Noncanonical recognition and degradation of a stable soluble protein by AAA protease FtsH

by

Juhee P. Morehouse

B.S. / M.S. in Biochemistry
Brandeis University, 2015

Submitted to the Department of Biology
in Partial Fulfillment of the Requirements for the Degree of

Doctor of Philosophy
at the
Massachusetts Institute of Technology

May 2022

Signature of Author: ………………………………………………………………………...

<div align="right">

Department of Biology
May 12, 2022

</div>

Certified by: …………………………………………………………………….......

<div align="right">

Robert T. Sauer
Salvador E. Luria Professor of Biology
Thesis Supervisor

</div>

Accepted by: …………………………………………………………………….

<div align="right">

Mary Gehring
Associate Professor of Biology
Member, Whitehead Institute
Co-Director, Biology Graduate Committee

</div>

Noncanonical recognition and degradation of a stable soluble protein by AAA protease FtsH

by

Juhee P. Morehouse

Submitted to the Department of Biology on May 13, 2022 in Partial Fulfillment of the
Requirements for the Degree of Doctor of Philosophy

ABSTRACT

AAA+ (ATPases associated with various cellular activities) proteolytic machines help maintain and adjust the cellular proteome in response to stress or changes in nutrients. AAA+ proteases bind degradation targets and utilize ATP-powered conformational changes in the AAA+ unfoldase ring to denature and translocate the substrate polypeptide into an associated, sequestered protease chamber for degradation. Of the five AAA+ proteases in *Escherichia coli*, FtsH is unique in being genetically essential, in its localization to the membrane, and in its function in degrading both membrane and cytosolic proteins. Prior *in vitro* characterization suggested that FtsH only degrades meta-stable proteins despite its ability to extract protein substrates from the membrane for degradation. These results motivated me to reinvestigate the determinants in a substrate required for effective FtsH unfolding. In this thesis, I present experiments that first test the hypothesis that FtsH may unfold and degrade a more stable protein *in vitro* with a sufficiently long degradation tag (degron) and then explore noncanonical recognition as one mechanism that may be employed in FtsH-dependent degradation.

In Chapter I, I review our current understanding of AAA+ protease structure and function, especially as it pertains to FtsH to provide background for the later chapters. In Chapter II, I test the hypothesis that a long degron may be required for FtsH to successfully bind and unfold *E. coli* dihydrofolate reductase (DHFR), a stable protein which was previously found to resist FtsH degradation. Strikingly, I find that detergent-solubilized FtsH can degrade DHFR *in vitro* with or without an appended degron. I then show that FtsH recognition of DHFR is noncanonical and not dependent on unstructured terminal degrons but suggest a model for how FtsH may unfold DHFR by engaging an internal site in a partially unfolded intermediate. In Chapter III, I test the hypothesis that FtsH may bind another stably folded soluble protein, cyclopropane fatty acid synthase (CFAS), at an internal site. In Chapter IV, I propose future directions that may further enrich our understanding of FtsH-DHFR degradation and experimental approaches that can be applied to assess the kinetics of assembly/disassembly of other enzyme-substrate complexes.

Thesis Supervisor: Robert T. Sauer
Title: Salvador E. Luria Professor of Biology

ACKNOWLEDGMENTS

I am grateful to many mentors, colleagues, friends and family, who have provided support and guidance in the path of earning a PhD. Below, I will name and thank a few of these people.

I would like to start by thanking my doctoral advisor Bob Sauer. I joined the Sauer lab in awe of Bob's scientific intuition that was evident in not only the classroom but also as a research advisor. I have admired and appreciated his ability to make precise yet detailed insights and his optimistic approach that translates to both perseverance and patience in life. I aspire to bring these values to my future endeavors. I would also like to thank my co-advisor Tania Baker for providing complementary insights and descriptive scientific pictures that have enriched many discussions. I would like to express my gratitude for my thesis committee members Amy Keating and Thomas Schwartz, who have provided unwavering support from my time rotating in their respective labs. Their questions and feedback significantly shaped my research and I feel lucky to have had these amazing mentors be so present in my time at MIT.

I am grateful for the incredible scientists and role models that I had the pleasure to work with from my alma mater, Brandeis. I would like to thank Chris Miller for letting me make bacterial media to help me see firsthand what it would be like to be in a lab and, eventually, setting me up with Janice Robertson, who worked with me on my first real hypothesis-driven project. I would like to thank Steve Goldstein for providing a nurturing lab environment to pursue my undergraduate thesis projects and Leigh Plant for mentoring me with such breadth and depth, from teaching me technical details to providing the framework to develop as a scientist. I would also like to thank Ruiming Zhao and Hui Dai who were always ready to help and brightened my days in the Goldstein Lab.

I would like to thank the current and former members of the Sauer Lab, especially Sanjay Hari, Xue Fei, Tristan Bell, Alireza Ghanbarpour, AJ Amor, Vlad Baytshtok and Karl Schmitz who have taught me so much and provided many laughs and genuine advice to propel me forward. I am especially grateful to Sanjay Hari for teaching me not only how to convert a hypothesis to a testable construct to clone, purify and validate, but also for candidly showing me how to be a 'cowboy biochemist.' I would also like to share my appreciation for the current and former members of the Baker lab: Sora Kim, Kristin Zuromski, Meghann Kasal, Irene Shih, Sara Kim, Jia Jia Zhang and Gina Mawla, who welcomed me to the south-side of the fifth floor and were always happy to lend a hand. Additionally, I am honored to have been part of the Building 68 community.

I am grateful to have wonderful friends who inspire me outside of my lab, especially Melissa Tannenbaum, Mary Thompson, Elaine Kuo, Theresa Hwang, and Alexandra Navarro.

I am forever grateful to my parents whose love and sacrifice have enabled me to pursue my passion and provided a home to always come back to rest and recharge. I would like to express gratitude to my brother, Juhun Park, whose smile lights up my world even during the most difficult times. I would also like to thank my extended family in Korea and in the US who have cheered me on.

Last but not least, I would like to thank my husband, Benjamin Morehouse, without whom, none of this would be possible. I am excited to embark on my next chapter with my best friend, Ben.

TABLE OF CONTENTS

Chapter I

Introduction

<u>Introduction to proteolysis</u>

Proteins can bind small molecules or macromolecules, perform chemical reactions, provide scaffolding and structure at multiple biological levels, produce energy, and even degrade other proteins. As a regulated post-translational mechanism, protein degradation can eliminate proteins, providing amino-acid building blocks that can be used to synthesize more proteins, or remodel proteins via partial degradation, which is a common mechanism to activate inactive forms of proteins. Protein degradation also alters the cellular proteome to adapt and respond to stress or changes in nutrients, making it an essential process in maintaining cell viability (Goldberg & Dice, 1974).

In 1942, Rudolf Scheonheimer and his colleagues challenged the then-prevailing idea that proteins that make up the body components are essentially stable material by proposing that proteins turn over via continuous and dynamic synthesis and degradation (Schoenheimer, 1942). Even though the idea of dynamic protein turnover was not widely accepted for more than a decade, the field has since expanded to show that there are organelles, like the lysosome, dedicated to the degradation of proteins and recycling of amino acids via proteolytic enzymes (proteases) and that the act of proteolysis is carried out in a precise manner that can be highly regulated and often requires metabolic energy (Ciechanover, 2005).

The catalytic mechanism of peptide-bond hydrolysis can be used to categorize proteases into six classes. The aspartic, glutamic, and metallo- classes of proteases utilize an activated water molecule as a nucleophile for attack on the peptide bond. The cysteine, serine, and threonine proteases use the side chains of the eponymous amino acids as the nucleophile (López-Otín &

Bond, 2008). The distinction in nucleophile identity dictates the hydrolysis mechanism, as an activated water molecule in the catalytic sites of aspartic, glutamic, and metalloproteases cleaves a peptide bond in one step. Cysteine, serine, and threonine proteases, by contrast, cleave a peptide bond in a two-step mechanism, in which a covalent acyl-enzyme intermediate is formed first, releasing the C-terminal product, and then an activated water molecule hydrolyzes the acyl-intermediate to release the N-terminal product and restore the catalytic site.

Serine-based enzymes make up more than 30% of known proteases (Di Cera, 2009). One might even argue that our understanding of how enzymes "work" or catalyze reactions is built on insights gathered from years of research on serine proteases, including chymotrypsin and trypsin (Warshel et al., 1989). Although no single amino-acid residue is a strong enough nucleophile at neutral pH to cleave a peptide bond, several features in the active site have been shown to allow serine proteases, like trypsin, to be incredibly effective enzymes (Buller & Townsend, 2013). The catalytic triad, a unique arrangement of aspartic acid, histidine, and serine side chains in the active site, makes the serine hydroxyl group a more reactive nucleophile, and a nearby oxyanion hole helps stabilize the transition state (the aforementioned acyl intermediate, which is negatively charged) and allows the reaction to move forward. These structural features are found in most serine proteases, but the specificity of these enzymes depends on the amino acids flanking the cleavage site. Which amino acids are recognized for cleavage are determined by the side chains lining the specificity pocket, for example chymotrypsin's high selectivity toward aromatic/hydrophobic residues versus trypsin's selectivity towards positively charged amino acids.

Metalloproteases make up the largest class of proteases (Rawlings & Barrett, 2004). These enzymes coordinate a network of waters and metal ion(s), usually one or two zinc ions but sometimes one or two cobalt or manganese ions. An HEXXH motif, as part of an alpha helix, most often coordinates a zinc ion in the active site. Examples of well-studied zinc metalloproteases include carboxypeptidase A and thermolysin.

Proteases can be divided into exopeptidases and endopeptidases. Exopeptidases hydrolyze terminal peptide bonds, whereas endopeptidases hydrolyze internal peptide bonds. Cleavage specificity in proteases can range widely from very promiscuous proteases to highly specific enzymes that may only attack a single peptide bond in one particular protein. To prevent proteases from wreaking havoc in the cell by nonspecifically destroying proteins at inopportune times, proteases are carefully regulated (López-Otín & Bond, 2008). Proteases can be regulated at the level of gene expression, by activation of their inactive zymogen forms, by inactivation by endogenous inhibitors, by localization to a specific compartment within the cell or the membrane, or by post-translational modifications.

Introduction to AAA and AAA+ proteases

The insight that some intracellular proteolysis requires metabolic energy led to the discovery of ubiquitin-dependent degradation by the 26S proteasome in eukaryotes and energy-dependent proteases in bacteria (Hershko & Ciechanover, 1982; Gottesman, 2003). Regulated proteolysis in the cell is carried out by AAA+ proteases. These enzymes harbor proteolytic active sites in a self-compartmentalized and protected chamber and contain at least one protein that belongs to the AAA+ (ATPases associated with diverse cellular activities) superfamily (Sauer & Baker, 2011).

AAA+ enzymes typically function as engines for cellular processes that require mechanical work (Fig. 1.1), and in the case of AAA+ proteases are used to unfold protein substrates and translocate the polypeptide into the peptidase compartment.
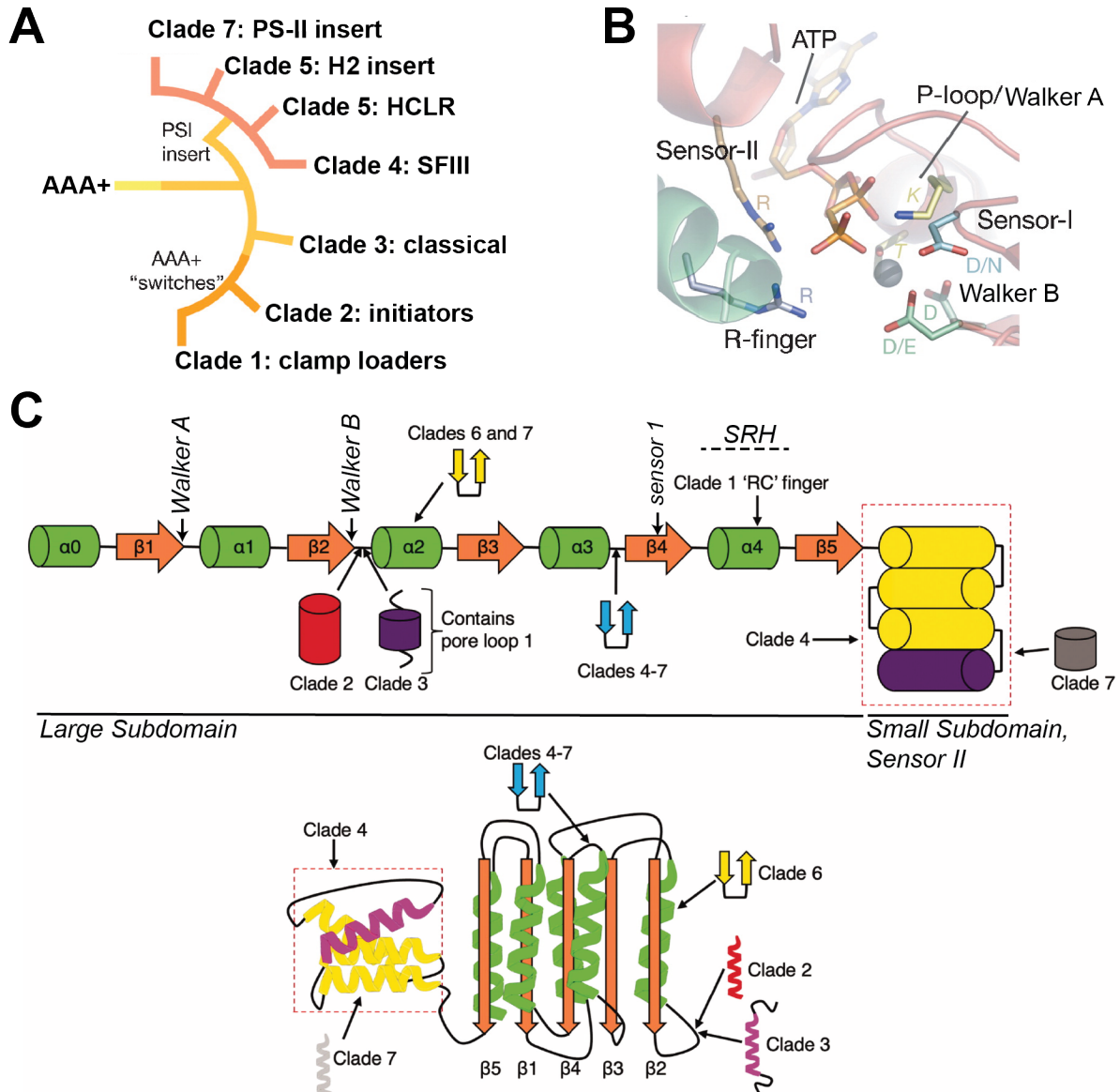

Figure 1.1. AAA+ ATPases. *A,* The seven clades of AAA+ ATPases as defined by Aravind and colleagues are classified according to their defining structural elements, adapted from (Erzberger & Berger, 2006). *B,* The nucleotide-interacting motifs and ATP of a AAA+ active site in DnaA are shown, adapted from (Erzberger & Berger, 2006) *C,* upper portion*:* Topological diagram with secondary structures in the large subdomain and small subdomain of AAA+ ATPases are illustrated. The various structural elements introduced with each clade and motif/regions highlighted in panels *A* and *B* are also depicted. SRH stands for second region of homology. *C,* lower portion*:* Cartoon model of the assembled core of a AAA+ ATPase subunit, highlighting structural elements that differ between clades, adapted from (Khan et al., 2021).

Features	Clade 1: clamp loader	Clade 2: initiators	Clade 3: classical	Clade 4: SFIII	Clade 5: HCLR	Clade 6: H2 insert	Clade 7: PS-II insert
Phylogeny	Viruses, Bacteria, Archaea, Eukarya	Bacteria, Archaea, Eukarya	Bacteria, Archaea, Eukarya	Viruses	Bacteria, Archaea, Eukarya	Bacteria, Archaea, Eukarya	Bacteria, Archaea, Eukarya
Biological functions	DNA replication	DNA replication	SNARE disassembly, chaperones, proteases, unfoldases, protein transport, cytoskeletal remodeling, etc	DNA replication	Chaperones, proteases, unfoldases, nuclear pore trafficking, ER morphology, DNA Helicase, etc	Restriction enzyme, transcription factor	DNA replication, metabolism, protein transport, ribosomal assembly, etc
Substrate	DNA	DNA	DNA, Protein, Membranes (indirectly)	DNA	DNA, Protein, Membranes	DNA, Protein	DNA, Protein
Oligomeric state	Pentamer, potentially octamer	Hexamer, filamentous	Hexamer, heptamer	Hexamer	Hexamer, multimer, filamentous	Hexamer, heptamer	Hexamer, heptamer, multimers

Table 1.1. Features of AAA+ ATPases as defined by clade. Adapted from (Khan et al., 2021)**.**

The AAA+ superfamily has members in all branches of life and can be subdivided into seven clades based on structural features that deviate from the core AAA structure (Fig. 1.1A, Table 1.1). These AAA+ motors use ATP hydrolysis to power mechanical work. Despite acting upon diverse substrates, AAA+ ATPases all consist of a large and a small AAA+ subdomains: the larger N-terminal AAA+ domain has a Rossman fold, whereas the smaller C-terminal AAA+ domain is mainly α-helical (Fig 1.1, Table 1.1). For the rest of this thesis, AAA will be used to refer to AAA ATPases from the classical AAA clade (*e.g.*, the AAA module of FtsH), whereas AAA+ will be used to denote the ATPases from the AAA+ superfamily outside of the classical clade (e.g., the AAA+ module of Lon).

The large AAA+ subdomain contains Walker-A, Walker-B, and sensor-1 motifs, as well as an arginine finger (Figs. 1.1B-1.1C). All of these motifs include residues that are important for binding and/or hydrolyzing ATP. The small AAA+ domain contains a sensor-2 motif, which is

also important for ATP hydrolysis (Figs. 1.1B-1.1C). The large AAA+ domain of one subunit packs against the small AAA+ domain of a neighboring to form the nucleotide-binding site. During the ATPase cycle, the large and the small domains in the apo-, ATP-bound, and ADP•P$_i$ and ADP-bound states change their orientation, which affects the conformation of the hexamer, and provides a mechanism for performing physical work (Sauer & Baker, 2011).

In bacteria, targeted ATP-dependent proteolysis is carried out by five AAA+ proteases: FtsH, Lon, HslUV, ClpXP, and ClpAP. The AAA+ components of these proteases form ring-shaped hexamers that couple ATP hydrolysis to the mechanical unfolding of captured protein substrates and the subsequent translocation of the unfolded polypeptide through an axial pore and into the peptidase chamber (Fig. 1.2). Two of the five AAA+ proteases, FtsH and Lon, contain the protease domain in the same polypeptide chain as the unfoldase (Fig. 1.2A). By contrast, ClpA hexamers, which contain D1 and D2 AAA+ rings, and ClpX hexamers combine with the double-ring ClpP$_{14}$ peptidase to form ClpAP and ClpXP. Similarly, HslU hexamers assemble with the double-ring HslV$_{12}$ peptidase to form HslUV (Fig. 1.2A). The AAA modules of FtsH and the ClpA D1 ring belong to the classic clade, whereas the AAA+ modules of ClpX, the D2 ring of ClpA, HslU, and Lon belong to the HCLR clade (Fig. 1.1A) (Zhang & Mao, 2020). The peptidase domain of FtsH is unique among the AAA+ proteases in being the only metalloprotease in this family (Ito & Akiyama, 2005). The Lon and ClpP peptidases are serine proteases, and HslV is a threonine protease.
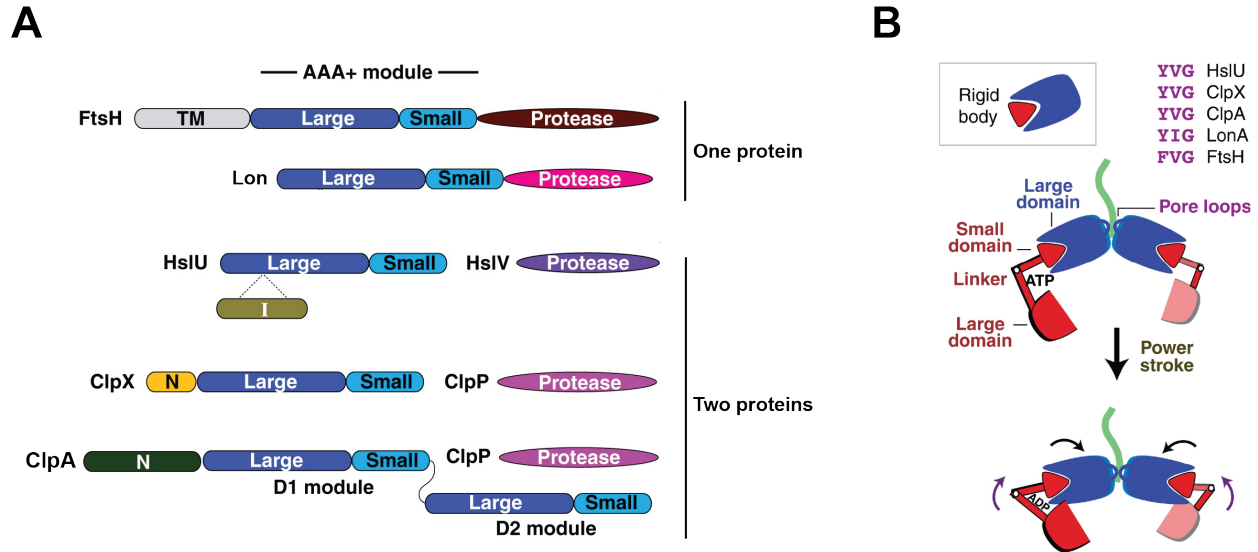
Figure 1.2. AAA+ proteases in *E. coli*. *A*, Domain structures of five AAA+ proteases in *E. coli*. FtsH and Lon have the unfoldase module and the protease domain on one polypeptide, whereas the unfoldase module and protease domains are on separate polypeptides for HslUV, ClpXP, and ClpAP. Adapted from (Sauer & Baker, 2011) *B*, The small domain in one subunit (red) and large domain of the neighboring subunit (blue) make up a rigid body (inset) in the AAA+ module. ATP-hydrolysis dependent power strokes result in translocation of the polypeptide (green) driven by the highly conserved pore loops (sequence alignment shown in upper corner) through the axial channel. Taken from (Sauer & Baker, 2011).

Post-translational modification of proteins by addition of ubiquitin targets them for degradation by the 26S proteasome in eukaryotes. By contrast, short peptide sequences, often called degradation tags or degrons, target proteins for proteolysis by AAA+ proteases in bacteria (Sauer & Baker, 2011). For example, the bacterial ssrA tag marks incompletely translated proteins for degradation and frees ribosomes that stall during protein synthesis (Keiler et al., 1996). Proteins bearing the ssrA tag are degraded efficiently by ClpXP, ClpAP, Lon, and FtsH in biochemical experiments but are mainly degraded by ClpXP (or Lon in Mycoplasma, which lack ClpXP) and FtsH in the cell (Moore & Sauer, 2007; Gur & Sauer Robert, 2008; Hari & Sauer, 2016). Adaptor proteins may also enhance or promote recognition of specific substrates by binding both to the substrate and to the AAA+ enzyme. Examples include SspB, which lowers K_M for degradation of ssrA-

tagged proteins by ClpXP, and ClpS, which enhances degradation of N-end-rule substrates by ClpAP (Sauer & Baker, 2011).

Multiple steps can be involved in recognition and unfolding of substrates by AAA+ proteases and have been best characterized for ClpXP (Fig. 1.3) (Fei et al., 2020; Saunders et al., 2020; Sauer et al., 2021). Minimally, a protein segment from the substrate that marks it for degradation must bind in the axial pore of the AAA+ ring to form an initial recognition complex. In most cases, ATP-dependent power strokes result in one or more translocation steps to form an intermediate complex(es) and finally an engaged complex, in which the native protein is pulled against the top of the AAA+ ring to generate an unfolding force. After engagement, repeated cycles of ATP binding and hydrolysis are typically required to successfully unfold the protein and then to translocate the polypeptide into the peptidase chamber for degradation (Kenniston et al., 2003).
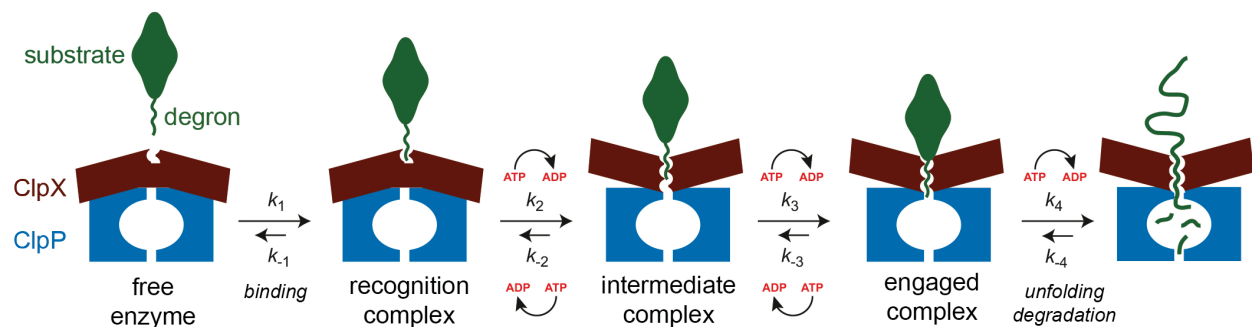

Figure 1.3. Mechanism of degradation by AAA+ protease ClpXP. Multistep model for ClpXP degradation of a substrate. ClpXP (ClpX in burgundy, ClpP in blue) binds a substrate via a degron (green) to form a recognition complex. ATP-dependent power strokes then translocate the degron to form an intermediate complex and finally an engaged complex. Once the substrate is engaged by being pulled against the AAA+ ring, repeated cycles of ATP binding and hydrolysis result in unfolding and translocation of the polypeptide into the ClpP chamber for degradation. Adapted from (Saunders et al., 2020).

Lon and HslUV play important roles in protein quality control during stress responses. In *E. coli*, Lon has been proposed to remove approximately 50% of misfolded proteins by recognizing hydrophobic motifs that would usually be buried in the native protein fold (Chung & Goldberg,

1981; Gur & Sauer, 2008; Mahmoud & Chien, 2018). HslUV is overexpressed under heat-shock conditions and its degradation activity *in vitro* has been shown to be maximal at heat-shock temperatures (Burton et al., 2005; Baytshtok et al., 2021).

FtsH is different in many ways from the other four *E. coli* AAA+ proteases. For example, FtsH is the only protease anchored to the inner membrane and is also the only essential AAA+ protease in *E. coli* (Tomoyasu et al., 1993; Tomoyasu et al., 1995; Langklotz et al., 2012). These features have made mechanistic investigation a challenge, leading to a gap in understanding of its activity when compared to cytosolic AAA+ enzymes. In addition, the AAA rings of FtsH and the D1 ring of ClpA are the only members of the classical clade, whereas the protease domain of FtsH is the only metalloprotease. As a consequence of these distinguishing features, it is possible that study of FtsH will reveal new biochemical insights. The remainder of this introduction is dedicated to background, discussing what is known and what remains to be discovered about the structure and function of FtsH, the focus of my thesis research.

Organization and structure of bacterial FtsH

FtsH is a homohexamer, with each subunit containing two transmembrane helices, an N-terminal periplasmic domain, a AAA module, and a zinc-metalloprotease domain (Figs. 1.4-1.5) (Ogura et al., 1991; Langklotz et al., 2012). Although a high-resolution structure of full-length FtsH has remained elusive, crystal structures of the AAA unfoldase and periplasmic domains of *E. coli* FtsH have been solved. The AAA module (residues 114-398) has the expected two-domain ATP-binding/hydrolyzing fold and is most similar to AAA modules from the p97 and NSF enzymes of the classical clade (Fig. 1.5A) (Krzywda et al., 2002). NMR and crystal structures show that

subunits of the periplasmic domain of *E. coli* FtsH (residues 25-96) form a compact α + β fold that assembled into a hexamer with stabilizing salt bridges between the subunits (Fig. 1.5B) (Scharfenberg et al., 2015).
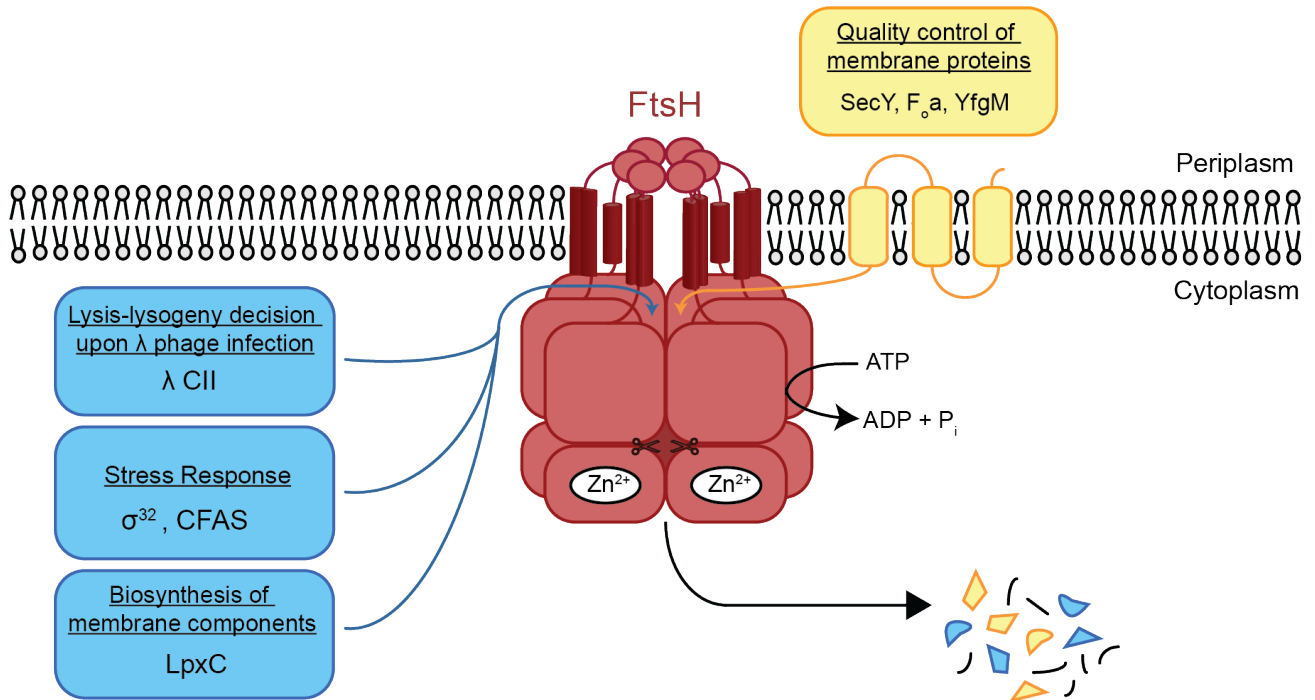

Figure 1.4. *E. coli* FtsH – structure, localization and substrates. A cartoon diagram of FtsH and its attachment to the inner membrane of *E. coli* with representative cytosolic and membrane-protein substrates. Biological functions ascribed to different regions are shown.
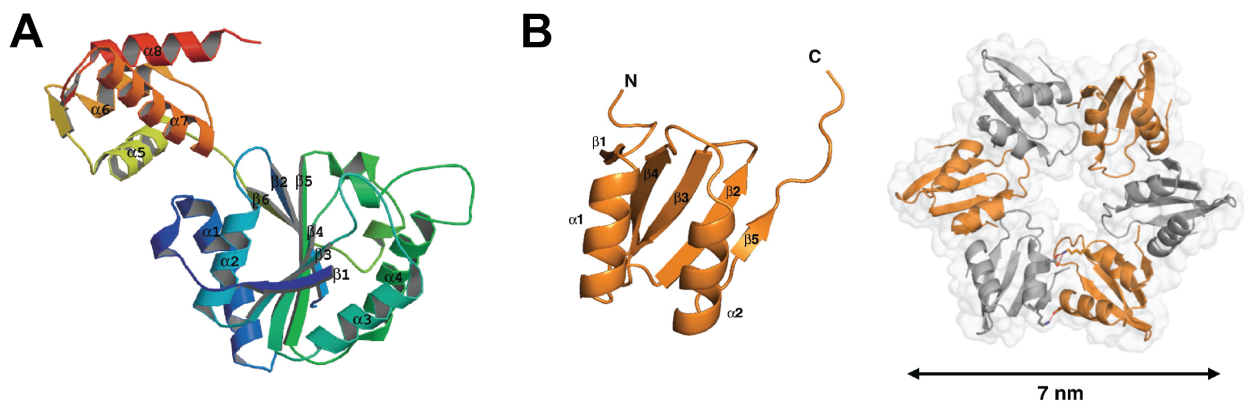

Figure 1.5. Structures of the AAA unfoldase and periplasmic N-domain of *E. coli* FtsH. *A,* Crystal structure of the large and small AAA subdomains of *E. coli FtsH* (residues 114 to 398 colored from blue to red; PDB code 1LV7. Taken from (Krzywda et al., 2002). *B,* Left – Monomeric NMR structure of the periplasmic domain of *E. coli* FtsH (residues 25-96; PDB code 2MUY). Right – Crystal structure of the hexameric periplasmic domain of *E. coli* FtsH (PDB code 4V0B; taken from (Scharfenberg et al., 2015).

Studies of thermophilic bacterial homologs of FtsH have also yielded valuable structural insights. The entire cytosolic portion of FtsH, including the unfoldase and protease domains from *Thermotoga maritima* has been solved in ADP-bound and nucleotide-free forms (Figs. 1.6A-1.6B) (Bieniossek et al., 2006; Bieniossek et al., 2009). Again, the AAA module contains a wedge-shaped large subdomain and a four-helical-bundle small subdomain (Fig. 1.6A). The AAA module is connected to the protease domain by a flexible glycine-rich linker (Fig. 1.6A). The protease ring has nearly perfect six-fold symmetry in these crystal structures, whereas the AAA ring has either two-fold or three-fold symmetry in the ADP-bound structures and six-fold symmetry in the apo structure (Fig. 1.6B). In addition, nucleotide binding appears to compress the cytosolic portion, with the conserved pore-1 and pore-2 loops moving inward towards the axis of the hexamer.

The apo-form of the structure of the cytosolic domain of *T. maritima* FtsH was used to generate a visual representation of the evolutionary rate of change of each residue based on a multiple-sequence alignment generated from ~1000 bacterial FtsH sequences (ConSurf, Fig. 1.6C). As expected, the AAA unfoldase is mostly well conserved, whereas residues of the AAA unfoldase contacting the protease domain and residues of the protease domain facing the cytosol are less conserved (Fig. 1.6C).

The C-terminal portion of the protease domain contains a canonical HEXXH motif, but the crystal structure revealed that the third zinc ligand is Asp[495] rather that the previously predicted Glu[476], making the protease a novel Asp-zincin (Bieniossek et al., 2009). Mutating this aspartate to alanine results in a loss of the zinc ion in the crystal structure.
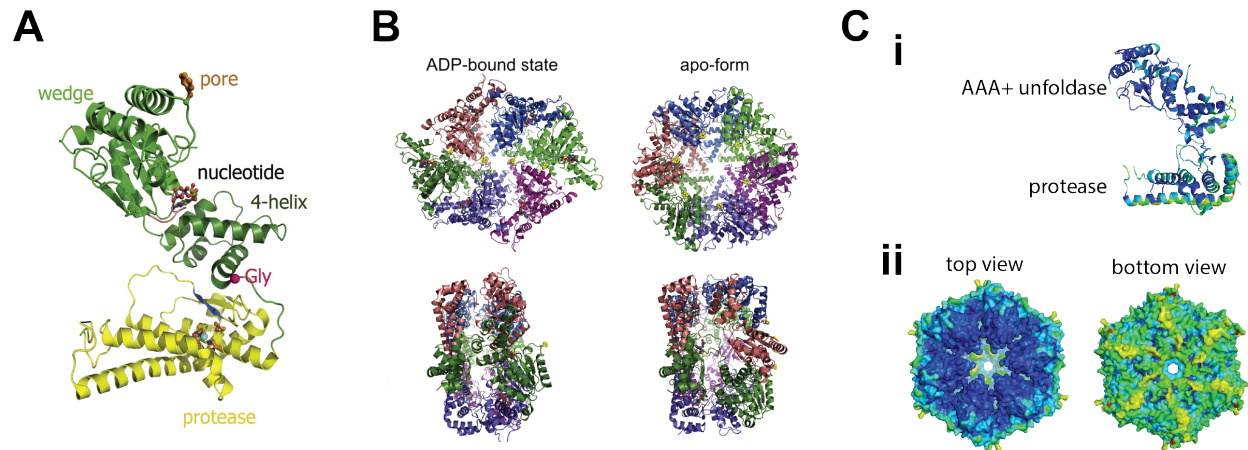
Figure 1.6. Cytosolic portion of *T. maritima* FtsH and conservation of bacterial FtsH sequences. *A,* Monomer structure of the ADP-bound form of the cytosolic portion of *T. maritima* FtsH (PDB code 2CE7). Cartoon representations of the wedge-like large AAA subdomain and helical small AAA subdomain are colored green; the protease domain is colored yellow. Stick representations are shown for the pore-1 loop residue F^{234} (orange), ADP nucleotide, and zinc-binding residues in the protease domain. The beginning of the glycine-rich linker is marked by a red sphere. *B,* ADP-bound (PDB code 2CE7) and apo *T. maritima* FtsH (PDB code 3KDS). Panels A and B are taken from (Langklotz et al., 2012) *C,* (i) side view of the monomer structure from panel *A* generated by ConSurf and colored based on evolutionary rates of change with cold/blue regions being most conserved and warm/red regions being least conserved; (ii) top and bottom views of the hexamer (similar to apo-form from panel *B*) colored by rates of evolutionary change.

A recent cryo-EM study of FtsH from another thermophilic bacterium, *Aquifex aeolicus,* has provided a low-resolution structure of the full-length detergent-solubilized enzyme and a model for how FtsH might access cytosolic and membrane-protein substrates (Carvalho et al., 2021). A structure calculated without imposing symmetry revealed that the periplasmic domain is off-set relative to the axis of the cytosolic portion of FtsH and the axial channel of the AAA ring is open (Fig. 1.7A). High-resolution cryo-EM structures of the cytosolic domain of the yeast mitochondrial YME1 protease, an FtsH homolog, in various nucleotide-binding states, fit well into the asymmetric structure (Fig. 1.7A).

The domain structures of *A. aeolicus* FtsH and *E. coli* FtsH closely resemble each other, including a highly conserved ~20-residue glycine-rich linker connecting the second transmembrane helix to the cytosolic portion of the enzyme (Fig. 1.7B). Based on the predicted flexible nature of this linker and the full-length *A. aeolicus* structure, Carvalho and colleagues propose that the cytosolic hexamer may tilt with respect to the membrane, allowing soluble and membrane protein substrates to access the axial pore of the AAA unfoldase ring through a gap of ~30 Å (Fig. 1.7B). A recent cryo-EM structure of full-length ADP-bound *Thermotoga maritima* FtsH in the membranous environment shows a similar tilted architecture of the cytosolic portion in relation to the membrane (Fig.1.7C). However, low resolution especially around the N-terminal periplasmic domain and transmembrane portion required the use of AlphaFold to build atomic models for these sections and will require further validation - potentially the structure of a well-formed complex bound to other membrane proteins to stabilize this region further (Fig. 1.7D).

FtsH binds two other membrane proteins, HflK and HflC, which are adaptors that modulate FtsH activity (Kihara et al., 1996, 1997, 1998; Saikawa et al., 2004). A recent cryo-EM structure shows a FtsH-HflKC supramolecular complex spanning 20 nm in diameter, in which HflK and HflC form a circular 24-unit assembly around four FtsH hexamers (Fig. 1.7E) (Ma et al., 2022). Based on this structure and biochemical results showing that purified FtsH-HflKC does not degrade the membrane substrate SecY but does degrade the cytosolic substrate λ cII, HflKC is proposed to inhibit degradation by forming a cage that would limit the access to potential substrates, especially membrane proteins with large periplasmic domains.
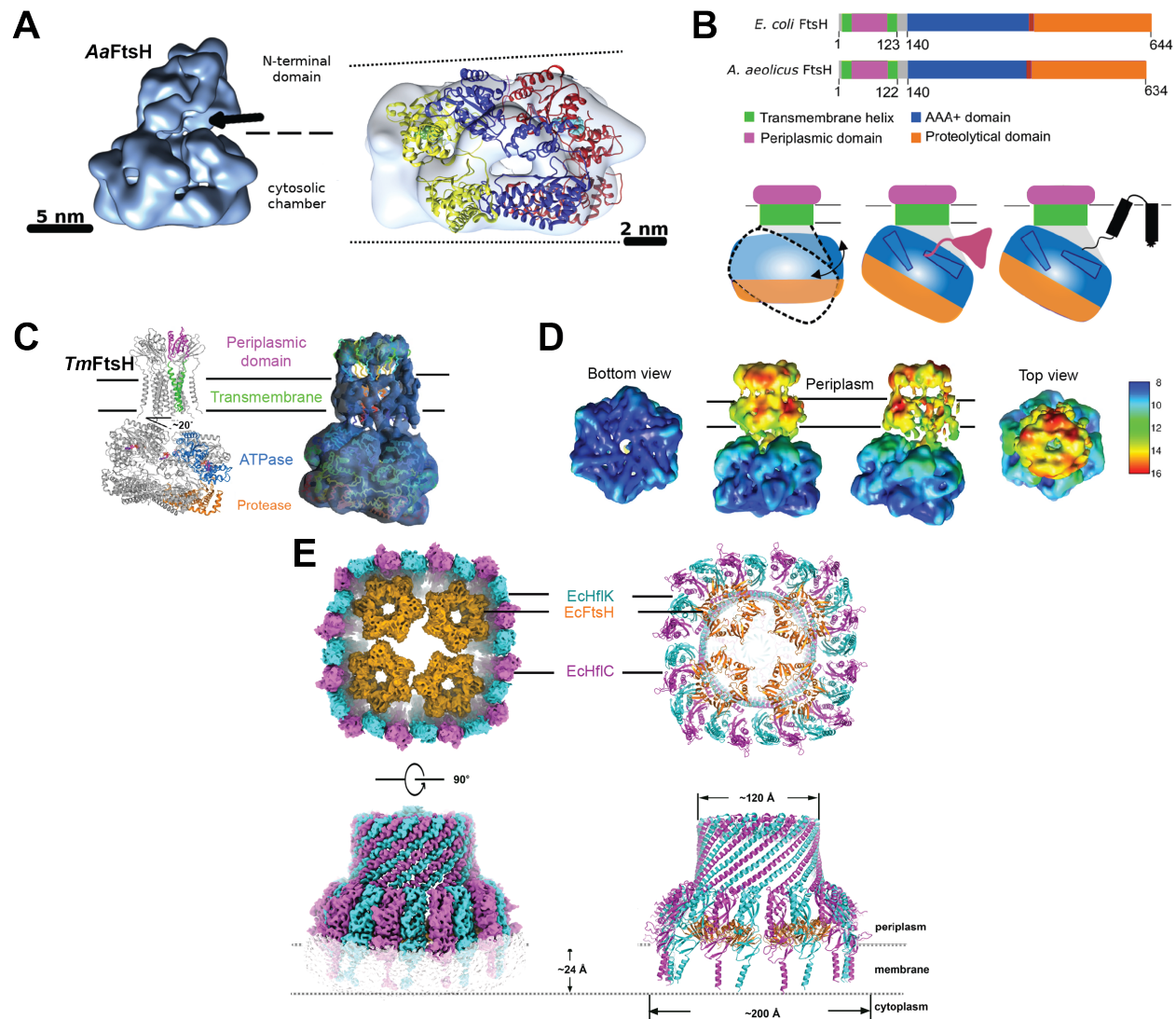
Figure 1.7. Cryo-EM structures of bacterial FtsH. *A,* left: Structure of *A. aeolicus* FtsH hexamer without symmetry constraints shows a tilted cytosolic domain and somewhat disordered periplasmic domain, with a potential access channel indicated by the black arrow. *A,* right: Three Yme1 cytosolic domains (PDB code 6AZ0) are fitted into the asymmetric structure. Yellow represents ADP-bound chain E, blue represents the nucleotide-free chain F, and red represents the ATP-bound chain A. *B,* The upper portion of the panel compares the sequence/domain organization of *E. coli* FtsH and *A. aeolicus* FtsH. The conserved ~20-residue glycine-rich linker (residues 122-140) is in gray. The lower portion of the panel shows a model for substrate entry based on a tilted cytosolic domain without substrate (left), with a cytosolic substrate (middle) and with a membrane protein substrate (right). Parts *A* and *B* are adapted from (Carvalho et al., 2021). *C,* Left – Full-length *Thermotoga maritima* FtsH model. Transmembrane and periplasmic domains were modeled using AlphaFold. Right – Full-length *T. maritima* FtsH model fit into 3D density map. *D,* 3D map of *T. maritima* FtsH colored by local resolution showing a bottom view, two side views, and a top view. Parts *C* and *D* are adapted from (Liu et al., 2022). *E,* Top – the FtsH-HflKC supramolecular complex viewed from the cytoplasm with the cryo-EM map (left) and an atomic-model (right). Bottom – side-view of FtsH-HflKC shows the cryo-EM map (left) and atomic-model (right). Adapted from (Ma et al., 2022).

FtsH substrates *in vivo*

FtsH substrates have been identified by numerous methods, including candidate-based approaches for proteins known to be rapidly degraded, genetics, and proteomics. Unsurprisingly, given its anchoring to the inner membrane, FtsH plays a role in quality control by degrading disassembled and misfolded membrane proteins (Fig. 1.4). For example, overexpression of membrane proteins, especially those that function as part of a larger complex, including SecY of the SecYEG translocon and F_o of the F_oF_1 ATPase, results in FtsH-dependent degradation (Akiyama et al., 1994; Kihara et al., 1995; Akiyama et al., 1996; Kihara et al., 1999). Some FtsH substrate were discovered by isolating *E. coli* proteins that co-purified with a proteolytically inactive variant of FtsH, using mass spectrometry for identification and validating candidates by degradation experiments *in vivo* (Westphal et al., 2012; Arends et al., 2016; Lindemann et al., 2018). Membrane-protein substrates identified in this way include DadA, which deaminates D-amino acids, FdoH, which is involved in adaptation to anaerobic conditions, and YfgM, an ancillary translocon subunit. The degradation of YfgM is most rapid under slow-growth conditions or in stationary phase (Bittner et al., 2015).

Several cytosolic proteins have been shown to be FtsH substrates (Fig. 1.4). FtsH degradation of LpxC, a cytoplasmic enzyme responsible for the first committed step of lipopolysaccharide (LPS) biosynthesis, is essential to maintain a proper ratio of the major components of the outer membrane (Ogura et al., 1999; Schäkermann et al., 2013). KdtA, an enzyme downstream of LpxC in the lipopolysaccharide synthesis pathway, has also been reported to be a substrate, illustrating a dual role for FtsH in this important pathway (Katz & Ron, 2008). An *E. coli ftsH* deletion strain can only survive with a suppressor mutation in the *fabZ* gene, the product of which is involved in the

production of phospholipids, the other major component of the outer membrane (Fig. 1.4) (Tatsuta et al., 1998).

FtsH was historically known as HflB because mutations in this protease result in a <u>h</u>igh <u>f</u>requency of <u>l</u>ysogeny upon infection of *E. coli* with λ phage (Banuett et al., 1986). This phenotype depends on FtsH degradation of the cytoplasmic λ cII protein, a key regulator controlling the λ lysis/lysogeny decision (Cheng et al., 1988; Herman et al., 1993; Kihara et al., 1997; Shotland et al., 1997; Shotland et al., 2000). Lower levels of cII promote the lytic pathway, whereas higher levels favor lysogen formation. λ cIII, a small membrane-associated protein, was also found to promote the stability of cII by competitively inhibiting FtsH (Herman et al., 1995; Tomoyasu et al., 1995; Kobiler et al., 2007).

FtsH also plays a role in stress responses by degrading the cytoplasmic RpoH (σ^{32}) sigma factor, which is the key regulator of the *E. coli* heat-shock response (Herman et al., 1995; Tomoyasu et al., 1995). At normal temperatures, RpoH associates with the DnaK and DnaJ molecular chaperones and is rapidly degraded by FtsH (Tatsuta et al., 1998). At elevated temperatures, unfolded and misfolded proteins compete for DnaK and DnaJ binding, freeing RpoH to associate with RNA polymerase and to induce transcription of heat-shock genes (Straus et al., 1990). FtsH also degrades cyclopropyl fatty acid synthase (CFAS), whose synthesis is controlled by σ^{s}, the stationary-phase transcription factor (Hari et al., 2018). Degradation of CFAS by FtsH is further explored in chapter III of this thesis.

Homologs of FtsH in organelles

Eukaryotic homologs of FtsH also play important roles in membrane-protein quality control. In mitochondria, there are two FtsH-like AAA proteases, *i*-AAA and *m*-AAA (Leonhard et al., 1996; Glynn, 2017). The *i*-AAA protease has the catalytic portion of the enzyme in the inner-membrane space with one transmembrane helix in the inner membrane; the *m*-AAA enzyme has the catalytic part of the protease in the matrix and two transmembrane helices in the inner membrane (Fig. 1.8A). One role of mitochondrial quality control is removing unassembled subunits of larger complexes, similar to the role of FtsH in *E. coli*. The mitochondrial AAA proteases degrade superfluous subunits of cytochrome c oxidase, also known as complex IV of the electron-transport chain, as well as subunits of ATP synthase (Nakai et al., 1995; Arlt et al., 1996). Mitochondrial AAA proteases also control the levels of proteins involved in metabolic pathways, including phospholipid homeostasis and stress response (Opalińska & Jańska, 2018). An organelle of the malaria parasite, *P. falciparum*, contains an essential FtsH homolog that can be inhibited by actinonin (Amberg-Johnson et al., 2017). This small-molecule antibiotic was known to inhibit the zinc-dependent peptide deformylase (Chen et al., 2000) and was subsequently found to inhibit FtsH *in vivo* and *in vitro.* In this thesis, I frequently use actinonin as an inhibitor of *E. coli* FtsH for negative controls.

In humans, mitochondrial *m*-AAA proteases can form hexamers consisting of six AFG3L2 proteins or assemble into heteromeric complexes containing AFG3L2 and paraplegin subunits. Malfunctioning *m*-AAA proteases have been implicated in neurodegenerative diseases, with mutations in AFG3L2 being associated with spinocerebellar ataxia type 28 (SCA28), and mutations in paraplegin being associated with spastic paraplegia (Patron et al., 2018). At least 17

single amino-acid substitutions in AFG3L2 have been associated with SCA28, the majority of which are found in the protease active site or the interface between subunits in the AAA unfoldase (Fig. 1.8) (Puchades et al., 2019).

A soluble hexamerization domain replacing the transmembrane portion has been a useful tool for studying the structure and degradation mechanism of these challenging membrane proteins (Fig. 1.8B-C). A soluble YME1 variant was shown to recognize and degrade model protein substrates tagged with AAA+ protease-specific degrons (Shi et al., 2016). Structural studies of soluble hexamers of YME1 and AFG3L2 yielded high-resolution cryo-EM structures of substrate-bound cytosolic portions of the enzymes, which showed that the AAA modules are organized in a spiral staircase formation unlike the symmetric hexameric crystal structures of bacterial FtsH (Puchades et al., 2017; Puchades et al., 2019). The aforementioned disease-associated mutations were found to cluster in different parts of the AFG3L2, suggesting connections to enzyme structure and function (Fig. 1.8C).
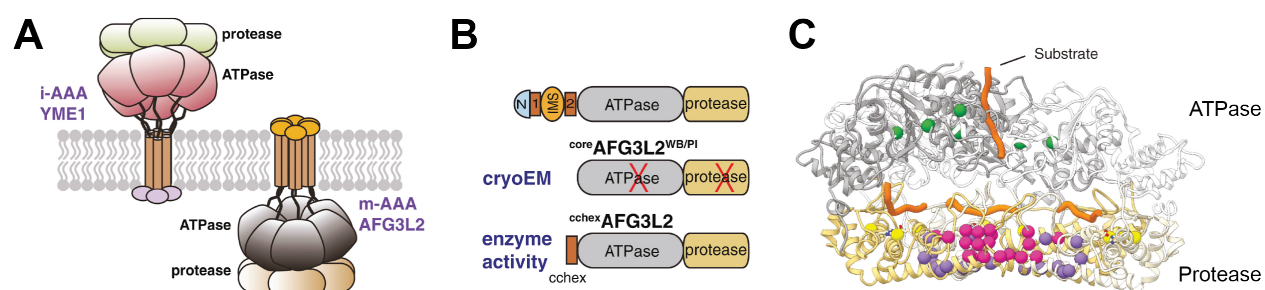

Figure 1.8. Mitochondrial AAA proteases. *A,* Cartoons depicting the *i*-AAA and *m*-AAA proteases in the mitochondrial inner membrane. *B,* Domain diagrams of wild-type AFG3L2 (top), a soluble inactivated variant (WB - Walker B mutation; PI - protease inactivated) used for cryo-EM studies (middle), and an active soluble construct used for biochemical studies (bottom). *C,* Cutaway side-view of AFG3L2 showing the substrate polypeptide (orange) in the ATPase ring and protease domains. The green, pink, purple, and yellow spheres highlight four types of disease-related mutations. All panels taken from (Puchades et al., 2019).

Multiple FtsH-like AAA proteases are found anchored to the thylakoid membrane in chloroplasts, with the catalytic domains facing the stroma (Lindahl et al., 1996). Similar to bacterial FtsH and the mitochondrial AAA proteases, chloroplast FtsH degrade unassembled proteins that normally assemble into larger complexes, like the Rieske iron-sulfur protein of the cytochrome b_6f complex, which is important for transferring electrons from photosystem II to I, as well as damaged proteins, including the photosystem II D1 protein (Lindahl et al., 2000; Adam & Ostersetzer, 2001).

In contrast to the single *ftsH* gene found in most bacteria, eukaryotes have an expanded number. Yeast and humans have three FtsH orthologs, whereas the plant *Arabidopsis thaliana* has 12 FtsH homologs. Despite this difference in the number of *ftsH* genes per species and the ability of subunits to form heteromeric enzymes, the sequences of FtsH in *E. coli, S. cerevisiae, H. sapiens,* and *A. thaliana* are highly conserved, with 40% sequence identity and similar three-domain structures (Opalińska & Jańska, 2018). FtsH-family enzymes across kingdoms appear to share the role of maintaining membrane-protein quality and adjusting levels of proteins involved in metabolic pathways, such as lipid biogenesis.

How FtsH recognizes substrates

FtsH utilizes diverse modes of recognition. Like other AAA+ proteases, a modular peptide sequence has been shown to target some substrates for FtsH degradation. The best studied example is the *E. coli* ssrA tag, as its addition to soluble proteins, like the λ cI N-domain and Arc repressor, result in their degradation by FtsH (Fig. 1.9) (Herman et al., 1998; Herman et al., 2003). Addition of an ssrA tag to a truncated variant of the ProW membrane protein also resulted in FtsH-dependent

degradation *in vivo* (Hari & Sauer, 2016). The ssrA sequence resembles the hydrophobic C-terminal sequence of LpxC which has been shown to be necessary for FtsH-dependent degradation (Fig. 1.9). The sequence Ser-Leu-Leu-Trp-Ser, called the 108 degron, was also found to be an FtsH-specific degron leading to degradation of λ cI N-domain when fused to the C-terminus *in vivo* and *in vitro* (Parsell et al., 1990; Herman et al., 1998). λ cII also possesses a modular C-terminal FtsH degron, but its sequence (Glu-Arg-Ser-Gln-Ile-Gln-Met-Glu-Phe) is quite different from the ssrA, 108, and LpxC degrons.

The FtsH membrane-protein substrates YfgM, ExbD, and YlaC have N-terminal degrons with three to five acidic residues (Fig. 1.9). Chiba and colleagues proposed that FtsH recognition of membrane proteins, including Ycca, SecY, and F_o, is sequence independent but requires a disordered N- or C-terminal sequence of ~20 residues (Chiba et al., 2000). The requirement for an unstructured stretch of polypeptide is reminiscent of substrate recognition by the 26S proteasome, which requires both a recognition tag (most commonly polyubiquitin chains) and an unstructured 'initiation region' for effective engagement (Prakash et al., 2004; Inobe et al., 2011).
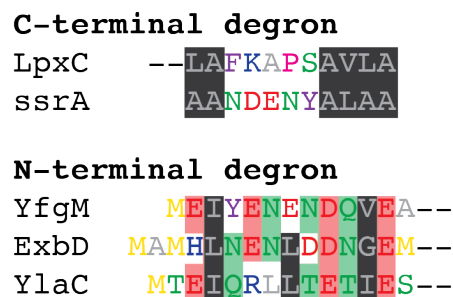
```
C-terminal degron
LpxC     --LAFKAPSAVLA
ssrA       AANDENYALAA

N-terminal degron
YfgM     METYENENDQVEA--
ExbD    MAMHLNENLDDNGEM--
YlaC     MTEIQRLLTETIES--
```

Figure 1.9. Degrons of FtsH. *Top,* C-terminal degron sequences of LpxC and the ssrA tag. *Bottom,* N-terminal degron sequences from YfgM, ExbD, and YlaC. Amino acid colors: acidic (red), basic (blue), small/polar (green), nonpolar (gray), aromatic (purple), proline (pink), and methionine (yellow). Adapted from (Bittner et al., 2017).

FtsH degradation of RpoH depends on an exposed alpha-helical motif in the internal region 2.1, but transferring this region to another sigma factor did not result in FtsH-dependent degradation (Obrist & Narberhaus, 2005; Obrist et al., 2007). DnaK and DnaJ binding also affects RpoH degradation *in vivo*, adding another layer of complexity (Rodriguez et al., 2008). It has also been suggested than an internal FtsH degron may be present in flavodoxin (Okuno et al., 2006a, 2006b).

FtsH degradation studies *in vitro*

The most thorough studies of FtsH degradation *in vitro* were performed using a suite of ssrA-tagged variants of model proteins of varying stabilities, including DHFR, GFP, barnase, Arc repressor, and the λ cI N-domain (Herman et al., 2003). The metastable Arc and cI proteins were degraded by FtsH, but the more stable DFHR, barnase, and GFP protein were not degraded. Notably, FtsH did degrade destabilized mutants of DHFR and barnase, showing a correlation between degradation susceptibility and thermodynamic instability. Another study – which assessed the unfolding/degradation activities of FtsH, ClpXP, ClpAP, Lon, HslUV, 20S/PAN, and the 26S proteasome – also reached the conclusion that FtsH has a weak unfolding ability (Koodathingal et al., 2009). Based on their results, Herman and colleagues proposed that the weak unfoldase activity of FtsH is an important determinant of its substrate specificity. Specifically, it seemed possible that substrates were only degraded when spontaneous thermal fluctuations resulted in partial denaturation that assisted FtsH-mediated unfolding attempts. However, recent studies have shown that FtsH has enough unfolding power to allow membrane extraction and degradation *in vitro* of GlpG, a thermodynamically and kinetically stable membrane protein (Yang et al., 2018). Thus, the issue of the strength of FtsH unfolding does not appear to have been resolved.

This thesis

Dr. William Jencks, an esteemed biochemist, once wrote that "*the principal difference between enzymic and most chemical catalysis lies precisely in these specific-binding interactions and that a separation between substrate binding and chemical mechanisms of catalysis leads to a misleading and incomplete picture of the mechanism of enzymic catalysis*" (Jencks, 1975). Due to the significance of the initial recognition step in determining catalysis, I endeavored to discover the determinants of recognition that would result in FtsH degradation of a stably folded protein *in vitro*. In Chapter II, I explore *E. coli* DHFR as a potential FtsH substrate. Because the work of Herman and colleagues that reported that FtsH cannot degrade DHFR-ssrA (Herman et al., 2003), I hypothesized that the proximity of the FtsH axial pore to the membrane might require the degron to be part of an unstructured polypeptide of sufficient length to allow FtsH recognition, engagement, and unfolding of DHFR. Indeed, I found that DHFR with a long linker between the native protein and ssrA tag could be degraded by FtsH. Surprisingly, however, I also discovered that FtsH can degrade DHFR-ssrA and even untagged DHFR, essentially as well as the long-degron substrate! I then performed additional experiments that support a model in which FtsH recognizes an internal degron in DHFR, most likely in an intermediate DHFR species in which a portion of the native fold is denatured. In Chapter III, I test one possibility for an internal degron within an unstructured region in CFAS for FtsH recognition. In Chapter IV, I discuss future experiments based on the development of a substrate binding assay that I believe will be important to advance our understanding of the FtsH substrate recognition and have the potential to be applied to studying substrate recognition with other AAA+ proteases.

REFERENCES

Adam, Z., & Ostersetzer, O. (2001). Degradation of unassembled and damaged thylakoid proteins. *Biochem Soc Trans*, *29*(Pt 4), 427-430. https://doi.org/10.1042/bst0290427

Akiyama, Y., Kihara, A., & Ito, K. (1996). Subunit a of proton ATPase F0 sector is a substrate of the FtsH protease in *Escherichia coli*. *FEBS Lett*, *399*(1-2), 26-28. http://onlinelibrary.wiley.com/store/10.1016/S0014-5793(96)01283-5/asset/feb2s0014579396012835.pdf?v=1&t=j7yvxxbi&s=af8c5729c7fab679402c5ded92d394c02227e05b

Akiyama, Y., Ogura, T., & Ito, K. (1994). Involvement of FtsH in protein assembly into and through the membrane. I. Mutations that reduce retention efficiency of a cytoplasmic reporter. *J Biol Chem*, *269*(7), 5218-5224. http://www.jbc.org/content/269/7/5218.full.pdf

Amberg-Johnson, K., Hari, S. B., Ganesan, S. M., Lorenzi, H. A., Sauer, R. T., Niles, J. C., & Yeh, E. (2017). Small molecule inhibition of apicomplexan FtsH1 disrupts plastid biogenesis in human pathogens. *Elife*, *6*. https://doi.org/10.7554/eLife.29865

Arends, J., Thomanek, N., Kuhlmann, K., Marcus, K., & Narberhaus, F. (2016). In vivo trapping of FtsH substrates by label-free quantitative proteomics. *Proteomics*, *16*(24), 3161-3172. https://doi.org/10.1002/pmic.201600316

Arlt, H., Tauer, R., Feldmann, H., Neupert, W., & Langer, T. (1996). The YTA10-12 complex, an AAA protease with chaperone-like activity in the inner membrane of mitochondria. *Cell*, *85*(6), 875-885. https://doi.org/10.1016/s0092-8674(00)81271-4

Banuett, F., Hoyt, M. A., McFarlane, L., Echols, H., & Herskowitz, I. (1986). hflB, a new *Escherichia coli* locus regulating lysogeny and the level of bacteriophage lambda cII protein. *J Mol Biol*, *187*(2), 213-224. https://doi.org/10.1016/0022-2836(86)90229-9

Baytshtok, V., Fei, X., Shih, T.-T., Grant, R. A., Santos, J. C., Baker, T. A., & Sauer, R. T. (2021). Heat activates the AAA+ HslUV protease by melting an axial autoinhibitory plug. *Cell Rep*, *34*(3), 108639-108639. https://doi.org/10.1016/j.celrep.2020.108639

Bieniossek, C., Niederhauser, B., & Baumann, U. M. (2009). The crystal structure of apo-FtsH reveals domain movements necessary for substrate unfolding and translocation. *Proc Natl Acad Sci U S A*, *106*(51), 21579-21584. https://doi.org/10.1073/pnas.0910708106

Bieniossek, C., Schalch, T., Bumann, M., Meister, M., Meier, R., & Baumann, U. (2006). The molecular architecture of the metalloprotease FtsH. *Proc Natl Acad Sci U S A*, *103*(9), 3066-3071. https://doi.org/10.1073/pnas.0600031103

Bittner, L. M., Arends, J., & Narberhaus, F. (2017). When, how and why? Regulated proteolysis by the essential FtsH protease in *Escherichia coli*. *Biol Chem*, *398*(5-6), 625-635. https://doi.org/10.1515/hsz-2016-0302

Bittner, L. M., Westphal, K., & Narberhaus, F. (2015). Conditional Proteolysis of the Membrane Protein YfgM by the FtsH Protease Depends on a Novel N-terminal Degron. *J Biol Chem*, *290*(31), 19367-19378. https://doi.org/10.1074/jbc.M115.648550

Buller, A. R., & Townsend, C. A. (2013). Intrinsic evolutionary constraints on protease structure, enzyme acylation, and the identity of the catalytic triad. *Proceedings of the National Academy of Sciences*, *110*(8), E653-E661. https://doi.org/doi:10.1073/pnas.1221050110

Burton, R. E., Baker, T. A., & Sauer, R. T. (2005). Nucleotide-dependent substrate recognition by the AAA+ HslUV protease. *Nat Struct Mol Biol*, *12*(3), 245-251. https://doi.org/10.1038/nsmb898

Carvalho, V., Prabudiansyah, I., Kovacik, L., Chami, M., Kieffer, R., van der Valk, R., de Lange, N., Engel, A., & Aubin-Tam, M. E. (2021). The cytoplasmic domain of the AAA+ protease FtsH is tilted with respect to the membrane to facilitate substrate entry. *J Biol Chem*, *296*, 100029. https://doi.org/10.1074/jbc.RA120.014739

Chen, D. Z., Patel, D. V., Hackbarth, C. J., Wang, W., Dreyer, G., Young, D. C., Margolis, P. S., Wu, C., Ni, Z. J., Trias, J., White, R. J., & Yuan, Z. (2000). Actinonin, a naturally occurring antibacterial agent, is a potent deformylase inhibitor. *Biochemistry*, *39*(6), 1256-1262. https://doi.org/10.1021/bi992245y

Cheng, H. H., Muhlrad, P. J., Hoyt, M. A., & Echols, H. (1988). Cleavage of the cII protein of phage lambda by purified HflA protease: control of the switch between lysis and lysogeny. *Proc Natl Acad Sci U S A*, *85*(21), 7882-7886. https://doi.org/10.1073/pnas.85.21.7882

Chiba, S., Akiyama, Y., Mori, H., Matsuo, E., & Ito, K. (2000). Length recognition at the N-terminal tail for the initiation of FtsH-mediated proteolysis. *EMBO Rep*, *1*(1), 47-52. https://doi.org/10.1093/embo-reports/kvd005

Chung, C. H., & Goldberg, A. L. (1981). The product of the lon (capR) gene in *Escherichia coli* is the ATP-dependent protease, protease La. *Proc Natl Acad Sci U S A*, *78*(8), 4931-4935. https://doi.org/10.1073/pnas.78.8.4931

Ciechanover, A. (2005). Intracellular protein degradation: from a vague idea thru the lysosome and the ubiquitin-proteasome system and onto human diseases and drug targeting. *Cell Death Differ*, *12*(9), 1178-1190. https://doi.org/10.1038/sj.cdd.4401692

Di Cera, E. (2009). Serine proteases. *IUBMB Life*, *61*(5), 510-515. https://doi.org/10.1002/iub.186

Erzberger, J. P., & Berger, J. M. (2006). EVOLUTIONARY RELATIONSHIPS AND STRUCTURAL MECHANISMS OF AAA+ PROTEINS. *Annual Review of Biophysics and Biomolecular Structure*, *35*(1), 93-114. https://doi.org/10.1146/annurev.biophys.35.040405.101933

Fei, X., Bell, T. A., Barkow, S. R., Baker, T. A., & Sauer, R. T. (2020). Structural basis of ClpXP recognition and unfolding of ssrA-tagged substrates. *Elife*, *9*. https://doi.org/10.7554/eLife.61496

Glynn, S. E. (2017). Multifunctional Mitochondrial AAA Proteases. *Frontiers in molecular biosciences*, *4*, 34-34. https://doi.org/10.3389/fmolb.2017.00034

Goldberg, A. L., & Dice, J. F. (1974). Intracellular protein degradation in mammalian and bacterial cells. *Annu Rev Biochem*, *43*(0), 835-869. https://doi.org/10.1146/annurev.bi.43.070174.004155

Gottesman, S. (2003). Proteolysis in Bacterial Regulatory Circuits. *Annual Review of Cell and Developmental Biology*, *19*(1), 565-587. https://doi.org/10.1146/annurev.cellbio.19.110701.153228

Gur, E., & Sauer Robert, T. (2008). Evolution of the ssrA degradation tag in Mycoplasma: Specificity switch to a different protease. *Proceedings of the National Academy of Sciences*, *105*(42), 16113-16118. https://doi.org/10.1073/pnas.0808802105

Gur, E., & Sauer, R. T. (2008). Recognition of misfolded proteins by Lon, a AAA(+) protease. *Genes Dev*, *22*(16), 2267-2277. https://doi.org/10.1101/gad.1670908

Hari, S. B., Grant, R. A., & Sauer, R. T. (2018). Structural and Functional Analysis of *E. coli* Cyclopropane Fatty Acid Synthase. *Structure*, *26*(9), 1251-1258.e1253. https://doi.org/10.1016/j.str.2018.06.008

Hari, S. B., & Sauer, R. T. (2016). The AAA+ FtsH Protease Degrades an ssrA-Tagged Model Protein in the Inner Membrane of *Escherichia coli. Biochemistry*, *55*(40), 5649-5652. https://doi.org/10.1021/acs.biochem.6b00920

Herman, C., Ogura, T., Tomoyasu, T., Hiraga, S., Akiyama, Y., Ito, K., Thomas, R., D'Ari, R., & Bouloc, P. (1993). Cell growth and lambda phage development controlled by the same essential *Escherichia coli* gene, ftsH/hflB. *Proc Natl Acad Sci U S A*, *90*(22), 10861-10865.

Herman, C., Prakash, S., Lu, C. Z., Matouschek, A., & Gross, C. A. (2003). Lack of a Robust Unfoldase Activity Confers a Unique Level of Substrate Specificity to the Universal AAA Protease FtsH. *Molecular Cell*, *11*(3), 659-669. https://doi.org/http://dx.doi.org/10.1016/S1097-2765(03)00068-6

Herman, C., Thevenet, D., Bouloc, P., Walker, G. C., & D'Ari, R. (1998). Degradation of carboxy-terminal-tagged cytoplasmic proteins by the *Escherichia coli* protease HflB (FtsH). *Genes Dev*, *12*(9), 1348-1355. https://www.ncbi.nlm.nih.gov/pmc/articles/PMC316767/pdf/x13.pdf

Herman, C., Thevenet, D., D'Ari, R., & Bouloc, P. (1995). Degradation of sigma 32, the heat shock regulator in *Escherichia coli*, is governed by HflB. *Proc Natl Acad Sci U S A*, *92*(8), 3516-3520.

Hershko, A., & Ciechanover, A. (1982). Mechanisms of Intracellular Protein Breakdown. *Annu Rev Biochem*, *51*(1), 335-364. https://doi.org/10.1146/annurev.bi.51.070182.002003

Inobe, T., Fishbain, S., Prakash, S., & Matouschek, A. (2011). Defining the geometry of the two-component proteasome degron. *Nature Chemical Biology*, *7*(3), 161-167. https://doi.org/10.1038/nchembio.521

Jencks, W. P. (1975). Binding Energy, Specificity, and Enzymic Catalysis: The Circe Effect. In *Advances in Enzymology and Related Areas of Molecular Biology* (pp. 219-410). https://doi.org/https://doi.org/10.1002/9780470122884.ch4

Katz, C., & Ron, E. Z. (2008). Dual role of FtsH in regulating lipopolysaccharide biosynthesis in *Escherichia coli. J Bacteriol*, *190*(21), 7117-7122. https://doi.org/10.1128/jb.00871-08

Keiler, K. C., Waller, P. R., & Sauer, R. T. (1996). Role of a peptide tagging system in degradation of proteins synthesized from damaged messenger RNA. *Science*, *271*(5251), 990-993. http://science.sciencemag.org/content/271/5251/990.long

Kenniston, J. A., Baker, T. A., Fernandez, J. M., & Sauer, R. T. (2003). Linkage between ATP consumption and mechanical unfolding during the protein processing reactions of an AAA+ degradation machine. *Cell*, *114*(4), 511-520.

Khan, Y. A., White, K. I., & Brunger, A. T. (2021). The AAA+ superfamily: a review of the structural and mechanistic principles of these molecular machines. *Critical Reviews in Biochemistry and Molecular Biology*, 1-32. https://doi.org/10.1080/10409238.2021.1979460

Kihara, A., Akiyama, Y., & Ito, K. (1995). FtsH is required for proteolytic elimination of uncomplexed forms of SecY, an essential protein translocase subunit. *Proc Natl Acad Sci U S A, 92*(10), 4532-4536.

Kihara, A., Akiyama, Y., & Ito, K. (1996). A protease complex in the *Escherichia coli* plasma membrane: HflKC (HflA) forms a complex with FtsH (HflB), regulating its proteolytic activity against SecY. *Embo j, 15*(22), 6122-6131. https://www.ncbi.nlm.nih.gov/pmc/articles/PMC452433/pdf/emboj00022-0118.pdf

Kihara, A., Akiyama, Y., & Ito, K. (1997). Host regulation of lysogenic decision in bacteriophage lambda: transmembrane modulation of FtsH (HflB), the cII degrading protease, by HflKC (HflA). *Proc Natl Acad Sci U S A, 94*(11), 5544-5549. https://www.ncbi.nlm.nih.gov/pmc/articles/PMC20815/pdf/pq005544.pdf

Kihara, A., Akiyama, Y., & Ito, K. (1998). Different pathways for protein degradation by the FtsH/HflKC membrane-embedded protease complex: an implication from the interference by a mutant form of a new substrate protein, YccA. *J Mol Biol, 279*(1), 175-188. https://doi.org/10.1006/jmbi.1998.1781

Kihara, A., Akiyama, Y., & Ito, K. (1999). Dislocation of membrane proteins in FtsH-mediated proteolysis. *Embo j, 18*(11), 2970-2981. https://doi.org/10.1093/emboj/18.11.2970

Kobiler, O., Rokney, A., & Oppenheim, A. B. (2007). Phage lambda CIII: a protease inhibitor regulating the lysis-lysogeny decision. *PLoS One, 2*(4), e363. https://doi.org/10.1371/journal.pone.0000363

Koodathingal, P., Jaffe, N. E., Kraut, D. A., Prakash, S., Fishbain, S., Herman, C., & Matouschek, A. (2009). ATP-dependent Proteases Differ Substantially in Their Ability to Unfold Globular Proteins. *J Biol Chem*, *284*(28), 18674-18684. https://doi.org/10.1074/jbc.M900783200

Krzywda, S., Brzozowski, A. M., Verma, C., Karata, K., Ogura, T., & Wilkinson, A. J. (2002). The crystal structure of the AAA domain of the ATP-dependent protease FtsH of *Escherichia coli* at 1.5 A resolution. *Structure*, *10*(8), 1073-1083.

Langklotz, S., Baumann, U., & Narberhaus, F. (2012). Structure and function of the bacterial AAA protease FtsH. *Biochim Biophys Acta*, *1823*(1), 40-48. https://doi.org/10.1016/j.bbamcr.2011.08.015

Leonhard, K., Herrmann, J. M., Stuart, R. A., Mannhaupt, G., Neupert, W., & Langer, T. (1996). AAA proteases with catalytic sites on opposite membrane surfaces comprise a proteolytic system for the ATP-dependent degradation of inner membrane proteins in mitochondria. *Embo j*, *15*(16), 4218-4229.

Lindahl, M., Spetea, C., Hundal, T., Oppenheim, A. B., Adam, Z., & Andersson, B. (2000). The thylakoid FtsH protease plays a role in the light-induced turnover of the photosystem II D1 protein. *Plant Cell*, *12*(3), 419-431. https://doi.org/10.1105/tpc.12.3.419

Lindahl, M., Tabak, S., Cseke, L., Pichersky, E., Andersson, B., & Adam, Z. (1996). Identification, characterization, and molecular cloning of a homologue of the bacterial FtsH protease in chloroplasts of higher plants. *J Biol Chem*, *271*(46), 29329-29334. https://doi.org/10.1074/jbc.271.46.29329

Lindemann, C., Thomanek, N., Kuhlmann, K., Meyer, H. E., Marcus, K., & Narberhaus, F. (2018). Next-Generation Trapping of Protease Substrates by Label-Free Proteomics. *Methods Mol Biol*, *1841*, 189-206. https://doi.org/10.1007/978-1-4939-8695-8_14

Liu, W., Schoonen, M., Wang, T., McSweeney, S., & Liu, Q. (2022). Cryo-EM structure of transmembrane AAA+ protease FtsH in the ADP state. *Commun Biol*, *5*(1), 257. https://doi.org/10.1038/s42003-022-03213-2

López-Otín, C., & Bond, J. S. (2008). Proteases: multifunctional enzymes in life and disease. *J Biol Chem*, *283*(45), 30433-30437. https://doi.org/10.1074/jbc.R800035200

Ma, C., Wang, C., Luo, D., Yan, L., Yang, W., Li, N., & Gao, N. (2022). Structural insights into the membrane microdomain organization by SPFH family proteins. *Cell Res*, *32*(2), 176-189. https://doi.org/10.1038/s41422-021-00598-3

Mahmoud, S. A., & Chien, P. (2018). Regulated Proteolysis in Bacteria. *Annu Rev Biochem*, *87*, 677-696. https://doi.org/10.1146/annurev-biochem-062917-012848

Moore, S. D., & Sauer, R. T. (2007). The tmRNA system for translational surveillance and ribosome rescue. *Annu Rev Biochem*, *76*, 101-124. https://doi.org/10.1146/annurev.biochem.75.103004.142733

Nakai, T., Yasuhara, T., Fujiki, Y., & Ohashi, A. (1995). Multiple genes, including a member of the AAA family, are essential for degradation of unassembled subunit 2 of cytochrome c oxidase in yeast mitochondria. *Mol Cell Biol*, *15*(8), 4441-4452. https://doi.org/10.1128/mcb.15.8.4441

Obrist, M., Milek, S., Klauck, E., Hengge, R., & Narberhaus, F. (2007). Region 2.1 of the *Escherichia coli* heat-shock sigma factor RpoH (sigma32) is necessary but not sufficient for degradation by the FtsH protease. *Microbiology (Reading)*, *153*(Pt 8), 2560-2571. https://doi.org/10.1099/mic.0.2007/007047-0

Obrist, M., & Narberhaus, F. (2005). Identification of a turnover element in region 2.1 of *Escherichia coli* sigma32 by a bacterial one-hybrid approach. *J Bacteriol*, *187*(11), 3807-3813. https://doi.org/10.1128/jb.187.11.3807-3813.2005

Ogura, T., Inoue, K., Tatsuta, T., Suzaki, T., Karata, K., Young, K., Su, L. H., Fierke, C. A., Jackman, J. E., Raetz, C. R., Coleman, J., Tomoyasu, T., & Matsuzawa, H. (1999). Balanced biosynthesis of major membrane components through regulated degradation of the committed enzyme of lipid A biosynthesis by the AAA protease FtsH (HflB) in *Escherichia coli. Mol Microbiol*, *31*(3), 833-844. http://onlinelibrary.wiley.com/store/10.1046/j.1365-2958.1999.01221.x/asset/j.1365-2958.1999.01221.x.pdf?v=1&t=j3yyjd2b&s=c46c4bad88fbdbada172d0dbecb9584baa1ead8d

Ogura, T., Tomoyasu, T., Yuki, T., Morimura, S., Begg, K. J., Donachie, W. D., Mori, H., Niki, H., & Hiraga, S. (1991). Structure and function of the ftsH gene in *Escherichia coli. Res Microbiol*, *142*(2-3), 279-282.

Okuno, T., Yamanaka, K., & Ogura, T. (2006a). An AAA protease FtsH can initiate proteolysis from internal sites of a model substrate, apo-flavodoxin. *Genes Cells*, *11*(3), 261-268. https://doi.org/10.1111/j.1365-2443.2006.00940.x

Okuno, T., Yamanaka, K., & Ogura, T. (2006b). Flavodoxin, a new fluorescent substrate for monitoring proteolytic activity of FtsH lacking a robust unfolding activity. *J Struct Biol*, *156*(1), 115-119. https://doi.org/10.1016/j.jsb.2006.02.001

Opalińska, M., & Jańska, H. (2018). AAA Proteases: Guardians of Mitochondrial Function and Homeostasis. *Cells*, *7*(10). https://doi.org/10.3390/cells7100163

Parsell, D. A., Silber, K. R., & Sauer, R. T. (1990). Carboxy-terminal determinants of intracellular protein degradation. *Genes Dev*, *4*(2), 277-286. https://doi.org/10.1101/gad.4.2.277

Patron, M., Sprenger, H. G., & Langer, T. (2018). m-AAA proteases, mitochondrial calcium homeostasis and neurodegeneration. *Cell Res*, *28*(3), 296-306. https://doi.org/10.1038/cr.2018.17

Prakash, S., Tian, L., Ratliff, K. S., Lehotzky, R. E., & Matouschek, A. (2004). An unstructured initiation site is required for efficient proteasome-mediated degradation. *Nat Struct Mol Biol*, *11*(9), 830-837. https://doi.org/10.1038/nsmb814

Puchades, C., Ding, B., Song, A., Wiseman, R. L., Lander, G. C., & Glynn, S. E. (2019). Unique Structural Features of the Mitochondrial AAA+ Protease AFG3L2 Reveal the Molecular Basis for Activity in Health and Disease. *Mol Cell*, *75*(5), 1073-1085.e1076. https://doi.org/10.1016/j.molcel.2019.06.016

Puchades, C., Rampello, A. J., Shin, M., Giuliano, C. J., Wiseman, R. L., Glynn, S. E., & Lander, G. C. (2017). Structure of the mitochondrial inner membrane AAA+ protease YME1 gives insight into substrate processing. *Science*, *358*(6363). https://doi.org/10.1126/science.aao0464

Rawlings, N. D., & Barrett, A. J. (2004). 67 - Introduction: metallopeptidases and their clans. In A. J. Barrett, N. D. Rawlings, & J. F. Woessner (Eds.), *Handbook of Proteolytic Enzymes (Second Edition)* (pp. 231-267). Academic Press. https://doi.org/https://doi.org/10.1016/B978-0-12-079611-3.50075-6

Rodriguez, F., Arsène-Ploetze, F., Rist, W., Rüdiger, S., Schneider-Mergener, J., Mayer, M. P., & Bukau, B. (2008). Molecular basis for regulation of the heat shock transcription factor sigma32 by the DnaK and DnaJ chaperones. *Mol Cell*, *32*(3), 347-358. https://doi.org/10.1016/j.molcel.2008.09.016

Saikawa, N., Akiyama, Y., & Ito, K. (2004). FtsH exists as an exceptionally large complex containing HflKC in the plasma membrane of *Escherichia coli. J Struct Biol*, *146*(1-2), 123-129. https://doi.org/10.1016/j.jsb.2003.09.020

Sauer, R. T., & Baker, T. A. (2011). AAA+ proteases: ATP-fueled machines of protein destruction. *Annu Rev Biochem*, *80*, 587-612. https://doi.org/10.1146/annurev-biochem-060408-172623

Sauer, R. T., Fei, X., Bell, T. A., & Baker, T. A. (2021). Structure and function of ClpXP, a AAA+ proteolytic machine powered by probabilistic ATP hydrolysis. *Critical Reviews in Biochemistry and Molecular Biology*, 1-17. https://doi.org/10.1080/10409238.2021.1979461

Saunders, R. A., Stinson, B. M., Baker, T. A., & Sauer, R. T. (2020). Multistep substrate binding and engagement by the AAA+ ClpXP protease. *Proc Natl Acad Sci U S A*, *117*(45), 28005-28013. https://doi.org/10.1073/pnas.2010804117

Schäkermann, M., Langklotz, S., & Narberhaus, F. (2013). FtsH-mediated coordination of lipopolysaccharide biosynthesis in *Escherichia coli* correlates with the growth rate and the alarmone (p)ppGpp. *J Bacteriol*, *195*(9), 1912-1919. https://doi.org/10.1128/JB.02134-12

Scharfenberg, F., Serek-Heuberger, J., Coles, M., Hartmann, M. D., Habeck, M., Martin, J., Lupas, A. N., & Alva, V. (2015). Structure and evolution of N-domains in AAA metalloproteases. *J Mol Biol*, *427*(4), 910-923. https://doi.org/10.1016/j.jmb.2014.12.024

Schoenheimer, R. a. T. C., Hans (1942). *The Dynamic State of Body Constituents*. Harvard university press.

Shi, H., Rampello, A. J., & Glynn, S. E. (2016). Engineered AAA+ proteases reveal principles of proteolysis at the mitochondrial inner membrane. *Nat Commun*, *7*, 13301. https://doi.org/10.1038/ncomms13301

Shotland, Y., Koby, S., Teff, D., Mansur, N., Oren, D. A., Tatematsu, K., Tomoyasu, T., Kessel, M., Bukau, B., Ogura, T., & Oppenheim, A. B. (1997). Proteolysis of the phage lambda CII regulatory protein by FtsH (HflB) of *Escherichia coli. Mol Microbiol*, *24*(6), 1303-1310. https://doi.org/10.1046/j.1365-2958.1997.4231796.x

Shotland, Y., Shifrin, A., Ziv, T., Teff, D., Koby, S., Kobiler, O., & Oppenheim, A. B. (2000). Proteolysis of bacteriophage lambda CII by *Escherichia coli* FtsH (HflB). *J Bacteriol*, *182*(11), 3111-3116. https://doi.org/10.1128/jb.182.11.3111-3116.2000

Straus, D., Walter, W., & Gross, C. A. (1990). DnaK, DnaJ, and GrpE heat shock proteins negatively regulate heat shock gene expression by controlling the synthesis and stability of sigma 32. *Genes Dev*, *4*(12a), 2202-2209. https://doi.org/10.1101/gad.4.12a.2202

Tatsuta, T., Tomoyasu, T., Bukau, B., Kitagawa, M., Mori, H., Karata, K., & Ogura, T. (1998). Heat shock regulation in the ftsH null mutant of *Escherichia coli*: dissection of stability and activity control mechanisms of sigma32 in vivo. *Mol Microbiol*, *30*(3), 583-593. https://doi.org/10.1046/j.1365-2958.1998.01091.x

Tomoyasu, T., Gamer, J., Bukau, B., Kanemori, M., Mori, H., Rutman, A. J., Oppenheim, A. B., Yura, T., Yamanaka, K., Niki, H., & et al. (1995). *Escherichia coli* FtsH is a membrane-bound, ATP-dependent protease which degrades the heat-shock transcription factor sigma 32. *Embo j*, *14*(11), 2551-2560. https://www.ncbi.nlm.nih.gov/pmc/articles/PMC398369/pdf/emboj00035-0161.pdf

Tomoyasu, T., Yuki, T., Morimura, S., Mori, H., Yamanaka, K., Niki, H., Hiraga, S., & Ogura, T. (1993). The *Escherichia coli* FtsH protein is a prokaryotic member of a protein family of putative ATPases involved in membrane functions, cell cycle control, and gene expression. *J Bacteriol*, *175*(5), 1344-1351. http://jb.asm.org/content/175/5/1344.full.pdf

Warshel, A., Naray-Szabo, G., Sussman, F., & Hwang, J. K. (1989). How do serine proteases really work? *Biochemistry*, *28*(9), 3629-3637. https://doi.org/10.1021/bi00435a001

Westphal, K., Langklotz, S., Thomanek, N., & Narberhaus, F. (2012). A trapping approach reveals novel substrates and physiological functions of the essential protease FtsH in *Escherichia coli*. *J Biol Chem*, *287*(51), 42962-42971. https://doi.org/10.1074/jbc.M112.388470

Yang, Y., Guo, R., Gaffney, K., Kim, M., Muhammednazaar, S., Tian, W., Wang, B., Liang, J., & Hong, H. (2018). Folding-Degradation Relationship of a Membrane Protein Mediated by the

Universally Conserved ATP-Dependent Protease FtsH. *J Am Chem Soc*, *140*(13), 4656-4665. https://doi.org/10.1021/jacs.8b00832

Zhang, S., & Mao, Y. (2020). AAA+ ATPases in Protein Degradation: Structures, Functions and Mechanisms. *Biomolecules*, *10*(4), 629. https://www.mdpi.com/2218-273X/10/4/629

Chapter II

FtsH degrades DHFR by recognizing a folding intermediate

This chapter is being prepared for publication with Tania A. Baker and Robert T. Sauer as coauthors. I did all of the experiments and the majority of the writing.

ABSTRACT

AAA+ proteolytic machines play essential roles in maintaining and rebalancing the cellular proteome in response to stress, developmental cues, and environmental changes. Of the five AAA+ proteases in *E. coli*, FtsH is unique in its attachment to the inner membrane and its function in degrading both membrane and cytosolic proteins. *E. coli* DHFR is a stable and biophysically well-characterized protein, which a previous study found resisted FtsH degradation *in vitro* despite the presence of an ssrA degron. By contrast, we find that FtsH degrades DHFR fused to a long peptide linker and ssrA tag. Surprisingly, we find that FtsH also degrades DHFR with shorter linkers and an ssrA tag, and without any linker or tag. Thus, FtsH must be able to recognize a sequence element or elements within DHFR. We find that FtsH degradation of DHFR is noncanonical in the sense that it does not rely upon recognition of an unstructured polypeptide at or near the N-terminus or C-terminus of the substrate. Results using peptide-array experiments, mutant DHFR proteins, and fusion proteins suggest that FtsH recognizes an internal sequence in a species of DHFR that is partially unfolded. Overall, our findings provide insight into substrate recognition by FtsH and indicate that its degradation capacity is broader than previously reported.

INTRODUCTION

Intracellular proteases enforce protein quality control and sculpt the cellular proteome in response to environmental stresses and changing nutritional landscapes. Within bacteria, most targeted proteolysis is carried out by proteases that belong to the AAA+ family (<u>A</u>TPases <u>A</u>ssociated with various cellular <u>A</u>ctivities) (Sauer & Baker, 2011). These proteases contain ring-shaped AAA+ hexamers that use the energy of ATP hydrolysis to mechanically unfold specific protein substrates and then translocate the unfolded polypeptide through a central channel and into an associated and sequestered degradation chamber for proteolysis. Initiation of degradation requires specific recognition of the substrate, usually by binding to a sequence-specific peptide recognition tag, called a degron. Degradation also requires engagement of an unstructured segment of substrate polypeptide, which can be the degron itself or another region, within the axial channel of the AAA+ ring (Varshavsky, 1991; Prakash et al., 2004; Inobe et al., 2011; Mahmoud & Chien, 2018; Fei et al., 2020; Saunders et al., 2020; Izert et al., 2021; Sauer et al., 2021).

Escherichia coli encodes five AAA+ proteases: FtsH, ClpXP, ClpAP, Lon, and HslUV (Sauer et al., 2004). The membrane-bound FtsH protease is the only member of this enzyme family essential for *E. coli* growth (Ogura et al., 1991). Starting at the N-terminus, each subunit of the FtsH homohexamer consists of a transmembrane helix, a periplasmic domain, a second transmembrane helix, a AAA unfoldase module, and a zinc metallopeptidase domain (Fig. 2.1) (Langklotz et al., 2012). The unfoldase and peptidase components, which constitute the proteolytic machinery of FtsH, reside on the cytoplasmic side of the inner membrane and play important roles in membrane-protein quality control and the degradation of some cytosolic proteins (Ito & Akiyama, 2005; Bittner et al., 2017). Well-characterized membrane substrates of FtsH include proteins that are

synthesized in excess of their usual partners, such as SecY of the SecYEG complex and subunit *a* of the F_oF_1-ATP synthase (Kihara et al., 1995; Akiyama et al., 1996). Cytosolic substrates of FtsH include LpxC, an essential enzyme required for lipopolysaccharide biosynthesis and maintenance of proper ratios of outer-membrane lipid components, as well as transcription factors, such as the RpoH heat-shock σ factor and the phage λ cII protein (Banuett et al., 1986; Cheng et al., 1988; Herman et al., 1993; Kihara et al., 1997; Shotland et al., 1997; Ogura et al., 1999; Schäkermann et al., 2013).

FtsH employs diverse modes of substrate recognition. The C-terminal sequences of LpxC, λ cII, and the ssrA tag, which is added to nascent polypeptides during ribosome rescue, contain degrons sufficient to target proteins for FtsH degradation (Keiler et al., 1996; Gottesman et al., 1998; Herman et al., 1998; Kobiler et al., 2002; Fuhrer et al., 2007; Hari & Sauer, 2016). N-terminal sequences of some known substrates can also direct FtsH recognition, as observed for the Ycca, YfgM, ExbD, and YlaC membrane proteins (Bittner et al., 2015; Yang et al., 2018). It has also been proposed that FtsH recognition of some of these membrane protein substrates is sequence-independent and only requires a ~20 residue cytosolic extension (Chiba et al., 2000). Finally, FtsH degradation of RpoH appears to depend on internal sequence elements as well as on interactions with the DnaK and DnaJ chaperones (Straus et al., 1990; Obrist & Narberhaus, 2005; Obrist et al., 2007; Rodriguez et al., 2008).

Based on biochemical studies of degron-tagged model proteins, FtsH was found to degrade a variety of meta-stable proteins but not to degrade *E. coli* dihydrofolate reductase (DHFR) or other stable substrates, unless these latter proteins were destabilized by mutation or circular permutation

(Herman et al., 2003). These results suggested that FtsH is a weak protein unfoldase, a property that could contribute to substrate selection *in vivo*. However, the idea that FtsH lacks robust unfoldase activity seems inconsistent with its ability to extract and degrade integral membrane proteins, which requires a substantial enzyme-generated force (Yang et al., 2018). In thinking about this apparent paradox, we reasoned that the location of the FtsH axial channel, which faces the membrane, might require a sufficiently long segment of unfolded polypeptide between a protein and degron to allow recognition and engagement of soluble substrates (Fig. 2.1). By this model, FtsH would only degrade metastable substrates, which unfold completely or partially to generate an accessible degron (Fig. 2.1, inset), or degrade stable substrates with a degron within an extended unstructured tail.
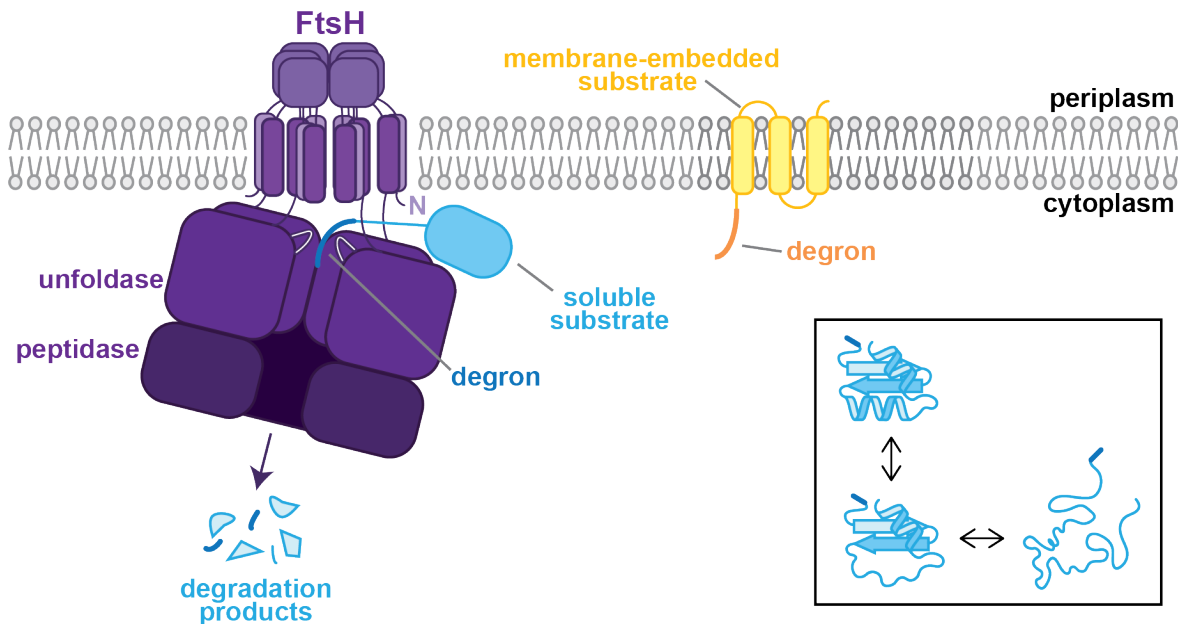

Figure 2.1. FtsH degrades membrane proteins and cytosolic proteins. The *E. coli* FtsH protease is anchored to the inner membrane and degrades cytosolic proteins (blue) and membrane proteins (yellow). Each FtsH subunit contains a periplasmic N-terminal domain, two transmembrane helices, and cytoplasmic AAA unfoldase and zinc metallopeptidase domains (colored from N to C-terminus in light to dark purple). The cut-away view of the cytoplasmic portion of FtsH shows it pulling on the degron tail (blue) of a soluble substrate using conserved pore loops (white) to apply an unfolding force. After unfolding, the substrate is translocated

through the axial channel and into the peptidase compartment for degradation. **Inset (box)**. A soluble protein (light blue) with a terminal degron (blue) is shown in three equilibrium states: a folded or native state (top), a partially unfolded intermediate state (bottom left), and a globally unfolded state (bottom right).

To test this model, we added ssrA tails of various lengths, composed of an unstructured polypeptide linker and an ssrA degron, to the C-terminus of DHFR and tested FtsH-dependent degradation. Indeed, a DHFR tail variant with a long linker and ssrA degron was degraded by FtsH. Surprisingly, however, DHFR-ssrA variants with shorter linkers or no linker were also degraded. Most surprisingly, FtsH degraded DHFR with no appended ssrA degron. We then explored potential mechanisms by which FtsH might recognize untagged DHFR. Our results indicate that FtsH can recognize an internal sequence in DHFR, which becomes accessible in a partially structured folding/unfolding intermediate that is populated under the conditions of our degradation reactions. In contrast to most substrates of AAA+ proteases, DHFR sequences near either its N- or C-terminus appear to play little role in FtsH recognition. We discuss the implications of these findings in terms of the role of FtsH in degradation of membrane and cytoplasmic proteins and in light of recent insights into FtsH structure from cryo-EM structural studies.

RESULTS

FtsH degrades *E. coli* DHFR with linker/degron containing tails.

We chose *E. coli* DHFR as a model protein for several reasons. First, DHFR is well characterized in terms of its structure, thermodynamic and kinetic stability, dynamics, and the effects of mutations on these properties (Rood & Williams, 1981; Touchette et al., 1986; Bystroff & Kraut, 1991). Second, prior studies reported that DHFR with a C-terminal ssrA degron was not degraded by FtsH (Herman et al., 2003), allowing us to test if extending the linker between DHFR and the

ssrA tag might allow degradation. Third, the inhibitor methotrexate (MTX) stabilizes DHFR and prevents or dramatically slows degradation by AAA+ proteases, and therefore provides a useful reagent for probing degradation mechanisms (Touchette et al., 1986; Bystroff & Kraut, 1991; Lee et al., 2001). We refer to unliganded DHFR as apo-DHFR and MTX-bound DHFR as MTX-DHFR.

As shown in Fig. 2.2A, we appended ssrA-containing tails of different lengths to the C-terminus of DHFR. For example, our first variant called DHFR-ssrA[60], contained a 49-residue linker plus the 11-residue ssrA tag (60 residues total). We anticipated that FtsH would bind and translocate the extended tail of this substrate at least until it reached the native DHFR domain. Then, we expected the release of a truncated degradation product consisting of undegraded DHFR with a portion of the 60-residue tail attached as an extension, as observed in similar experiments with other AAA+ proteases (Lee et al., 2001).

Indeed, we observed this outcome in degradation reactions in the presence of MTX as assayed by SDS-PAGE (Fig. 2.2B, left panel). Specifically, degradation of 20 µM substrate by 1 µM FtsH for 120 min resulted in two product bands slightly smaller than full-length DHFR-ssrA[60], as well as undegraded substrate. Comparison with standards containing DHFR with ssrA tails of different lengths suggested that the undegraded extensions in the partial degradation products were 28 and 39 residues long, respectively. Based on the size of the enzyme, most of the 28-residue extension C-terminal to the DHFR domain is likely to have been within the FtsH channel or protease chamber when degradation stopped, suggesting that the native portion of MTX-bound DHFR in the product is pulled against the opening to the FtsH channel. We then assayed the kinetics of degradation of DHFR-ssrA[60] by FtsH in the absence of MTX (Fig. 2.2B, right panel). To our surprise, FtsH

degraded the entire DHFR-ssrA^{60} protein as judged by the absence of partial degradation fragments at the 60-min time point, when little of the original substrate remained.
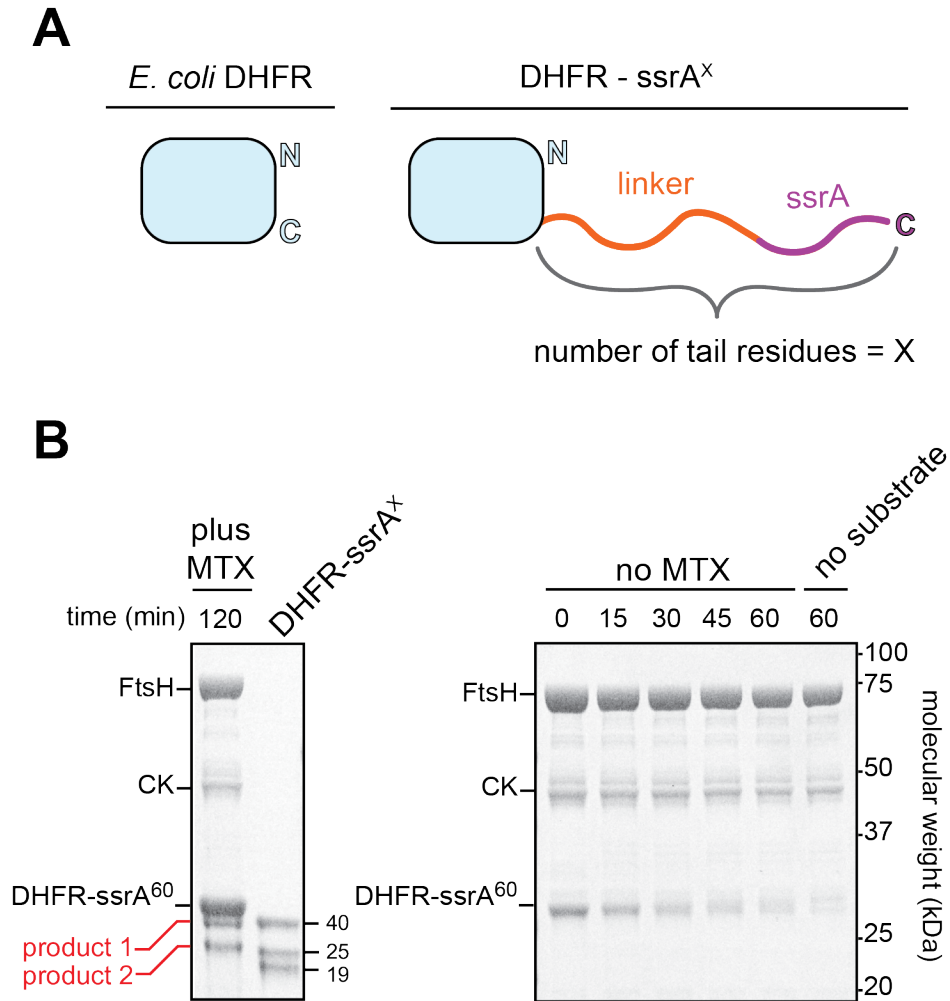

Figure 2.2. FtsH degrades DHFR-ssrA^{60}. *A,* Cartoon depiction of DHFR with the N- and C-termini indicated (left) and of DHFR with a C-terminal tail consisting of linker (orange) and ssrA tag (purple; right). *B,* SDS-PAGE of degradation assays. The left lane of the left panel shows DHFR-ssrA^{60} (20 µM) incubated for 120 min at 42 °C with FtsH$_6$ (1 µM), ATP, a creatine kinase regeneration mix (CK), and MTX (100 µM). The right lane shows DHFR-ssrA^{40}, DHFR-ssrA^{25}, and DHFR^{19} standards (5 µM each). The right panel shows DHFR-ssrA^{60} (4 µM) incubated with FtsH$_6$ (1 µM), ATP, and a creatine-kinase based regeneration mix (CK), for different times at 42 °C in the absence of MTX. The rightmost lane shows a control without DHFR-ssrA^{60}. For both panels, the gel shown is representative of two independent experiments.

FtsH degrades untagged DHFR similarly to degron-tagged DHFR variants.

We anticipated from our original model that FtsH would fail to degrade variants when the ssrA-tail reached some minimum length, below the required engagement length (Fig 2.1). However, as assayed by SDS-PAGE, FtsH degraded variants with tails shorter than 60 residues – including DHFR-ssrA[40], DHFR-ssrA[19], and DHFR-ssrA[11] – and even degraded untagged DHFR (Fig. 2.3A). Although untagged DHFR had been included as a negative control in this experiment, we were surprised to find that it was degraded at a rate similar to some degron-tagged variants in the SDS-PAGE degradation experiments.

Next, we tested the possibility that FtsH might degrade some of the ssrA-tailed DHFR substrates with substantially different steady-state kinetic parameters. For these experiments, we labeled the only solvent-exposed cysteine residue of DHFR, Cys[152], with a maleimide-fluorophore and used time-dependent increases in acid-soluble fluorescent peptides as an assay for the rate of FtsH degradation of DHFR-ssrA[40], DHFR-ssrA[19], DHFR-ssrA[11], and untagged DHFR. Fig. 2.3B shows the linear time-dependent increase in acid-soluble fluorescent peptides for FtsH degradation of 16 µM DHFR-ssrA[11]. This degradation was prevented or greatly slowed when FtsH was omitted from the assay, when methotrexate was added to stabilize DHFR, or in the presence of actinonin, a small molecule that inhibits the peptidase activity of FtsH (Fig. 2.3B) (Amberg-Johnson et al., 2017).

We determined K_M and k_{deg} for degradation of untagged DHFR or different ssrA-tagged DHFR variants by measuring degradation rates as a function of substrate concentration and fitting the results to the Michaelis-Menten equation (Fig. 2.3C, left panel). Although these values varied within a ~2-fold range between different substrates, the only trend was that the two shortest

proteins, untagged DHFR and DHFR-ssrA[11], were degraded somewhat faster at saturating substrate concentrations. Overall, however, FtsH degraded untagged DHFR, DHFR-ssrA[11], DHFR-ssrA[19], and DHFR-ssrA[40] with similar degradation parameters (Fig. 2.3C, right panel), indicating that the addition of an ssrA-tail does not significantly increase the degradation rate of untagged DHFR.
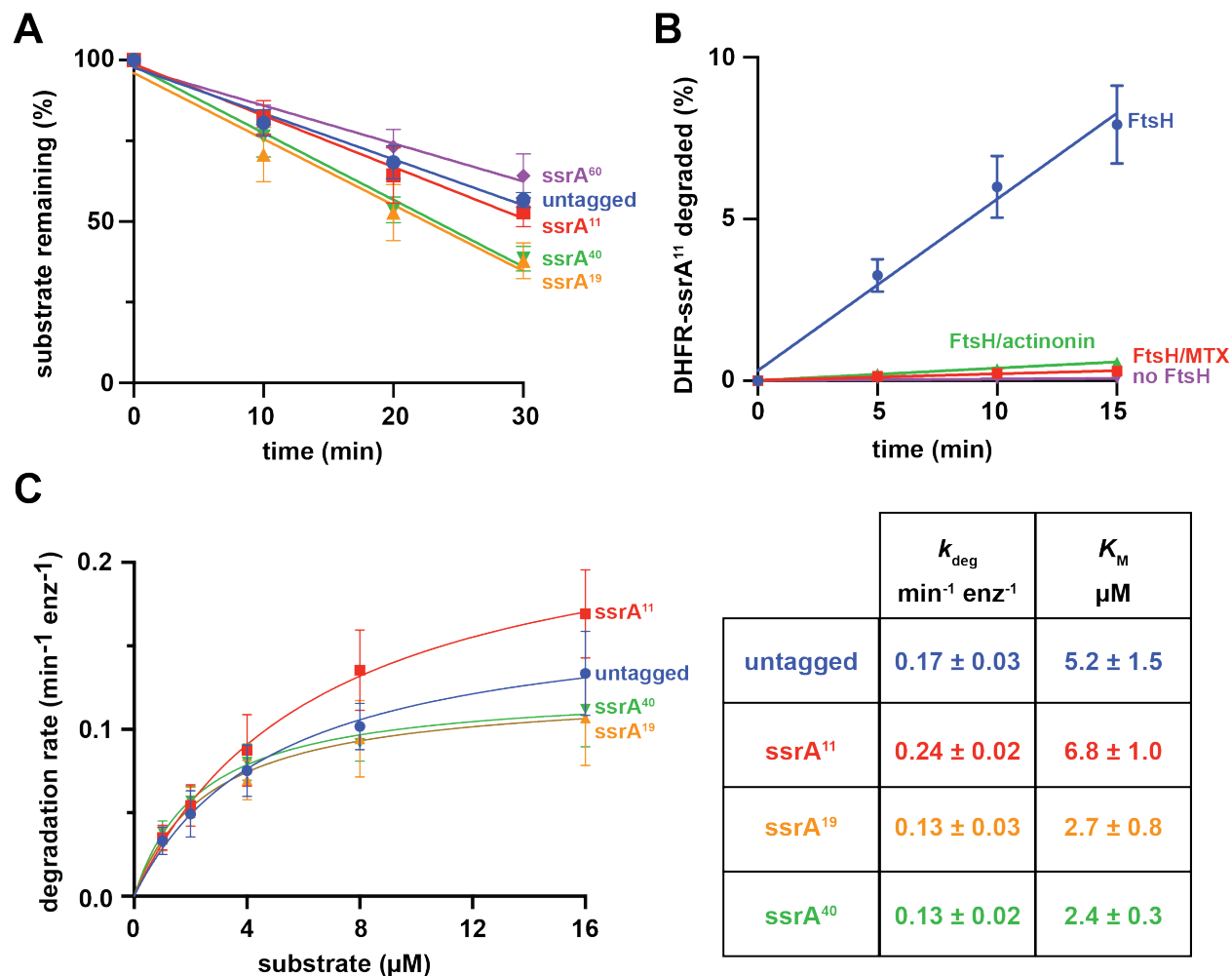

	k_{deg} min^{-1} enz^{-1}	K_M μM
untagged	0.17 ± 0.03	5.2 ± 1.5
ssrA[11]	0.24 ± 0.02	6.8 ± 1.0
ssrA[19]	0.13 ± 0.03	2.7 ± 0.8
ssrA[40]	0.13 ± 0.02	2.4 ± 0.3

Figure 2.3. FtsH degradation of DHFR constructs. *A,* Rates of FtsH$_6$ (1 μM) degradation of untagged DHFR or different DHFR-ssrA tail variant proteins (5 μM each) at 42 °C. Values are means (n ≥ 3) ± 1 SD, and lines are linear least square fits. *B,* Fluorophore-labelled DHFR-ssrA[11] (16 μM) was incubated with FtsH$_6$ (0.5 μM), ATP, and a creatine-kinase based regeneration mix at 37 °C, and degradation kinetics were monitored by measuring the fluorescence of acid-soluble peptides released. Experiments are also shown in the presence of the actinonin inhibitor (10 μM), methotrexate (125 μM), or the absence of FtsH. *C,* (left) Rates of FtsH$_6$ degradation of different concentrations of untagged DHFR or the various DHFR-ssrA tail variant proteins at 37 °C. Values

are means (n ≥ 3) ± 1 SD. Lines represents non-linear least squares fits to the Michaelis-Menten equation. (right) Average k_{deg} and K_M values ± 1 SD from three or four independent experiments.

ATP cost of degradation. Substrates typically alter the rate of ATP hydrolysis by AAA+ proteases (Kenniston et al., 2003). Indeed, near-saturating concentrations of untagged DHFR, DHFR-ssrA[11], DHFR-ssrA[19], or DHRF-ssrA[40] increased the rate of ATP hydrolysis by FtsH by 10-20% (Fig. 2.4). For untagged DHFR as well as the ssrA-tagged variants, these results support our model that these proteins are being engaged, unfolded, and degraded by FtsH. By dividing the substrate-stimulated ATP-hydrolysis rates by the corresponding k_{deg} values for each protein (0.13 to 0.24 min^{-1}), we calculated that 430-890 ATPs are hydrolyzed by FtsH in the time required to bind, unfold, translocate, and degrade one molecule of each DHFR substrate. For comparison, FtsH degradation of the degron-tagged GlpG membrane protein uses 380-550 ATPs ($k_{deg} \approx 0.25$ min^{-1}; Yang et al., 2018) and ClpXP degradation of the titin[27]-ssrA substrate uses ~640 ATPs ($k_{deg} \approx 0.18$ min^{-1}; Kenniston et al., 2003). Hence, the energetic cost of DHFR degradation by FtsH is on par with degradation of other substrates that are degraded at comparably slow rates by either FtsH or ClpXP.
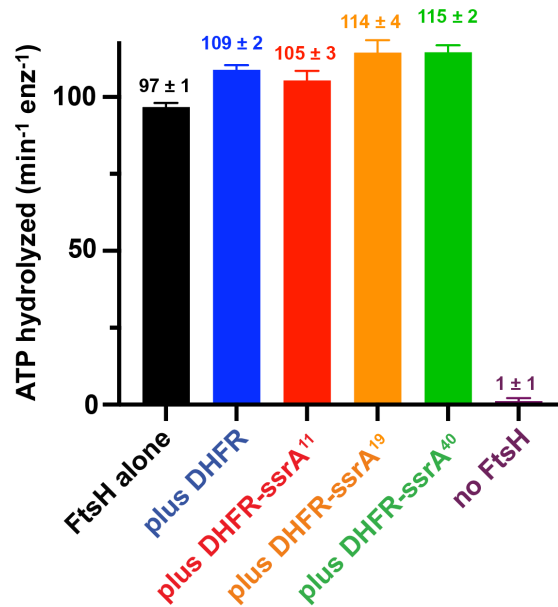
Figure 2.4. **Stimulation of FtsH rates of ATP hydrolysis by substrates.** Rates of ATP hydrolysis at 37 °C by FtsH$_6$ (0.5 µM) were measured in the absence of substrate or presence of untagged or ssrA-tagged DHFR proteins (20 µM each). A control reaction with no FtsH is included to show background. Values are means (n = 3) ± 1 SD.

Which molecular DHFR species does FtsH degrade?

Most substrates of AAA+ proteases have unstructured degrons at or near a terminus, which provide both a specific recognition region and an unstructured peptide segment where the protease initiates the translocation/unfolding cycles required for degradation (Sauer et al., 2004; Sauer & Baker, 2011). However, the terminal residues of native DHFR make interactions that are part of its three-dimensional fold (Bystroff & Kraut, 1991; Sawaya & Kraut, 1997). Thus, it appears unlikely that the termini function as FtsH recognition and/or initiation elements. Moreover, as we show in a subsequent section, the M20 loop of DHFR, which contains the only unstructured residues in apo-DHFR, is not required for FtsH degradation. Hence, native DHFR does not appear to be the species degraded by FtsH. We asked next if globally unfolded DHFR was the molecular species recognized for degradation.

If FtsH only degrades the small population of DHFR molecules that are globally unfolded under equilibrium conditions, then a mutation that increases the thermodynamic stability of native DHFR relative to globally unfolded DHFR should decrease the degradation rate. This model predicts that the A145T mutation, which increases DHFR stability by ~3 kcal/mol (Ohmae et al., 1998), would decrease the equilibrium fraction of unfolded DHFR by a factor of ~100-fold and thus slow FtsH degradation dramatically. By contrast, as shown in Fig. 2.5A, FtsH degraded [A145T]DHFR slightly faster than untagged, wild-type DHFR ([WT]DHFR). We interpret this result as evidence that globally-unfolded DHFR is not the primary FtsH degradation target.

Next, we tested FtsH degradation of two destabilized mutants, [W133V]DHFR and [I155A]DHFR, which are ~4 kcal/mol less stable than the wild-type protein (Ohmae et al., 2001; Arai et al., 2003). FtsH degraded these variants ~3-fold faster than [WT]DHFR (Fig. 2.5B). However, these increased degradation rates would be expected to be substantially larger if FtsH exclusively recognized and degraded globally denatured DHFR. Hence, the rates of FtsH degradation of both stabilized and destabilized variants are inconsistent with a model in which only globally unfolded DHFR is the primary recognition target. Nevertheless, the W133V and I155A mutations appear to increase the equilibrium population of a molecular species that FtsH does recognize and degrade. We note that an ensemble of structural intermediates between fully denatured and fully native DFHR are populated during folding/unfolding (Kuwajima et al., 1991; Heidary et al., 2000; Kasper et al., 2014). For example, Fig. 2.5C shows regions of DHFR that experience more structural fluctuations based on H/D exchange studies (Yamamoto et al., 2004). It seems likely, therefore, that one or more of these partially folded protein species is recognized and degraded by FtsH.
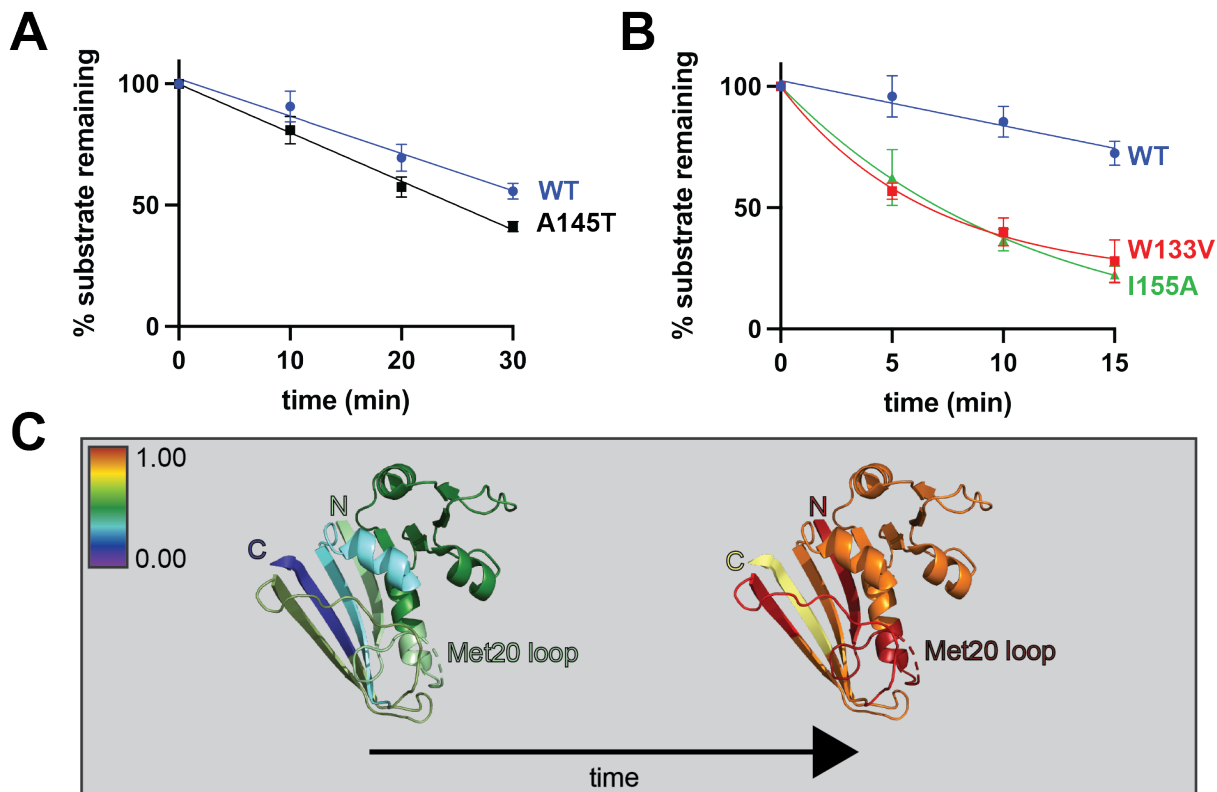
Figure 2.5. Effect of DHFR mutations on FtsH degradation. *A,* [WT]DHFR or [A145T]DHFR (5 µM each) were incubated with $FtsH_6$ (1 µM), ATP, and a creatine-kinase regeneration mix for different times at 42 °C, prior to assessing degradation by SDS-PAGE. The lines are linear least square fits. Data points are means (n ≥ 3) ± 1 SD. *B,* FtsH degradation of [WT]DHFR, [W133V]DHFR, and [I155A]DHFR with conditions as in panel B. A linear least-squares fit is shown for [WT]DHFR and single-exponential fits are shown for [W133V]DHFR and [I155A]DHFR. *C,* Fluctuation map of DHFR with colors of different segments based on the fraction of deuterium incorporation from 0.00 (purple) to 1.00 (dark red) at the beginning (left) and end (right) of the H/D exchange experiment (Yamamoto et al., 2004).

Sequence determinants of DHFR recognition

To investigate potential FtsH binding sites in DHFR, we used ^{35}S-FtsH to probe a peptide microarray consisting of 15-residue DHFR peptides offset from each other by two amino acids (Fig. 2.6A). FtsH bound a group of overlapping peptides from three internal regions of DHFR: residues 19-47 (region 1); residues 43-67 (region 2); and residues 93-117 (region 3) (Figs. 2.6A-2.6C). The DHFR peptides bound by FtsH surround the MTX-binding site in the three-dimensional structure (Fig. 2.6C) and also overlap sequences with high B-factors in the crystal structure of apo-

DHFR (Bystroff & Kraut, 1991; Sawaya & Kraut, 1997; Rajagopalan et al., 2002). The peptide-binding regions also overlap with α-helical regions of DHFR and regions that experience the highest degree of H/D exchange (Fig. 2.5C). Notably, FtsH did not bind to either N- or C-terminal peptides of DHFR.
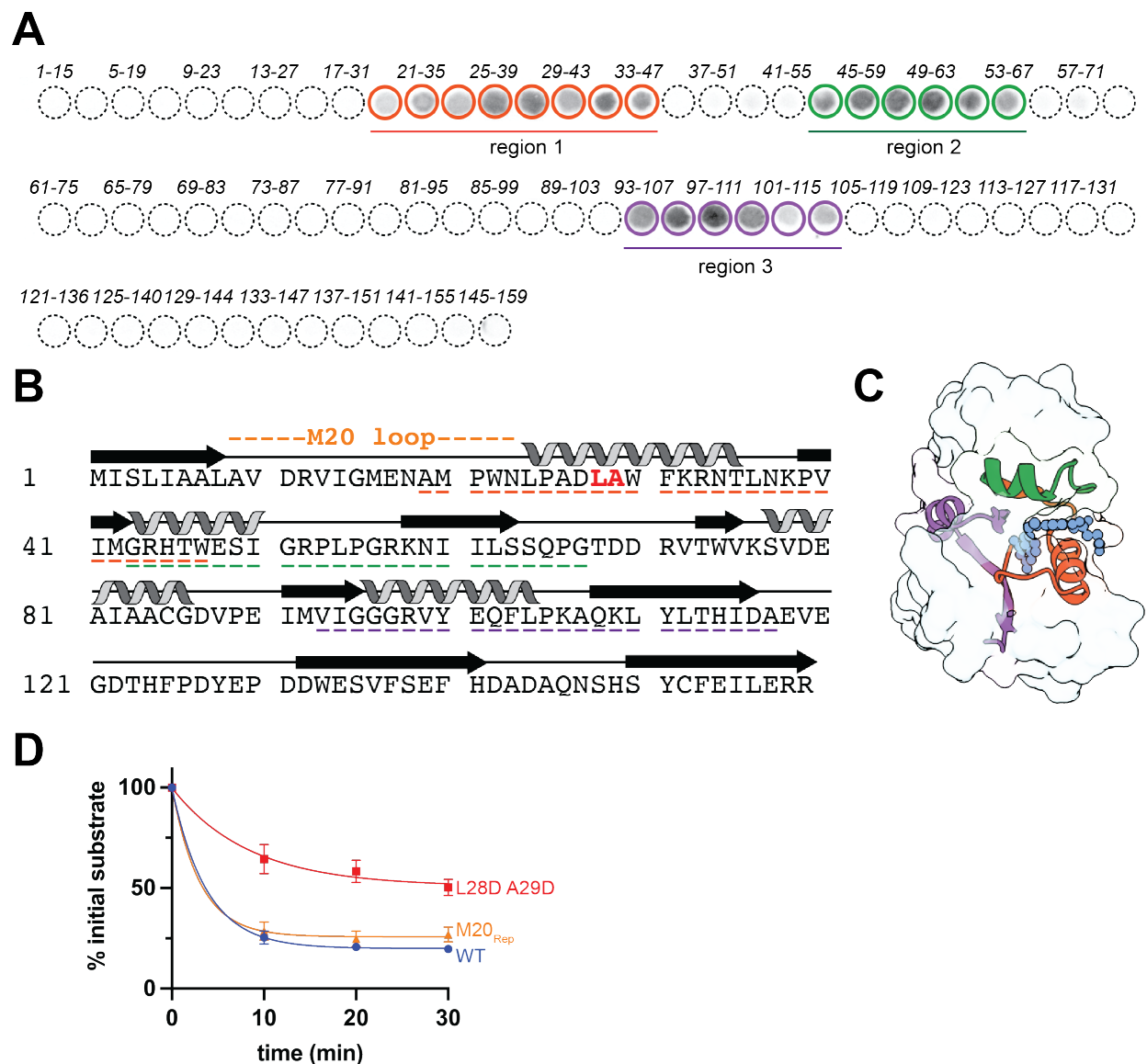

Figure 2.6. Identification of DHFR peptides that bind FtsH. *A,* ^{35}S-FtsH binding detected by autoradiography to an array of *E. coli* DHFR peptides. Each circle represents a 15-residue DHFR peptide (every other spot labeled in italics), with the rightward neighboring spot shifted towards the C-terminus by two amino acids. Circles with solid lines highlight peptides that bound ^{35}S-FtsH.

B, E. coli DHFR sequence and secondary structure. The Met20 (M20) loop is labeled and Leu28 and Ala29 are colored in red. Underlined residues are present in one or more peptide from panel A that bound FtsH. *C, E. coli* DHFR (PDB code 1RG7) is shown as an outlined, transparent surface with methotrexate (blue) shown in ball-and-stick representation. Secondary structural elements in regions 1 (orange), 2 (green), and 3 (purple) are shown in cartoon representation. *D,* FtsH$_6$ (3 μM) degradation of ^{WT}DHFR, M20$_{rep}$ DHFR and $^{L28D/A29D}$DHFR (5 μM each) at 42 °C in the presence of ATP and a creatine-kinase (CK) regeneration mix was monitored by SDS-PAGE. Values are means (n = 3) ± 1 SD; lines are single-exponential fits.

The side chains of Leu^{28} and Ala^{29} are exposed on the surface of the first α-helix in DHFR and are present in the first five peptide spots of region 1 (Figs. 2.6A-2.6C). When we mutated both residues to aspartic acids (L28D/A29D), the rate of FtsH degradation was reduced 2- to 3-fold compared to ^{WT}DHFR (Fig. 2.6D), suggesting that the wild-type side chains at these positions contribute to recognition. However, the modest decrease in degradation also indicates that the full recognition element is more complex. We probed the effects of additional mutations throughout DHFR in an attempt to find alterations that slowed FtsH degradation by disrupting the potential recognition elements. For example, we introduced N23D/L24D, K32A/R33A/K38A, R33A, R33D, or R52D mutations, but FtsH degraded the corresponding mutants at rates similar to ^{WT}DHFR. We did find that FtsH degraded variants with the A6D/A7D, R52A, K58A, K58D, R52A/R57A/K58A, G67T, or K106A/K109A mutations 2- to 3-fold faster than ^{WT}DHFR. Enhanced degradation of these variants probably results from an increase in the equilibrium population of a partially folded intermediate that is recognized and degraded by FtsH.

The M20 loop is highly dynamic in H/D exchange experiments (Fig. 2.5C), and residues 16-20 of this loop are the only amino acids lacking electron density in the crystal structure of apo-DHFR (Bystroff & Kraut, 1991). To test if engagement/initiation of FtsH degradation requires this loop, we replaced the complete M20 sequence (residues 9-24) with a GGGGS linker. However, FtsH

degraded the resulting variant (M20$_{rep}$) at a rate similar to ^{WT}DHFR (Fig. 2.6D). Hence, the M20 loop is dispensable for FtsH degradation, providing additional evidence that native DHFR is not the target. Assuming that a partially folded intermediate is the target, then another disordered region must allow FtsH engagement.

Domain fusions provide insight into initiation of FtsH degradation

If the FtsH recognition element in DHFR is accessible in a partially unfolded species, then residues at either the N or C terminus of DHFR might still serve as sites where FtsH begins translocation and subsequent unfolding. To test this model, we fused a HaloTag domain (Halo) to both termini of DHFR to create Halo-DHFR-Halo (Fig. 2.7A). We chose Halo because it is not degraded by FtsH and can be covalently modified with tetramethylrhodamine (TMR), allowing visualization of any Halo-containing degradation products using fluorescence (Los et al., 2008; Zuromski et al., 2020). FtsH degraded Halo-DHFR-Halo, albeit slowly, generating lower molecular-weight fluorescent products (Fig. 2.7A). This result indicates that access to residues at the N or C terminus of DHFR is not necessary for FtsH degradation and provides additional support for noncanonical recognition and engagement of an internal sequence or sequences in DHFR.
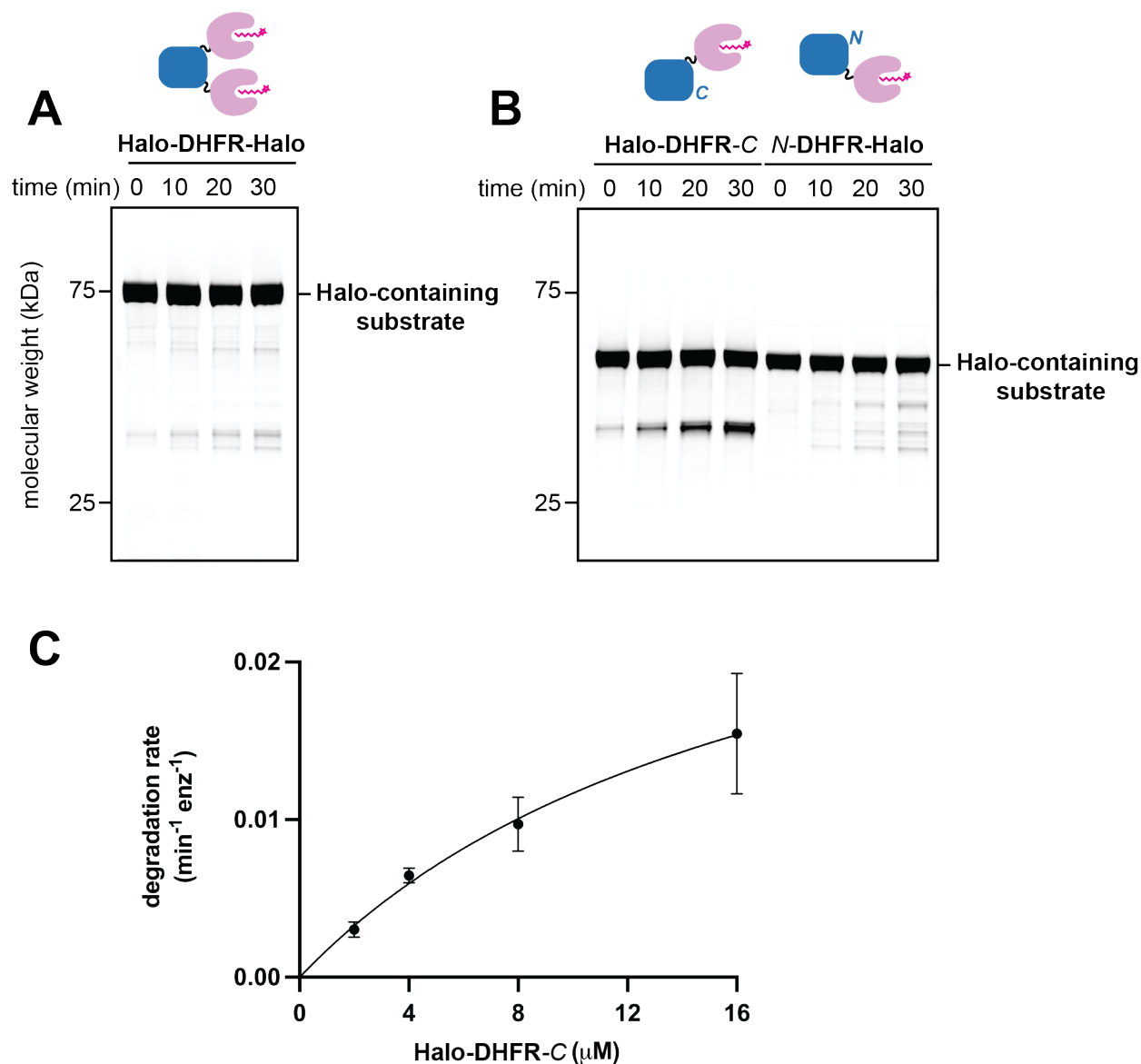
Figure 2.7. FtsH degrades DHFR with Halo domains fused to the N-terminus, C-terminus, or both termini. For panels *A* and *B,* cartoons of fusion constructs are shown above the gel degradation experiment. Prior to these reactions, Halo domains were covalently modified with TMR ligand. The kinetics of degradation were monitored by SDS-PAGE and visualized by the fluorescence of the TMR Halo-ligand. *A,* DHFR-Halo-DHFR (5 μM) was incubated at 42 °C with FtsH$_6$ (1 μM), ATP, and CK regeneration mix. *B,* Halo-DHFR-*C* or *N*-DHFR-Halo was incubated at 42 °C with FtsH$_6$ (1 μM), ATP, and CK regeneration mix. *C,* Rates of FtsH$_6$ (0.5 μM) degradation of different concentrations of Halo-DHFR-*C* at 37 °C were determined by SDS-PAGE to allow for direct comparison with DHFR degradation from Figure 2.3. The line is a non-linear least square fit of the data to the Michaelis-Menten equation; $k_{deg} = 0.03 \pm 0.02$ min^{-1} enz^{-1} and K_M = 18.0 ± 6.9 μM. Values are means (n ≥ 3) ± 1 SD.

We also tested degradation of DHFR blocked with Halo at just the N-terminus (Halo-DHFR-*C*) or just the C-terminus (*N*-DHFR-Halo), where the italicized letter indicates the native DHFR terminus (Fig. 2.7B). FtsH degraded Halo-DHFR-*C* more rapidly than *N*-DHFR-Halo. The presence of an easily identifiable major degradation product of Halo-DHFR-*C* allowed determination of steady-state kinetic parameters for its degradation by FtsH (Fig. 2.7C). Compared to ^{WT}DHFR, k_{deg} for the fusion protein decreased ~6-fold, whereas K_M increased ~6-fold. These changes in k_{deg} and K_M suggest that fusion of the Halo domain to the N-terminus affects FtsH binding to DHFR and a step that is rate limiting in degradation, presumably DHFR unfolding. The termini of native DHFR are located on the same side of the native molecule and close in space (~14 Å). It is plausible, therefore, that fusions to either terminus of DHFR weaken FtsH binding to a partially folded intermediate and thus hinder substrate recognition and possibly unfolding by steric interference.

DISCUSSION

We began this study by testing the hypothesis that FtsH might degrade DHFR with a sufficiently long degron. At a minimum, we expected to see a DHFR product with a partially trimmed extension that would provide information about how closely degron-tagged DHFR could approach FtsH. Instead, we discovered that FtsH can degrade DHFR attached to C-terminal ssrA-containing tails of different lengths and can also degrade DHFR lacking an appended degron. We suspect that differences in our degradation conditions or how FtsH or the substrates were purified account for the discrepancy between our results and the previously reported finding that FtsH cannot degrade DHFR with an appended ssrA degron (Herman et al., 2003).

Although the steady-state degradation parameters were similar for untagged DHFR and DHFR ssrA-tail variants, untagged DHFR and DHFR-ssrA[11] have slightly higher K_M and slightly higher k_{deg} values compared to DHFR-ssrA[19] and DHFR-ssrA[20]. This difference may be attributed to several factors, including but not limited to the possibility that degradation can occur via multiple pathways for the ssrA-tagged substrates. Force may be applied at a different site or with different geometry between the untagged DHFR, DHFR-ssrA[11] and longer ssrA-tail containing DHFR variants. The significance of both the site and geometry with which an unfolding force is applied in determining the fate of the substrate protein has been illustrated with other AAA+ proteases (Kenniston et al., 2004; Olivares et al., 2017; Kotamarthi et al., 2020). Additionally, fewer amino acids would need to be translocated for complete degradation of the shorter substrates, which were degraded at slightly faster maximal rates.

Which species of DHFR does FtsH recognize?

In the simplest case, a single short unstructured peptide in a native protein can act both as a recognition determinant and as the initiation site where translocation through the axial channel begins the unfolding and subsequent degradation of a substrate by a AAA+ protease. For example, appending just the C-terminal pentapeptide of the ssrA tag to the last structured residue at the C-terminus of GFP is sufficient for its degradation by ClpXP (Fei et al., 2020). A small portion of the M20 loop of DHFR is the only unstructured region in the crystal structure of apo-DHFR (Bystroff & Kraut, 1991), but we find that replacing the entire loop with a short linker has no significant effect on FtsH degradation. Hence, the M20 loop does not appear to be required for any step of FtsH degradation of DHFR.

In globally denatured DHFR, the N and C termini and other peptide sequences would be exposed and could plausibly be bound by FtsH. Importantly, however, FtsH degrades the hyper-stable A145T variant of DHFR slightly faster than the parental protein. As globally denatured [A145T]DHFR should be present at ~1% of the concentration of denatured wild-type DHFR under our assay conditions, the fully denatured recognition model incorrectly predicts that [A145T]DHFR should be degraded far more slowly than wild-type DHFR. We conclude that FtsH is unlikely to recognize fully denatured DHFR as its primary target.

As biophysical studies have identified meta-stable intermediates in DFHR folding/unfolding (Kuwajima et al., 1991; Heidary et al., 2000; Ionescu et al., 2000; Kasper et al., 2014), we propose that one or more of these species is recognized by FtsH (Fig. 2.8). These partially folded DHFR molecules should be populated at reasonable levels at the temperatures (37 to 42 °C) we use for degradation (Ohmae et al., 1996; Ionescu et al., 2000) and would have unstructured regions for engagement as well as native regions that might provide additional recognition determinants. We note that this model predicts that any DHFR mutation that increases the equilibrium population of the intermediate without directly affecting recognition would result in faster degradation by FtsH, a result that we observed for many mutant DHFR variants.

Figure 2.8. A model for how FtsH may recognize DHFR for degradation. Folded, native DHFR (left, M20 loop illustrated in dynamic motion) is in equilibrium with a partially unfolded

64

state (middle, indicated by the unfolding of the internal region in dark blue). This partially denatured species is likely to be recognized, unfolded, and degraded by FtsH.

Possibility of multiple degrons within DHFR

Mutation of residues 28 and 29, present in peptide-binding region 1, slowed FtsH degradation modestly, suggesting that these residues make up a part of a more complex recognition element. It is possible that one sequence element in partially unfolded DHFR binds FtsH, allowing a second disordered region to bind non-specifically in the axial channel to initiate translocation and engagement. There are multiple precedents for two-degron models in other AAA+ proteases. For example, most substrates of the 26S proteasome have a polyubiquitin moiety that binds to the 19S regulatory particle and an unstructured region that is needed to initiate proteolysis (Prakash et al., 2004; Inobe et al., 2011). Similarly, some substrates of ClpXP and ClpAP have one sequence that tethers the substrate to the N-terminal domains of these proteases and another sequence that is engaged in the axial pore (Neher et al., 2003; Hoskins & Wickner, 2006).

In the absence of a long unstructured polypeptide that contains a degron, our results suggest that untagged DHFR must approach FtsH closely enough to allow recognition and engagement of a partially folded substrate. Recent structural insights from bacterial FtsH homologs in membranous environments indicate that it may be possible for the cytosolic portion of FtsH to engage a cytosolic substrate of considerable size without requiring an extended degron. For example, cryo-EM structures of FtsH from *Aquifex aeolicus* and *Thermotoga maritima* show that the cytoplasmic domain of FtsH can tilt with respect to the membrane, which would facilitate interaction with substrates lacking a long degron tail (Carvalho et al., 2021; Liu et al., 2022).

Implications of internal recognition

Several results suggest that the N- or C-terminal sequences of DHFR do not play roles in FtsH recognition or engagement. For example, these sequences do not bind FtsH in peptide-blot experiments and blocking these terminal DHFR sequences by fusion to other proteins did not prevent DHFR degradation by FtsH. In combination, these results suggest that FtsH recognition of untagged DHFR is noncanonical and involves engagement of internal DHFR sequences. This model, in turn, predicts that FtsH must be able to translocate multiple polypeptide strands simultaneously, an activity that has been demonstrated for the 26S proteasome, ClpXP, and HslUV (Burton et al., 2001; Lee et al., 2002; Liu et al., 2003; Bolon et al., 2004; Kwon et al., 2004). FtsH degradation of RpoH and flavodoxin has also been proposed to depend on engagement of internal sequences in these substrates (Obrist & Narberhaus, 2005; Okuno et al., 2006a, 2006b; Obrist et al., 2007), and another study suggested that FtsH degrades proteins in non-native conformations (Ayuso-Tejedor et al., 2010).

One biological consequence of internal engagement by FtsH would be an ability to degrade inner-membrane proteins whose topologies place both their N- and C-termini in the periplasm. The rate of substrate unfolding by AAA+ proteases can depend on whether the enzyme is pulling from the N- or C-terminus or from an internal position, as mechanical stability can vary with the direction of the unfolding force (Lee et al., 2001; Kenniston et al., 2003; Kenniston et al., 2004; Gur et al., 2012; Olivares et al., 2017; Kotamarthi et al., 2020). In principle, therefore, recognition of internal degrons might allow FtsH to unfold proteins that would be more difficult to denature by pulling on a terminal degron.

Is FtsH a weak protein unfoldase?

The inability of FtsH to degrade degron-tagged DHFR was originally cited as one piece of evidence for a weak unfoldase activity (Herman et al., 2003). Although we find that FtsH does degrade DHFR, our results suggest that the actual target may be a less stable intermediate in folding/unfolding, leaving the question of unfolding strength open. The finding that FtsH can extract and degrade the stable GlpG protein from the membrane provides the strongest evidence that FtsH possesses a robust unfolding activity (Yang et al., 2018). In general, however, we note that AAA+ proteases and substrates co-evolve to allow degradation of appropriate cellular proteins when necessary. Thus, we find it unlikely that the substrate specificity of the only membrane-bound AAA+ protease in bacteria and eukaryotic organelles is limited by an inherently weak unfoldase activity.

MATERIALS AND METHODS

Strains, plasmids, and proteins. *E. coli* strain T7 Express (NEB) was used for FtsH expression. For expression of other proteins, *E. coli* strain ER2566 (lab stock) was used. Constructs containing all or part of *E. coli* DHFR were expressed from HTUA vectors. *E. coli* FtsH was expressed from a pET21b vector. FtsH was purified as described (Hari & Sauer, 2016). For preparation of ^{35}S-labeled FtsH for the spot-array assay, *E. coli* T7 Express cells harboring a pET21-based plasmid with a gene encoding FtsH-myc-H$_6$ were grown in 100 mL of minimal media (without methionine or cysteine) to log-phase and induced with 0.5 mM IPTG and EasyTag™ EXPRESS^{35}S Protein Labeling Mix (40 µCi/mL, PerkinElmer) for 3 h at 30 °C. The harvested pellet was subjected to three cycles of freeze-thaw and then resuspended in lysis buffer (50 mM Tris-HCl, pH 8.0, 100 mM NaCl, 20 mM imidazole, 10% glycerol) before incubating with lysozyme and BugBuster

reagent (Sigma Aldrich) at 4 °C for 20 min. After centrifugation, the supernatant was added to 100 μL of Ni-NTA slurry, washed extensively with lysis buffer, and the protein was eluted with lysis buffer containing 300 mM imidazole. After dialyzing into lysis buffer overnight at 4 °C, the solution was frozen rapidly for storage.

Cells expressing untagged DHFR, mutants of untagged DHFR, and DHFR-ssrA[11] were grown in LB broth to log phase, induced with 1 mM IPTG, harvested by centrifugation, and resuspended in Q buffer (25 mM HEPES, pH 7.5, 50 mM NaCl, and 10% glycerol). After sonication and centrifugation, the supernatant was loaded onto a Source-Q anion-exchange column and eluted using a 0-50% gradient from Q buffer to Q buffer plus 750 mM NaCl. Fractions were analyzed by SDS-PAGE, pooled, and further purified by Superdex-75 size-exclusion chromatography in DHFR storage buffer (25 mM HEPES, pH 7.5, 150 mM KCl, and 10% glycerol). Fractions containing pure protein were pooled, concentrated, and flash frozen for storage at −80 °C.

DHFR-ssrA[19], DHFR-ssrA[40], and DHRF-ssrA[60] were purified by Ni^{++}-NTA affinity chromatography, Source-15Q anion-exchange chromatography, and Superdex-75 size-exclusion chromatography, and stored frozen. Constructs containing Halo were initially fused to an N-terminal H$_7$-SUMO protein, purified by Ni^{++}-NTA affinity chromatography, cleaved overnight with purified Ulp1 protease, passed over a second Ni^{++}-NTA affinity column to remove the cleaved H$_7$-SUMO protein, and finally purified by Superdex-200 size-exclusion chromatography in DHFR storage buffer. Purified Halo fusion proteins were pooled, concentrated and then labelled at molar ratios of 1 HaloTag TMR ligand (Promega) to 3 proteins for 15 min at room temperature and desalted using Zeba columns (Thermo Scientific) into storage buffer before being used for

degradation reactions. The concentrations of labeled Halo fusion proteins were measured using the Bradford assay with the unlabeled version as standards and flash frozen for storage at –80 °C.

Gel assays of degradation. Substrates and enzymes were incubated at 37 °C or 42 °C in PD buffer (50 mM Tris-HCl, pH 8.0, 10 mM KCl, 5 mM $MgSO_4$, 10 µM $ZnCl_2$, 10% glycerol, 2 mM βME, and 0.1% Igepal CA-630) supplemented with ATP (4 mM) and a regeneration system (16 mM creatine phosphate, 75 µg/mL creatine kinase). Samples were quenched at different times by addition of SDS-loading buffer and heated before separation by SDS-PAGE, and visualized by Coomassie staining or by TMR fluorescence. Gels were imaged using a Typhoon FLA7000 (GE Healthcare) with the Coomassie setting or Alexa 532 setting. ATP-hydrolysis rates were measured using a NADH-coupled continuous spectrophotometric assay as described (Burton et al., 2003).

Enzyme kinetics. Alexa 488-maleimide (Thermo Fisher) was used to label DHFR or its ssrA-tail variants. Different concentrations of fluorescent protein were incubated at 37 °C with $FtsH_6$ (0.5 µM) in PD buffer with ATP (4 mM) and a creatine-kinase regeneration system. At different times, samples were quenched by addition of trichloroacetic acid (final 10% v/v) and allowed to precipitate overnight at 4 °C. After centrifugation, the soluble fraction was monitored for fluorescence (excitation 495 nm; emission 515 nm).

SPOT array. Peptides of 15 amino acids were synthesized by standard Fmoc techniques using a ResPep SL peptide synthesizer (Intavis) linked via their C termini to a cellulose membrane. Arrays were incubated with gentle agitation in methanol for 5 min, washed with TBST (TBS + 0.1% Tween20) 3X, and blocked overnight with blocking solution (TBST plus 5% bovine serum

albumin) at room temperature. Blocked arrays were washed twice with TBST and then washed twice in with PD buffer or binding buffer (PD buffer supplemented with an additional 90 mM KCl). The washed array was incubated with binding buffer, 0.5% BSA, 30 nM ^{35}S-FtsH, and 1.25 mM ATPγS for 1 h at 4 °C. After this incubation, the array was washed with PD or binding buffer, 5% dry milk, and 1 mM ATP for 5 min at 4 °C, dried, exposed to a Storage Phosphor Screen (Amersham) overnight, and imaged using a Typhoon FLA7000 (GE Healthcare).

REFERENCES

Akiyama, Y., Kihara, A., & Ito, K. (1996). Subunit a of proton ATPase F0 sector is a substrate of the FtsH protease in Escherichia coli. *FEBS Lett*, *399*(1-2), 26-28. http://onlinelibrary.wiley.com/store/10.1016/S0014-5793(96)01283-5/asset/feb2s0014579396012835.pdf?v=1&t=j7yvxxbi&s=af8c5729c7fab679402c5ded92d394c02227e05b

Amberg-Johnson, K., Hari, S. B., Ganesan, S. M., Lorenzi, H. A., Sauer, R. T., Niles, J. C., & Yeh, E. (2017). Small molecule inhibition of apicomplexan FtsH1 disrupts plastid biogenesis in human pathogens. *Elife*, *6*. https://doi.org/10.7554/eLife.29865

Arai, M., Maki, K., Takahashi, H., & Iwakura, M. (2003). Testing the relationship between foldability and the early folding events of dihydrofolate reductase from Escherichia coli. *J Mol Biol*, *328*(1), 273-288. https://doi.org/10.1016/s0022-2836(03)00212-2

Banuett, F., Hoyt, M. A., McFarlane, L., Echols, H., & Herskowitz, I. (1986). hflB, a new Escherichia coli locus regulating lysogeny and the level of bacteriophage lambda cII protein. *J Mol Biol*, *187*(2), 213-224. https://doi.org/10.1016/0022-2836(86)90229-9

Bittner, L. M., Arends, J., & Narberhaus, F. (2017). When, how and why? Regulated proteolysis by the essential FtsH protease in Escherichia coli. *Biol Chem*, *398*(5-6), 625-635. https://doi.org/10.1515/hsz-2016-0302

Bittner, L. M., Westphal, K., & Narberhaus, F. (2015). Conditional Proteolysis of the Membrane Protein YfgM by the FtsH Protease Depends on a Novel N-terminal Degron. *J Biol Chem*, *290*(31), 19367-19378. https://doi.org/10.1074/jbc.M115.648550

Bolon, D. N., Grant, R. A., Baker, T. A., & Sauer, R. T. (2004). Nucleotide-dependent substrate handoff from the SspB adaptor to the AAA+ ClpXP protease. *Mol Cell*, *16*(3), 343-350. https://doi.org/10.1016/j.molcel.2004.10.001

Burton, R. E., Baker, T. A., & Sauer, R. T. (2003). Energy-dependent degradation: Linkage between ClpX-catalyzed nucleotide hydrolysis and protein-substrate processing. *Protein Sci*, *12*(5), 893-902. https://www.ncbi.nlm.nih.gov/pmc/articles/PMC2323860/pdf/0120893.pdf

Burton, R. E., Siddiqui, S. M., & Kim, Y. I. (2001). Effects of protein stability and structure on substrate processing by the ClpXP unfolding and degradation machine. *20*(12), 3092-3100. https://doi.org/10.1093/emboj/20.12.3092

Bystroff, C., & Kraut, J. (1991). Crystal structure of unliganded Escherichia coli dihydrofolate reductase. Ligand-induced conformational changes and cooperativity in binding. *Biochemistry*, *30*(8), 2227-2239. https://doi.org/10.1021/bi00222a028

Carvalho, V., Prabudiansyah, I., Kovacik, L., Chami, M., Kieffer, R., van der Valk, R., de Lange, N., Engel, A., & Aubin-Tam, M. E. (2021). The cytoplasmic domain of the AAA+ protease FtsH is tilted with respect to the membrane to facilitate substrate entry. *J Biol Chem*, *296*, 100029. https://doi.org/10.1074/jbc.RA120.014739

Cheng, H. H., Muhlrad, P. J., Hoyt, M. A., & Echols, H. (1988). Cleavage of the cII protein of phage lambda by purified HflA protease: control of the switch between lysis and lysogeny. *Proc Natl Acad Sci U S A*, *85*(21), 7882-7886. https://doi.org/10.1073/pnas.85.21.7882

Chiba, S., Akiyama, Y., Mori, H., Matsuo, E., & Ito, K. (2000). Length recognition at the N-terminal tail for the initiation of FtsH-mediated proteolysis. *EMBO Rep*, *1*(1), 47-52. https://doi.org/10.1093/embo-reports/kvd005

Fei, X., Bell, T. A., Barkow, S. R., Baker, T. A., & Sauer, R. T. (2020). Structural basis of ClpXP recognition and unfolding of ssrA-tagged substrates. *Elife*, *9*. https://doi.org/10.7554/eLife.61496

Fuhrer, F., Muller, A., Baumann, H., Langklotz, S., Kutscher, B., & Narberhaus, F. (2007). Sequence and length recognition of the C-terminal turnover element of LpxC, a soluble substrate of the membrane-bound FtsH protease. *J Mol Biol*, *372*(2), 485-496. https://doi.org/10.1016/j.jmb.2007.06.083

Gottesman, S., Roche, E., Zhou, Y. N., & Sauer, R. T. (1998). The ClpXP and ClpAP proteases degrade proteins with carboxy-terminal peptide tails added by the SsrA-tagging system. *Genes Dev*, *12*(9), 1338-1347. https://www.ncbi.nlm.nih.gov/pmc/articles/PMC316764/pdf/x10.pdf

Gur, E., Vishkautzan, M., & Sauer, R. T. (2012). Protein unfolding and degradation by the AAA+ Lon protease. *Protein Sci*, *21*(2), 268-278. https://doi.org/10.1002/pro.2013

Hari, S. B., & Sauer, R. T. (2016). The AAA+ FtsH Protease Degrades an ssrA-Tagged Model Protein in the Inner Membrane of Escherichia coli. *Biochemistry*, *55*(40), 5649-5652. https://doi.org/10.1021/acs.biochem.6b00920

Heidary, D. K., O'Neill, J. C., Jr., Roy, M., & Jennings, P. A. (2000). An essential intermediate in the folding of dihydrofolate reductase. *Proc Natl Acad Sci U S A*, *97*(11), 5866-5870. https://doi.org/10.1073/pnas.100547697

Herman, C., Ogura, T., Tomoyasu, T., Hiraga, S., Akiyama, Y., Ito, K., Thomas, R., D'Ari, R., & Bouloc, P. (1993). Cell growth and lambda phage development controlled by the same essential Escherichia coli gene, ftsH/hflB. *Proc Natl Acad Sci U S A*, *90*(22), 10861-10865.

Herman, C., Prakash, S., Lu, C. Z., Matouschek, A., & Gross, C. A. (2003). Lack of a Robust Unfoldase Activity Confers a Unique Level of Substrate Specificity to the Universal AAA Protease FtsH. *Molecular Cell*, *11*(3), 659-669. https://doi.org/http://dx.doi.org/10.1016/S1097-2765(03)00068-6

Herman, C., Thevenet, D., Bouloc, P., Walker, G. C., & D'Ari, R. (1998). Degradation of carboxy-terminal-tagged cytoplasmic proteins by the Escherichia coli protease HflB (FtsH). *Genes Dev*, *12*(9), 1348-1355. https://www.ncbi.nlm.nih.gov/pmc/articles/PMC316767/pdf/x13.pdf

Hoskins, J. R., & Wickner, S. (2006). Two peptide sequences can function cooperatively to facilitate binding and unfolding by ClpA and degradation by ClpAP. *Proc Natl Acad Sci U S A*, *103*(4), 909-914. https://doi.org/10.1073/pnas.0509154103

Inobe, T., Fishbain, S., Prakash, S., & Matouschek, A. (2011). Defining the geometry of the two-component proteasome degron. *Nature Chemical Biology*, *7*(3), 161-167. https://doi.org/10.1038/nchembio.521

Ionescu, R. M., Smith, V. F., O'Neill, J. C., Jr., & Matthews, C. R. (2000). Multistate equilibrium unfolding of Escherichia coli dihydrofolate reductase: thermodynamic and spectroscopic description of the native, intermediate, and unfolded ensembles. *Biochemistry*, *39*(31), 9540-9550. https://doi.org/10.1021/bi000511y

Ito, K., & Akiyama, Y. (2005). Cellular functions, mechanism of action, and regulation of FtsH protease. *Annu Rev Microbiol*, *59*, 211-231. https://doi.org/10.1146/annurev.micro.59.030804.121316

Izert, M. A., Klimecka, M. M., & Górna, M. W. (2021). Applications of Bacterial Degrons and Degraders — Toward Targeted Protein Degradation in Bacteria [Review]. *Frontiers in molecular biosciences*, *8*. https://doi.org/10.3389/fmolb.2021.669762

Kasper, J. R., Liu, P.-F., & Park, C. (2014). Structure of a partially unfolded form of Escherichia coli dihydrofolate reductase provides insight into its folding pathway. *Protein Sci*, *23*(12), 1728-1737. https://doi.org/10.1002/pro.2555

Keiler, K. C., Waller, P. R., & Sauer, R. T. (1996). Role of a peptide tagging system in degradation of proteins synthesized from damaged messenger RNA. *Science*, *271*(5251), 990-993. http://science.sciencemag.org/content/271/5251/990.long

Kenniston, J. A., Baker, T. A., Fernandez, J. M., & Sauer, R. T. (2003). Linkage between ATP consumption and mechanical unfolding during the protein processing reactions of an AAA+ degradation machine. *Cell*, *114*(4), 511-520.

Kenniston, J. A., Burton, R. E., Siddiqui, S. M., Baker, T. A., & Sauer, R. T. (2004). Effects of local protein stability and the geometric position of the substrate degradation tag on the efficiency of ClpXP denaturation and degradation. *J Struct Biol*, *146*(1-2), 130-140. https://doi.org/10.1016/j.jsb.2003.10.023

Kihara, A., Akiyama, Y., & Ito, K. (1995). FtsH is required for proteolytic elimination of uncomplexed forms of SecY, an essential protein translocase subunit. *Proc Natl Acad Sci U S A*, *92*(10), 4532-4536.

Kihara, A., Akiyama, Y., & Ito, K. (1997). Host regulation of lysogenic decision in bacteriophage lambda: transmembrane modulation of FtsH (HflB), the cII degrading protease, by HflKC (HflA). *Proc Natl Acad Sci U S A*, *94*(11), 5544-5549. https://www.ncbi.nlm.nih.gov/pmc/articles/PMC20815/pdf/pq005544.pdf

Kobiler, O., Koby, S., Teff, D., Court, D., & Oppenheim Amos, B. (2002). The phage λ CII transcriptional activator carries a C-terminal domain signaling for rapid proteolysis. *Proceedings of the National Academy of Sciences*, *99*(23), 14964-14969. https://doi.org/10.1073/pnas.222172499

Kotamarthi, H. C., Sauer, R. T., & Baker, T. A. (2020). The Non-dominant AAA+ Ring in the ClpAP Protease Functions as an Anti-stalling Motor to Accelerate Protein Unfolding and Translocation. *Cell Rep*, *30*(8), 2644-2654.e2643. https://doi.org/10.1016/j.celrep.2020.01.110

Kuwajima, K., Garvey, E. P., Finn, B. E., Matthews, C. R., & Sugai, S. (1991). Transient intermediates in the folding of dihydrofolate reductase as detected by far-ultraviolet circular dichroism spectroscopy. *Biochemistry*, *30*(31), 7693-7703. https://doi.org/10.1021/bi00245a005

Kwon, A. R., Trame, C. B., & McKay, D. B. (2004). Kinetics of protein substrate degradation by HslUV. *J Struct Biol*, *146*(1-2), 141-147. https://doi.org/10.1016/j.jsb.2003.11.003

Langklotz, S., Baumann, U., & Narberhaus, F. (2012). Structure and function of the bacterial AAA protease FtsH. *Biochim Biophys Acta*, *1823*(1), 40-48. https://doi.org/10.1016/j.bbamcr.2011.08.015

Lee, C., Prakash, S., & Matouschek, A. (2002). Concurrent translocation of multiple polypeptide chains through the proteasomal degradation channel. *J Biol Chem*, *277*(38), 34760-34765. https://doi.org/10.1074/jbc.M204750200

Lee, C., Schwartz, M. P., Prakash, S., Iwakura, M., & Matouschek, A. (2001). ATP-dependent proteases degrade their substrates by processively unraveling them from the degradation signal. *Mol Cell*, *7*(3), 627-637.

Liu, C. W., Corboy, M. J., DeMartino, G. N., & Thomas, P. J. (2003). Endoproteolytic activity of the proteasome. *Science*, *299*(5605), 408-411. https://doi.org/10.1126/science.1079293

Liu, W., Schoonen, M., Wang, T., McSweeney, S., & Liu, Q. (2022). Cryo-EM structure of transmembrane AAA+ protease FtSH in the ADP state. *Commun Biol*, *5*(1), 257. https://doi.org/10.1038/s42003-022-03213-2

Los, G. V., Encell, L. P., McDougall, M. G., Hartzell, D. D., Karassina, N., Zimprich, C., Wood, M. G., Learish, R., Ohana, R. F., Urh, M., Simpson, D., Mendez, J., Zimmerman, K., Otto, P., Vidugiris, G., Zhu, J., Darzins, A., Klaubert, D. H., Bulleit, R. F., & Wood, K. V. (2008). HaloTag: a novel protein labeling technology for cell imaging and protein analysis. *ACS Chem Biol*, *3*(6), 373-382. https://doi.org/10.1021/cb800025k

Mahmoud, S. A., & Chien, P. (2018). Regulated Proteolysis in Bacteria. *Annu Rev Biochem*, *87*, 677-696. https://doi.org/10.1146/annurev-biochem-062917-012848

Neher, S. B., Sauer, R. T., & Baker, T. A. (2003). Distinct peptide signals in the UmuD and UmuD' subunits of UmuD/D' mediate tethering and substrate processing by the ClpXP protease. *Proc Natl Acad Sci U S A*, *100*(23), 13219-13224. https://doi.org/10.1073/pnas.2235804100

Obrist, M., Milek, S., Klauck, E., Hengge, R., & Narberhaus, F. (2007). Region 2.1 of the Escherichia coli heat-shock sigma factor RpoH (sigma32) is necessary but not sufficient for degradation by the FtsH protease. *Microbiology (Reading)*, *153*(Pt 8), 2560-2571. https://doi.org/10.1099/mic.0.2007/007047-0

Obrist, M., & Narberhaus, F. (2005). Identification of a turnover element in region 2.1 of Escherichia coli sigma32 by a bacterial one-hybrid approach. *J Bacteriol*, *187*(11), 3807-3813. https://doi.org/10.1128/jb.187.11.3807-3813.2005

Ogura, T., Inoue, K., Tatsuta, T., Suzaki, T., Karata, K., Young, K., Su, L. H., Fierke, C. A., Jackman, J. E., Raetz, C. R., Coleman, J., Tomoyasu, T., & Matsuzawa, H. (1999). Balanced biosynthesis of major membrane components through regulated degradation of the committed enzyme of lipid A biosynthesis by the AAA protease FtsH (HflB) in Escherichia coli. *Mol Microbiol*, *31*(3), 833-844. http://onlinelibrary.wiley.com/store/10.1046/j.1365-2958.1999.01221.x/asset/j.1365-2958.1999.01221.x.pdf?v=1&t=j3yyjd2b&s=c46c4bad88fbdbada172d0dbecb9584baa1ead8d

Ogura, T., Tomoyasu, T., Yuki, T., Morimura, S., Begg, K. J., Donachie, W. D., Mori, H., Niki, H., & Hiraga, S. (1991). Structure and function of the ftsH gene in Escherichia coli. *Res Microbiol*, *142*(2-3), 279-282.

Ohmae, E., Ishimura, K., Iwakura, M., & Gekko, K. (1998). Effects of point mutations at the flexible loop alanine-145 of Escherichia coli dihydrofolate reductase on its stability and function. *J Biochem*, *123*(5), 839-846. https://doi.org/10.1093/oxfordjournals.jbchem.a022013

Ohmae, E., Kurumiya, T., Makino, S., & Gekko, K. (1996). Acid and Thermal Unfolding ofEseherichia coli Dihydrofolate Reductase. *The Journal of Biochemistry*, *120*(5), 946-953. https://doi.org/10.1093/oxfordjournals.jbchem.a021511

Ohmae, E., Sasaki, Y., & Gekko, K. (2001). Effects of five-tryptophan mutations on structure, stability and function of Escherichia coli dihydrofolate reductase. *J Biochem*, *130*(3), 439-447. https://doi.org/10.1093/oxfordjournals.jbchem.a003004

Okuno, T., Yamanaka, K., & Ogura, T. (2006a). An AAA protease FtsH can initiate proteolysis from internal sites of a model substrate, apo-flavodoxin. *Genes Cells*, *11*(3), 261-268. https://doi.org/10.1111/j.1365-2443.2006.00940.x

Okuno, T., Yamanaka, K., & Ogura, T. (2006b). Flavodoxin, a new fluorescent substrate for monitoring proteolytic activity of FtsH lacking a robust unfolding activity. *J Struct Biol*, *156*(1), 115-119. https://doi.org/10.1016/j.jsb.2006.02.001

Olivares, A. O., Kotamarthi, H. C., Stein, B. J., Sauer, R. T., & Baker, T. A. (2017). Effect of directional pulling on mechanical protein degradation by ATP-dependent proteolytic machines. *Proc Natl Acad Sci U S A*, *114*(31), E6306-e6313. https://doi.org/10.1073/pnas.1707794114

Prakash, S., Tian, L., Ratliff, K. S., Lehotzky, R. E., & Matouschek, A. (2004). An unstructured initiation site is required for efficient proteasome-mediated degradation. *Nat Struct Mol Biol*, *11*(9), 830-837. https://doi.org/10.1038/nsmb814

Rodriguez, F., Arsène-Ploetze, F., Rist, W., Rüdiger, S., Schneider-Mergener, J., Mayer, M. P., & Bukau, B. (2008). Molecular basis for regulation of the heat shock transcription factor sigma32 by the DnaK and DnaJ chaperones. *Mol Cell*, *32*(3), 347-358. https://doi.org/10.1016/j.molcel.2008.09.016

Rood, J. I., & Williams, J. W. (1981). Characterization of the cloned Escherichia coli dihydrofolate reductase. *Biochim Biophys Acta*, *660*(2), 214-218. https://doi.org/10.1016/0005-2744(81)90162-5

Sauer, R. T., & Baker, T. A. (2011). AAA+ proteases: ATP-fueled machines of protein destruction. *Annu Rev Biochem*, *80*, 587-612. https://doi.org/10.1146/annurev-biochem-060408-172623

Sauer, R. T., Bolon, D. N., Burton, B. M., Burton, R. E., Flynn, J. M., Grant, R. A., Hersch, G. L., Joshi, S. A., Kenniston, J. A., Levchenko, I., Neher, S. B., Oakes, E. S. C., Siddiqui, S. M., Wah, D. A., & Baker, T. A. (2004). Sculpting the Proteome with AAA+ Proteases and Disassembly Machines. *Cell*, *119*(1), 9-18. https://doi.org/10.1016/j.cell.2004.09.020

Sauer, R. T., Fei, X., Bell, T. A., & Baker, T. A. (2021). Structure and function of ClpXP, a AAA+ proteolytic machine powered by probabilistic ATP hydrolysis. *Critical Reviews in Biochemistry and Molecular Biology*, 1-17. https://doi.org/10.1080/10409238.2021.1979461

Saunders, R. A., Stinson, B. M., Baker, T. A., & Sauer, R. T. (2020). Multistep substrate binding and engagement by the AAA+ ClpXP protease. *Proc Natl Acad Sci U S A*, *117*(45), 28005-28013. https://doi.org/10.1073/pnas.2010804117

Sawaya, M. R., & Kraut, J. (1997). Loop and Subdomain Movements in the Mechanism of Escherichia coli Dihydrofolate Reductase: Crystallographic Evidence. *Biochemistry*, *36*(3), 586-603. https://doi.org/10.1021/bi962337c

Schäkermann, M., Langklotz, S., & Narberhaus, F. (2013). FtsH-mediated coordination of lipopolysaccharide biosynthesis in Escherichia coli correlates with the growth rate and the alarmone (p)ppGpp. *J Bacteriol*, *195*(9), 1912-1919. https://doi.org/10.1128/JB.02134-12

Shotland, Y., Koby, S., Teff, D., Mansur, N., Oren, D. A., Tatematsu, K., Tomoyasu, T., Kessel, M., Bukau, B., Ogura, T., & Oppenheim, A. B. (1997). Proteolysis of the phage lambda CII regulatory protein by FtsH (HflB) of Escherichia coli. *Mol Microbiol*, *24*(6), 1303-1310. https://doi.org/10.1046/j.1365-2958.1997.4231796.x

Straus, D., Walter, W., & Gross, C. A. (1990). DnaK, DnaJ, and GrpE heat shock proteins negatively regulate heat shock gene expression by controlling the synthesis and stability of sigma 32. *Genes Dev*, *4*(12a), 2202-2209. https://doi.org/10.1101/gad.4.12a.2202

Touchette, N. A., Perry, K. M., & Matthews, C. R. (1986). Folding of dihydrofolate reductase from Escherichia coli. *Biochemistry*, *25*(19), 5445-5452. https://doi.org/10.1021/bi00367a015

Varshavsky, A. (1991). Naming a targeting signal. *Cell*, *64*(1), 13-15. https://doi.org/10.1016/0092-8674(91)90202-a

Yamamoto, T., Izumi, S., & Gekko, K. (2004). Mass spectrometry on segment-specific hydrogen exchange of dihydrofolate reductase. *J Biochem*, *135*(1), 17-24. https://doi.org/10.1093/jb/mvh002

Yang, Y., Guo, R., Gaffney, K., Kim, M., Muhammednazaar, S., Tian, W., Wang, B., Liang, J., & Hong, H. (2018). Folding-Degradation Relationship of a Membrane Protein Mediated by the Universally Conserved ATP-Dependent Protease FtsH. *J Am Chem Soc*, *140*(13), 4656-4665. https://doi.org/10.1021/jacs.8b00832

Zuromski, K. L., Sauer, R. T., & Baker, T. A. (2020). Modular and coordinated activity of AAA+ active sites in the double-ring ClpA unfoldase of the ClpAP protease. *Proceedings of the National Academy of Sciences*, *117*(41), 25455. https://doi.org/10.1073/pnas.2014407117

Chapter III

FtsH degrades kinetically stable dimers of cyclopropane fatty acid synthase via an internal

degron

This chapter has been submitted for publication as:

Hari, SB, Morehouse, JP, Sauer, RT. (2022). FtsH degrades kinetically stable dimers of cyclopropane fatty acid synthase via an internal degron.

JPM performed experiments that contributed to Figures 3.4E, 3.5A, 3.5B. SBH performed all other experiments in this manuscript. RTS oversaw research. RTS, SBH, and JPM contributed to writing and/or revising the manuscript.

ABSTRACT

Targeted protein degradation plays important roles in stress responses in all cells. In *E. coli*, the membrane-bound AAA+ FtsH protease degrades cytoplasmic and membrane proteins. Here, we demonstrate that FtsH degrades cyclopropane fatty acid (CFA) synthase, whose synthesis is induced upon nutrient deprivation and entry into stationary phase. We find that neither the disordered N-terminal residues nor the structured C-terminal residues of the kinetically stable CFA-synthase dimer are required for FtsH recognition and degradation. Experiments with fusion proteins support a model in which an internal degron mediates FtsH recognition as a prelude to unfolding and proteolysis. These findings elucidate the terminal step in the life cycle of CFA synthase and provide new insight into FtsH function.

SIGNIFICANCE STATEMENT

The cellular proteome is in a constant state of flux, as changes in the environment necessitate rapid functional responses. A key part of this process is regulated protein degradation; in bacteria, most protein degradation is performed by ATP-dependent proteases which use energy from ATP hydrolysis to mechanically unfold proteins and feed them into a central chamber for degradation. Here, we report that the membrane-bound ATP-dependent protease FtsH degrades cyclopropane fatty acid synthase, an enzyme that is transiently upregulated upon entrance into stationary phase. Interestingly, FtsH does not appear to use the N- or C-terminus of CFA synthase for recognition but more likely recognizes an internal region. Our findings highlight the role of ATP-dependent proteases, specifically FtsH, in restoring cellular homeostasis.

INTRODUCTION

Proteases of the AAA+ superfamily bind specific protein targets and use the energy of ATP hydrolysis to mechanically unfold and then translocate the substrate into a sequestered proteolytic chamber for destruction (Sauer and Baker, 2011). These proteolytic machines consist of a AAA+ ring hexamer with a central axial channel and a self-compartmentalized peptidase. The AAA+ ring is responsible for substrate recognition, unfolding, and translocation. Several AAA+ proteases are upregulated in bacteria as part of the heat-shock response, helping to limit cytotoxicity by degrading misfolded or partially unfolded proteins (Meyer and Baker, 2011). In addition, AAA+ proteases degrade two transcription factors, σ^{32} and σ^{S}, the respective master regulators of heat-shock stress and nutrient-starvation stress in *Escherichia coli*, to help restore homeostasis (Herman et al., 1995; Zhou et al., 2001). After the SOS response to DNA damage, AAA+ proteases also degrade many of the induced proteins, allowing a return to homeostasis once transcription of their genes returns to pre-stress levels (Flynn et al., 2003; Neher et al., 2003a; 2003b; 2006).

Upon entry of *E. coli* into stationary phase, levels of cyclopropane fatty acid (CFA) synthase increase as a consequence of enhanced transcription from a σ^{S}-regulated promoter (Wang and Cronan, 1994). This enzyme converts the alkene groups within unsaturated fatty acids of the lipid membrane into cyclopropyl moieties (Law, 1971), a reaction that provides increased resistance of *E. coli* to acid shock (Chang and Cronan, 1999) and repeated freeze-thaw cycles (Grogan and Cronan, 1986). Proteolysis of CFA synthase in a σ^{32}-dependent manner subsequently helps return enzyme activity to pre-transition levels (Chang et al., 2000). Here, we report that FtsH, a membrane-anchored AAA+ protease, degrades CFA synthase *in vitro* and *in vivo*. CFA synthase is enzymatically active as a dimer (Hari et al. 2018), which we show is kinetically stable and the direct target of FtsH degradation. Like other AAA+ proteases, FtsH typically recognizes

disordered peptide sequences (degrons) at the N- or C-termini of characterized substrates (Führer et al., 2007; Herman et al., 2003). The N-terminal residues of CFA synthase are disordered, but we find that they play no role in FtsH recognition. The C-terminal residues of CFA synthase are inaccessible in the native dimer. Although these residues can function as an FtsH degron when appended to another protein, our mutational experiment indicate that they do not mediate degradation of CFA synthase. Thus, internal sequences in CFA synthase appear to be responsible for recognition by FtsH. These results demonstrate that FtsH plays a role in the life cycle of CFA synthase and suggest that it can degrade native proteins with substantial kinetic stability.

RESULTS

FtsH degrades CFA synthase. We initially asked if any of the five AAA+ proteases in *E. coli* (FtsH, HslUV, Lon, ClpXP, or ClpAP) could degrade CFA synthase. Purified FtsH degraded purified CFA synthase but the remaining proteases catalyzed little or no degradation (Fig. 3.1A). FtsH did not degrade CFA synthase in the absence of ATP, and a Walker-B [E252Q]FtsH mutant deficient in ATP hydrolysis-deficient was inactive in degradation (Fig. 3.1B). Thus, degradation of CFA synthase is energy dependent as well as specific with respect to the AAA+ protease involved.
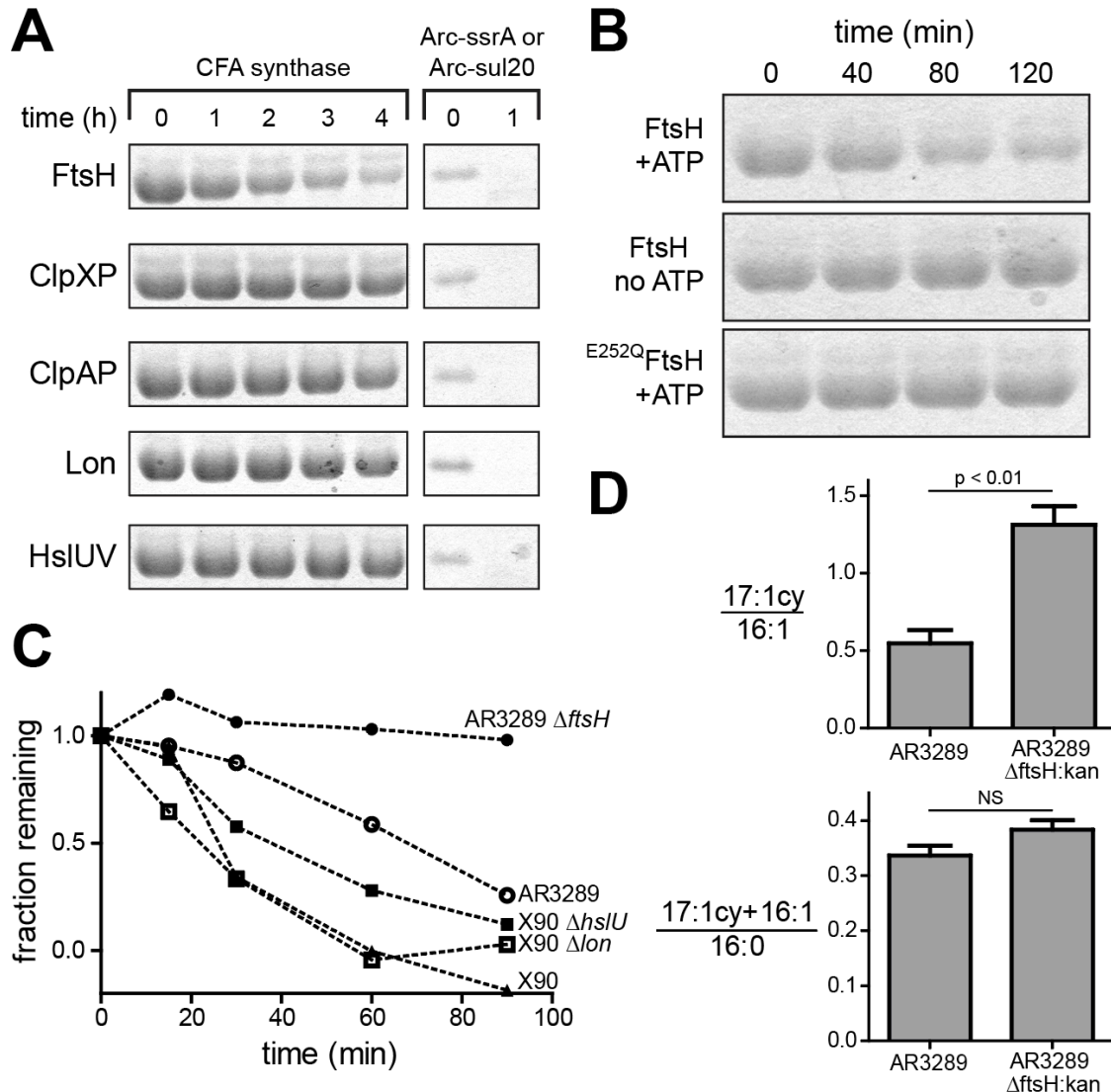
Figure 3.1. FtsH degrades CFA synthase. (**A**) CFA synthase (20 μM; left panel) or degron-tagged Arc repressor (20 μM; right panel) were incubated at 37 °C with FtsH (0.3 μM hexamer), HslUV (0.3 μM $HslU_6$; 1 μM $HslV_{12}$), Lon (0.3 μM hexamer), ClpXP (0.3 μM $ClpX_6$; 0.9 μM $ClpP_{14}$), or ClpAP (0.3 μM $ClpA_6$; 0.9 μM $ClpP_{14}$) and degradation kinetics were monitored by SDS-PAGE. Reactions contained 4 mM ATP and a regeneration system. Arc-ssrA was used for FtsH, HslUV, ClpXP, and ClpAP. Arc-sul20 was used for Lon. The faint band above CFA synthase is creatine kinase from the regeneration system. (**B**) CFA synthase (20 μM) was incubated with FtsH (0.5 μM hexamer; top two panels) or ^{E252Q}FtsH (0.5 μM hexamer; bottom panel) in the presence or absence of 4 mM ATP and a regeneration system. Degradation reactions were performed and analyzed as described in panel A. (**C**) After briefly expressing CFA synthase from a plasmid, ^{35}S-labeled methionine and cysteine were added to the indicated *E. coli* strains for 5 min, and a chase was initiated with unlabeled amino acids and phenyl-β-D-galactoside to represses transcription. At different times, samples were taken, separated by SDS-PAGE, and the gel was autoradiographed. Quantified bands from one replicate are shown in the plot. Based on independent experiments, the half-lives of CFA synthase were 20 and 34 min in strain X90; 34 and 29 min in strain X90 *ΔhslU*; and 12 and 18 min in strain X90 *Δlon*. CFA synthase half-lives

were 53, 52, and 60 min in strain AR3289; and >90, >90, and >90 min in strain AR3289 *ΔftsH*. **(D)** Phospholipids were extracted from overnight cultures of *E. coli* strains AR3289 or AR3289 *ΔftsH* grown at 30 °C, then converted into fatty acid methyl esters and analyzed by GC/MS. NS: not significant. Error bars represent the standard error of the mean (SEM, n = 3 separately grown cultures started from the same colony).

A previous study showed that the intracellular half-life of CFA synthase was not affected by a *clpP* mutation (Chang et al., 2000), which prevents degradation by ClpXP or ClpAP. To analyze the stability of CFA synthase in *E. coli* strains containing single-gene knockouts of *ftsH*, *hslU*, or *lon*, we performed radiolabeled pulse-chase experiments using plasmid-borne CFA synthase (Fig. 3.1C). Consistent with our results *in vitro*, chromosomal deletions of either *lon* or *hslU* had little effect on intracellular degradation of CFA synthase. However, the half-life of CFA synthase was longer in *ΔftsH:kan* cells than in an otherwise isogenic strain, showing that FtsH plays a role in regulating intracellular levels of CFA synthase.

In *E. coli* lacking the *ftsH* gene, higher steady-state levels of CFA synthase might result in increased lipid cyclopropanation. To test this possibility, we extracted phospholipids from overnight cultures of strains AR3289 and AR3289/*ΔftsH:kan* and analyzed lipid fatty acid methyl esters by GC/MS. Importantly, the level of the major cyclopropanated species (17:1cy) relative to its precursor with a double bond (16:1) was ~2.5-fold higher in AR3289/*ΔftsH* than in the parental strain (Fig. 3.1D, top panel). Adding the concentrations of the 17:1cy and 16:1 species and dividing by the concentration of the corresponding lipid species lacking a double bond (16:0) resulted in similar values in the *ftsH*[+] and *ΔftsH:kan* strains (Fig. 3.1D, bottom panel). Thus, the degree of cyclopropanation but not overall biosynthesis of these lipid variants is increased by the *ΔftsH:kan* allele.

FtsH degrades native dimers of CFA synthase. CFA synthase forms a dimer that is stable at μM concentrations (Hari and Sauer, 2018). In principle, however, a small equilibrium population of native or denatured monomer could be the species recognized and degraded by FtsH. This model predicts that destabilization of the native dimer should increase the rate of FtsH degradation. To test this hypothesis, we first used Michaelis-Menten analysis to determine the steady-state kinetic parameters for FtsH degradation of ^{35}S-labelled CFA synthase (Fig. 3.2A), yielding a K_M of 0.5 μM and a substrate turnover number (V_{max}/E_{total}) of 0.16 min^{-1} FtsH$_6$$^{-1}$. Next, we studied degradation of E308Q CFA synthase, which has a mutation in the dimer interface and chromatographs as a monomer in gel filtration (Hari and Sauer, 2018). FtsH degraded the E308Q variant at about half of the maximal rate of the wild-type dimer but with a similar K_M (Fig. 3.2A). Thus, CFA-synthase dimerization is not required for FtsH recognition. Moreover, because monomers are degraded more slowly than dimers, it is unlikely that native CFA synthase dimers must dissociate prior to recognition by FtsH.
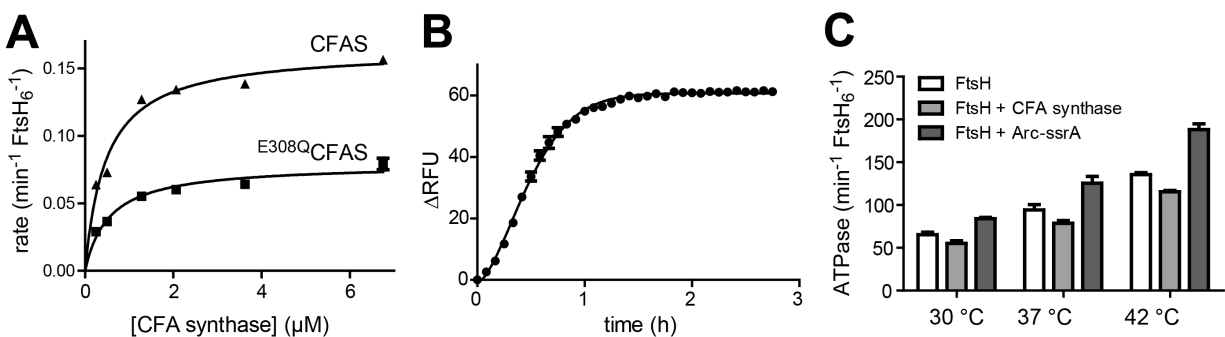

Figure 3.2. Steady-state FtsH degradation, subunit exchange, and ATP hydrolysis. (**A**) Rates of FtsH degradation of different concentrations of ^{35}S-labeled CFA synthase or ^{E308Q}CFA synthase at 37 °C were determined by scintillation counting of TCA-soluble fractions. The graph shows non-linear least squares fits of the data to the Michaelis-Menten equation (CFAS: K_M = 0.48 ± 0.06 μM; V_{max} = 0.16 ± 0.01 min^{-1}. ^{E308Q}CFAS: K_M = 0.55 ± 0.08 μM; V_{max} = 0.079 ± 0.003 min^{-1}). Error bars represent the standard error of the mean (SEM, n = 3 trials prepared using the same substrate and enzyme stocks). (**B**) Samples of CFA synthase labeled with Dylight-488 or -650 were mixed and FRET as a function of time was monitored at 37 °C (excitation 480 nm; emission 675 nm). The solid line is a fit to a growth equation (Weibull, 1951) to account for the initial lag

phase (see text). (**D**) The rate of ATPase hydrolysis by FtsH was measured alone or in the presence of either CFA synthase or Arc-ssrA (20 µM each) at different temperatures.

A second prediction of the monomer-degradation model is that the rate of dimer dissociation should be faster than the steady-state rate of FtsH degradation. To determine kinetic stability, we mixed equal concentrations of CFA synthase labeled separately with fluorescent donor or acceptor dyes and monitored the kinetics of heterodimer formation by FRET (Fig. 3.2B). Under these conditions, the heterodimer concentration approaches its equilibrium value with kinetics determined by the rate of subunit dissociation (Jonsson et al., 1996). After a short lag, the half-life of subunit mixing was ~23 min at 37 °C. This time is substantially longer than the ~4 min half-life of CFA synthase degradation by FtsH under V_{max} conditions and thus supports a model in which FtsH recognizes CFA-synthase dimers prior to the initiation of global unfolding and degradation. Alternatively, FtsH binding might induce more rapid dissociation of CFA-synthase dimers. However, because FtsH would have to expend energy to force dimer dissociation, this model predicts that K_M for degradation of the monomeric variant should be substantially lower than K_M for degradation of the wild-type dimer, which was not observed (Fig. 3.2A).

We assayed the rate of ATP hydrolysis by FtsH in the absence of substrate or presence of CFA-synthase dimers or Arc-ssrA dimers at 30, 37, and 42 °C (Fig. 3.2C). At each temperature, CFA synthase reduced the rate of ATP hydrolysis by FtsH, whereas Arc-ssrA increased this rate. For other AAA+ proteases, faster ATP hydrolysis is often correlated with translocation being the rate-determining step in degradation, whereas slow ATP hydrolysis suggests that unfolding is rate limiting (Kenniston et al., 2003). FtsH degraded Arc-ssrA with a steady-state maximum velocity ~6-fold faster (see Fig. 3.3C) than it degraded CFA synthase. The rate of ATP hydrolysis in the presence of substrate divided by V_{max} for degradation provides an estimate of the ATP cost of

degradation of a single molecule of substrate. At 37 °C, these values were ~460 ATPs for FtsH

degradation of CFA synthase and ~140 ATPs for Arc-ssrA. Thus, FtsH uses more energy to engage,

unfold, and translocate CFA synthase than Arc, which is probably a consequence of the larger size

and increased stability of CFA synthase compared to Arc-ssrA.

Sequence determinants of FtsH recognition. Unstructured peptide degrons at either the N-

terminus or C-terminus of a protein substrate are typically recognized and engaged by the axial

channel of AAA+ proteases (Sauer and Baker, 2011). Internal sequences can also serve as degrons

and engagement sites, albeit more rarely (Hoskins et al., 2002; Okuno et al., 2006; Piwko and

Jentsch, 2006; Gur and Sauer, 2008; Kraut and Matouschek, 2011). The 12 N-terminal residues of

CFA synthase are disordered in the crystal structure and thus represented a plausible degron.

However, when we fused the N-terminal 15 residues of CFA synthase to the N-terminus of Arc,

FtsH degraded this substrate (N15[CFAS]-Arc) more slowly than parental Arc (Fig. 3.3A). Moreover,

FtsH degraded a purified CFA-synthase variant missing the 15 N-terminal residues (ΔN15-CFAS)

slightly faster than wild-type CFA synthase at 30 °C (Fig. 3.3B). This temperature was used

because the variant precipitated at 37 °C. Thus, N-terminal residues of CFA synthase are not
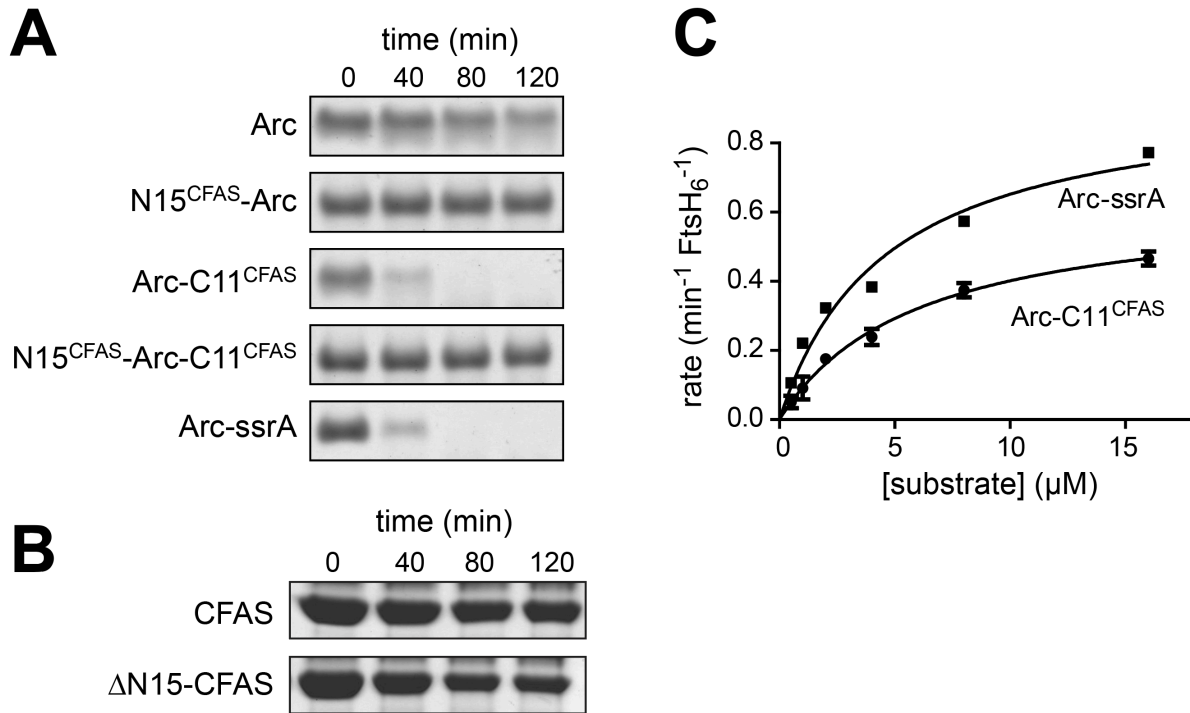
required for FtsH degradation.

Figure 3.3. Effects of terminal CFA-synthase sequences on degradation. (**A**) Degradation of Arc repressor fusions with different termini of CFA synthase by FtsH at 30 °C. (**B**) Degradation of wild-type CFA synthase and the ΔN15 mutant by FtsH at 30 °C. (**C**) Rates of degradation of different concentrations of Dylight-488-labeled Arc-C11^{CFAS} or Arc-ssrA by FtsH at 37 °C were determined by monitoring fluorescence dequenching (Baytshtok et al., 2016). The graph shows non-linear least squares fits of the data to the Michaelis-Menten equation (Arc-C11^{CFAS}: $K_M = 5.9 \pm 1.1$ µM; $V_{max} = 0.64 \pm 0.05$ min^{-1}; Arc-ssrA $- K_M = 4.6 \pm 0.8$ µM; $V_{max} = 0.95 \pm 0.07$ min^{-1}).

Next, we probed the C-terminal residues of CFA synthase, as FtsH has been shown to recognize C-terminal ssrA and 108 degradation tags (Herman et al., 1988). When we appended the 11 C-terminal residues of CFA synthase to the C-terminus of Arc (Arc-C11^{CFAS}), FtsH degraded this substrate faster than untagged Arc and at a rate similar to degradation of Arc-ssrA (Fig. 3.3A). Michaelis-Menten analysis showed that K_M for both degradation reactions was ~5 µM and V_{max} for FtsH degradation of Arc-C11^{CFAS} was about ~30% lower that of Arc-ssrA (Fig. 3.3C). Surprisingly, an Arc substrate containing the 15 N-terminal and 11 C-terminal residues of CFA synthase was not degraded by FtsH (Fig. 3.3A), indicating that the N15 sequence of CFA synthase inhibits FtsH degradation of this substrate. We propose that acidic residues in N15

(NGSSSSCI<u>EE</u>VP<u>DD</u>S) might interact with basic residues in C11 (<u>R</u>GVENGL<u>R</u>VA<u>R</u>), as the two termini of Arc are close in space, allowing an electrostatic interaction to mask recognition of C11 by FtsH.

Although the C-terminal 11 residues of CFA synthase can function as a modular degron for FtsH, K_M for recognition of these residues fused to Arc was ~5 µM, whereas K_M for degradation of CFA synthase was ~0.5 µM. Moreover, residues 375-382 pack into the dimer interface of CFA synthase in the crystal structure (Fig. 3.4A). For example, the side chain of Arg^{382}, the C-terminal residue in each subunit, forms multiple salt bridges and hydrogen bonds in the native structure (Fig. 3.4B). Thus, the C-terminus of CFA synthase would only be accessible in a transiently disordered conformation. To test for Arg^{382} availability, we assayed binding of anhydrotrypsin, which binds tightly to accessible C-terminal arginines (Yokosawa and Ishii, 1977). Specifically, we immobilized different His-tagged proteins onto sensor tips coated with anti-His1K antibody and monitored binding using bio-layer interferometry (BLI; Abdiche et al., 2008). To validate the assay, we first compared binding responses of His_7-SUMO-Arc-$C11^{CFAS}$ (C-terminal arginine) and His_7-SUMO-Arc-$C11^{CFAS/R11A}$ (C-terminal alanine). The equilibrium response signal of anhydrotrypsin binding to His_7-SUMO-Arc-$C11^{CFAS}$ was ~6-fold greater than to the control protein, which gave a response similar to another control reaction without loaded protein (Fig. 3.4C). We then assayed anhydrotrypsin binding to His_6-CFA synthase and to an otherwise identical R382A mutant. The response of CFA synthase was only slightly higher than the R382A mutant or His_7-SUMO-Arc-$C11^{CFAS/R11A}$, which has a C-terminal alanine. By contrast, His_6-$CFAS^{ext}$, a mutant in which the last 10 residues were duplicated to generate an exposed C-terminal arginine, produced robust anhydrotrypsin binding. Thus, conformational shielding dramatically reduces the accessibility of the C-terminus of CFA synthase to macromolecular binding.
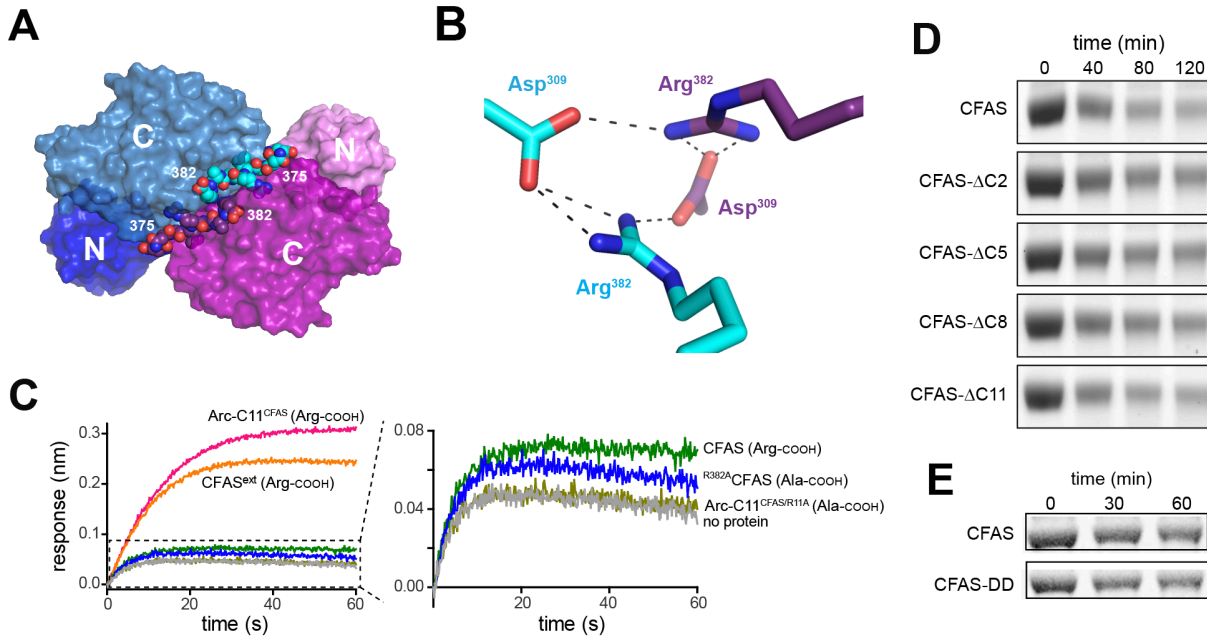
Figure 3.4. The C-terminus of CFA synthase is part of the structure and not required for FtsH degradation. (A) CFA synthase dimer (PDB code 6BQC) shown in surface representation. Subunits are colored shades of blue or purple and the N-terminal and C-terminal domains are designated. Residues 375-382 of each subunit are shown in space-filling representation and are part of the dimer interface. **(B)** In both subunits, the side chains of Arg^{382} point down into the dimer interface, and make multiple hydrogen-bonded salt bridges (indicated by dashed lines) with the side chains of Asp^{309}. **(C)** Variants of H$_7$-SUMO-Arc-C11^{CFAS} or H$_6$-CFA synthase (CFAS) were loaded onto bio-layer interferometry tips coated with anti-His1K antibody and anhydrotrypsin binding was monitored. The reference control omitted his-tagged protein loading. **(D)** Degradation of C-terminal truncations of CFA synthase (20 μM) by FtsH (0.5 μM hexamer). **(E)** Degradation of CFA synthase or the Asp^{381}-Asp^{382} CFAS-DD variant (20 μM) by FtsH (0.5 μM hexamer). The experiments in panels D and E were performed at 37 °C in the presence of 5 mM ATP and were monitored by SDS-PAGE.

To test more directly if the C-terminal residues play a role in FtsH degradation, we truncated two, five, eight, or eleven residues from CFA synthase and observed little effect on degradation (Fig. 3.4D). FtsH does not degrade an Arc-ssrA variant with the C-terminal Ala-Ala dipeptide changed to Asp-Asp (Herman et al., 2003). However, changing the C-terminal dipeptide of CFA synthase from Ala-Arg to Asp-Asp (CFAS-DD) did not slow FtsH degradation (Fig. 3.4E). Hence, neither the N-terminal nor C-terminal residues of CFA synthase are required for FtsH degradation.

94

An internal disordered sequence is not required for FtsH degradation. The N-domain of CFA

synthase is connected to the C-terminal domain by a sequence (residues 100-120) that is disordered

in the crystal structure (Hari and Sauer, 2018). We hypothesized that FtsH might recognize and/or

initiate degradation within this linker and then degrade CFA synthase in both C-to-N and N-to-C

directions, as proposed for other substrates (Chiba et al., 2002; Okuno et al. 2006). We tested this

model in two ways. First, we replaced the wild-type ARLFN[105] LQSKK[110] RAWIV[115] GKEHY[120]

sequence with a GGGSG[105] SGGGG[110] SGSGG[115] GGSGS[120] segment composed solely of

glycines and serines. Notably, FtsH degraded this mutant (GS[linker]-CFAS) as fast as it degraded

wild-type CFA synthase (Fig. 3.5A). Thus, the sequence of the wild-type linker is required neither

for recognition by FtsH nor for the initiation of degradation. The distance between residues 99 and

121 is ~25 residues, which in principle could be spanned by a linker of only nine residues. Thus,

we tested if linker length was important by deleting residues 110-120 from CFA synthase or

GS[linker]-CFAS. In each case, the deletion mutant was degraded at a rate similar to wild-type CFA

synthase (Fig. 3.5B), indicating that linker length plays little role in FtsH recognition.

As described previously (Hari and Sauer, 2018), the two domains of CFA synthase remain

associated after Ni^{++}-NTA affinity purification from a strain harboring a plasmid-borne gene (Fig.

3.5C) that expresses a His$_6$-tagged N domain and untagged C domain separately. When this split

protein was incubated with FtsH, the N-domain was degraded rapidly and the C-domain was

degraded more slowly (Fig. 3.5D). Interestingly, C-domain degradation ceased once the N-domain

was completely degraded, indicating that C-domain degradation requires the presence of the N-

domain. This result could be explained if FtsH binds to a sequence within the N-domain of the

split substrate and efficiently initiates degradation of this domain, while less efficiently initiating degradation of the C-domain.
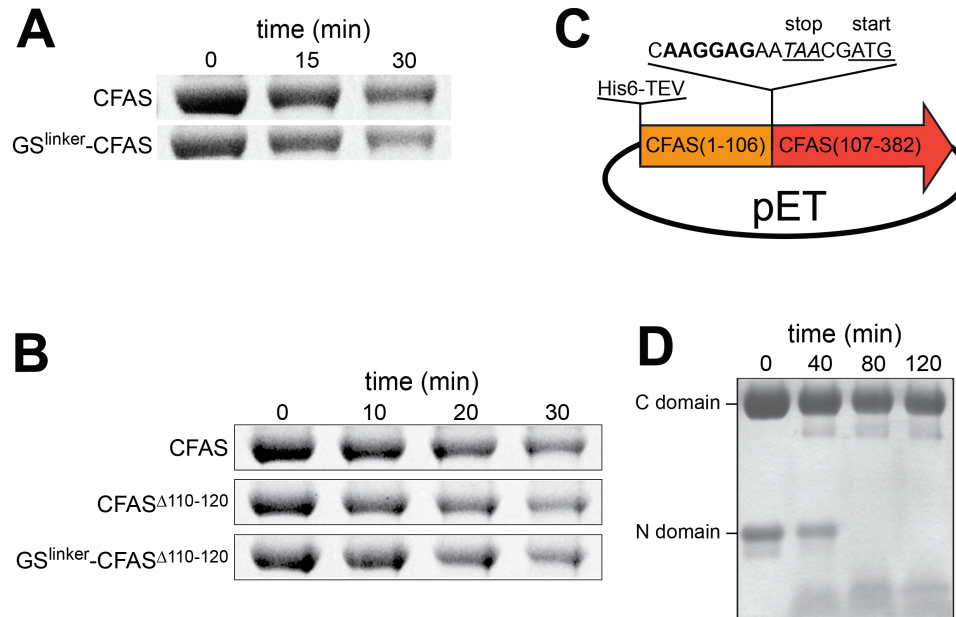

Figure 3.5. Degradation of linker variants and split CFA synthase. (**A**) FtsH (0.5 µM hexamer) degrades CFA synthase and GS^{linker}-CFAS (20 µM each) at similar rates. (**B**) FtsH degrades linker deletion variants of CFA synthase at similar rates. Conditions as in panel A. (**C**) An engineered gene (Shine-Dalgarno sequence in bold) was used to express the N-terminal and C-terminal domains of CFA synthase as separate polypeptides. (**D**) The complex of both domains was purified by Ni^{++}-NTA affinity and incubated with FtsH under the same conditions as in Fig. 1B.

Effects of blocking the N-terminus or C-terminus. An internal recognition model predicts that blocking the CFA synthase termini by fusion to other proteins should still allow degradation unless the fusion protein clashes with FtsH during recognition. Indeed, we found that FtsH degraded SUMO-CFAS and CFAS-SUMO fusion proteins (Fig. 3.6A), whereas SUMO as a free protein was not degraded (Fig. 3.6B).
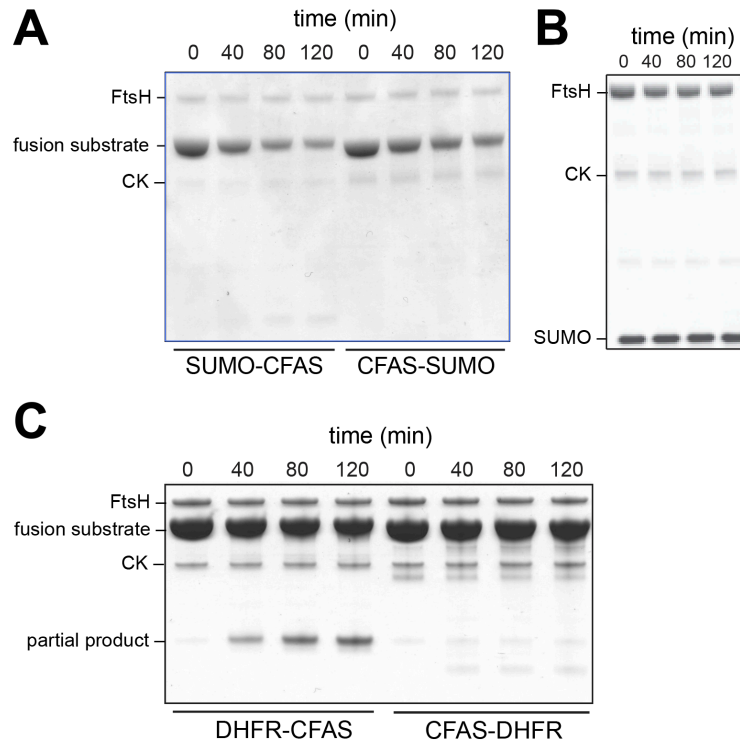
Figure 3.6. **Degradation of fusion proteins**. (**A**) Degradation of SUMO-CFAS and CFAS-SUMO (20 µM each) by FtsH (0.5 µM hexamer) at 37 °C. (**B**) SUMO was purified by size-exclusion chromatography following overnight cleavage of SUMO-CFAS with Ulp1 (1:100 mol. eq.) and 20 µM was incubated with FtsH (0.5 µM hexamer) at 37 °C. (**C**) Incubation of DHFR-CFAS and CFAS-DHFR (20 µM each) with FtsH (0.5 µM hexamer) at 37 °C.

We also fused *E. coli* dihydrofolate reductase (DHFR) either to the N-terminus (DHFR-CFAS) or C-terminus (CFAS-DHFR) of CFA synthase. In the presence of methotrexate, which prevents FtsH proteolysis of DHFR (Koodathingal et al., 2009), FtsH degradation of DHFR-CFAS produced a partially degraded species, which electrophoresed in SDS-PAGE at a molecular weight slightly larger than DHFR (Fig. 3.6C, left side). After excising this intermediate from the gel, sequential Edman degradation revealed an N-terminal sequence (Gly-Ser-Ser-His-His) identical to that of the DHFR construct. These results support a model in which FtsH degradation of DHFR-CFAS begins at an internal CFA-synthase sequence but cannot proceed through DHFR. Little FtsH degradation of the CFAS-DHFR fusion protein was observed (Fig. 3.6C, right side), likely because

the fusion protein at the C-terminus interferes indirectly with FtsH recognition of sequence determinants in the N-domain of CFA synthase.

Discussion

CFA synthase converts unsaturated fatty acids in the lipid bilayer of *E. coli* into cyclopropyl fatty acids at the onset of stationary phase (Law, 1971; Taylor and Cronan, 1979). Its subsequent depletion is dependent on the heat-shock promoter σ^{32}, which controls the transcription of several AAA+ family proteases, including FtsH (Chang et al., 2000; Zhao et al., 2005). In this work, we demonstrate that the membrane-anchored AAA+ protease FtsH degrades CFA synthase both in biochemical experiments *in vitro* and in *E. coli*. CFA synthase was not identified as a substrate for FtsH in proteomic studies (Westphal et al., 2012; Arends et al., 2016), possibly because of its relatively low abundance. Interestingly, CFA synthase itself is not regulated by σ^{32} but by σ^{S}, the stationary-phase transcription factor. LpxC and YfgM are also degraded by FtsH during stationary phase (Bittner et al., 2017; Thomanek et al., 2019). Hence, these findings raise the possibility that FtsH plays a more global role in stress response and suggest that additional substrates might be discovered through targeted proteomic studies performed under stress conditions other than heat shock.

An important and influential early study suggested that FtsH is a 'weak unfoldase' (Hermann et al., 2003). For example, many of its soluble substrates (e.g., σ^{32}, degron-tagged Arc repressor, and the N-terminal domain of λ repressor) equilibrate rapidly between folded and unfolded species. Moreover, FtsH did not degrade stable native substrates, like GFP-ssrA, which can be degraded by the AAA+ ClpXP and ClpAP proteases (Hermann et al., 2003). More recent investigations, however, show that FtsH can degrade integral membrane proteins, overcoming the large energetic

barrier needed to dislodge these proteins from the membrane (Langklotz et al., 2012; Hari and Sauer, 2106; Yang et al. 2018; 2019). We also recently found that FtsH degrades *E. coli* DHFR (Morehouse et al., 2022), a protein thought to be refractory to FtsH proteolysis (Herman et al., 2003). Hence, accumulating evidence suggests that FtsH may not be an inherently weak protein unfoldase. CFA synthase represents another example of FtsH degrading a protein with substantial kinetic stability. At 37 °C, we find that CFA synthase can be degraded by FtsH at a rate about 5-fold faster than dimers, the predominant oligomeric species, dissociate to monomers, implying that a dimeric and not a monomeric form is the proteolytic target. As discussed below, it is possible that a dimeric CFA synthase species with a transiently unfolded region is recognized and degraded by FtsH.

AAA+ proteases need to recognize a target protein and also to engage an unstructured segment of this substrate in their axial channel to initiate the unfolding and translocation reactions that are required for degradation (Sauer and Baker, 2011). In principle, recognition and engagement could both involve the same disordered segment, as demonstrated for ClpXP and the ssrA tag (Fei et al., 2020), or recognition could involve binding regions of the AAA+ protease other than the axial channel with engagement of a peptide being relatively non-specific. FtsH and many other AAA+ proteases have been shown to recognize disordered sequences at the N-terminus or C-terminus of substrates (Herman et al., 1998; Gottesman et al., 1998; Chiba et al., 2002; Flynn et al., 2003; Herman et al., 2003; Neher et al., 2003a; 2003b; Fuhrer et al., 2007; Sauer and Baker, 2011; Chiba et al., 2002). FtsH degradation of CFA synthase, by contrast, does not depend on sequences at either protein terminus. Specifically, deletion of the N-terminal 15 residues or C-terminal 10 residues of CFA synthase results in almost no change in the rate of FtsH degradation. These results suggest that FtsH recognizes an internal degron in CFA synthase. Consistent with this proposal,

blocking either terminus of CFA synthase by fusion to the SUMO protein has little effect on degradation. Fusion of DHFR to the C-terminus but not the N-terminus of CFA synthase did prevent degradation, which would normally be taken as evidence for degradation that begins at the C-terminus and proceeds to the N-terminus. We cannot rigorously eliminate this possibility, but it seems unlikely in light of the SUMO result, the structure, and our biochemical and mutational results.

Residues 100-120 form a disordered linker between the N-terminal and C-terminal domains in the crystal structure of *E. coli* CFA synthase (Hari and Sauer, 2018) and thus were a good candidate for an internal FtsH degron and/or a site at which degradation initiates. However, our mutational studies show that the sequence of residues 100-120 can be changed dramatically without affecting FtsH degradation. Moreover, no other internal CFA synthase sequences are disordered in the crystal structure. Thus, our results seem to rule out the obvious N-terminal, C-terminal, or disordered internal sequence candidates of CFA synthase as acting as degrons for FtsH degradation. How then does FtsH recognize and degrade CFA synthase? A model in which a segment of dimeric CFA synthase, probably within the N domain, unfolds transiently to provide a disordered polypeptide that is recognized and engaged by the axial channel of FtsH is consistent with our experimental results. However, the identity of this segment remains to be determined. Another possibility, which is less likely in our opinion, is that CFA synthase contains redundant degrons (e.g., the 100-120 region or the C-terminal region or the N-terminal region) and thus that mutation of any one of these regions has little effect of FtsH degradation.

Our findings establish CFA synthase as a substrate of FtsH. In light of this discovery and prior work (Flynn et al., 2003; Neher et al., 2003a; 2006; Lim et al., 2013), we believe that additional proteins that are upregulated during cellular responses to stress are likely to be FtsH substrates.

MATERIALS AND METHODS

Bacterial strains. *E. coli* strain X90 (*Δlac pro XIII, ara, nalA, argE(am), thi⁻, rifʳ, [F'lacI^{q1}, lacZY^{+,} proAB^{+}]*) was obtained from laboratory stocks. Deletion strains lacking *lon* or *hslU* were generated by P1 transduction and verified by Sanger sequencing. Strain AR3289 (W3110 *sfhC21 zad220::Tn10*) and AR3289 *ΔftsH::kan* were kindly provided by Teru Ogura (Kumamoto University).

Plasmids. The *cfa* gene from *E. coli* was amplified from genomic DNA and cloned downstream of an encoded His$_6$ tag and TEV site into a pET21-based plasmid. It was also cloned without any tags into pTrc99a. Further modifications were made as needed by site-directed mutagenesis. All sequences were verified by Sanger sequencing. The base Arc gene used for all studies was Arc-(Cys^{54})-st11. All other plasmids were obtained from laboratory stocks.

Proteins. Purified Lon, HslU, HslV, ClpA, and Arc-sul20 were kindly provided by V. Baytshtok (MIT). ClpX, ClpP, FtsH, and Arc-ssrA were expressed and purified as described (Hari and Sauer, 2016). CFA synthase as well as mutants and fusion proteins were purified as described (Hari and Sauer, 2018).

^{35}S-labeled CFA synthase was prepared as follows: *E. coli* T7 Express cells harboring a pET21-based plasmid with a gene encoding His$_6$-TEV-CFA synthase were grown in 100 mL of minimal media (without methionine or cysteine) to log-phase and induced with 0.5 mM IPTG and EXPRE^{35}S^{35}S protein labeling mix (40 µCi/mL, PerkinElmer) for 3 h at 30 °C. The harvested pellet was subjected to three cycles of freeze-thawing, then resuspended in lysis buffer (50 mM Tris-HCl, pH 8.0, 100 mM NaCl, 20 mM imidazole, 10% glycerol) before incubating with lysozyme and PopCulture reagent (Novagen) at 4 °C for 30 min. After centrifugation, the

supernatant was added to 100 μL of Ni-NTA slurry, washed extensively with lysis buffer, and the protein was eluted with lysis buffer containing 300 mM imidazole. After incubation with TEV protease and dialyzing into lysis buffer overnight at 4 °C, the solution was applied to 100 μL of Ni-NTA slurry. The flow-through was concentrated and snap-frozen for storage.

Biochemical assays. Substrates and enzymes were incubated at the indicated concentrations in PD buffer (50 mM Tris-HCl, pH 8.0, 10 mM KCl, 5 mM $MgSO_4$, 10 μM $ZnCl_2$, 10% glycerol, 1 mM DTT, 0.1% Igepal CA-630) with ATP (4 mM) and a regeneration system (16 mM creatine phosphate, 75 μg/mL creatine kinase). Samples were quenched at indicated times with SDS loading buffer, separated by SDS-PAGE, and visualized by Coomassie staining. ATP-hydrolysis rates were measured using a continuous spectrophotometric assay (Norby,1988).

Enzyme kinetics. Unlabeled and ^{35}S-labeled CFA synthase were mixed to the indicated concentrations and incubated with FtsH (0.1 or 0.2 μM hexamer) in PD buffer with ATP (4 mM) in a regeneration system at 37 °C. Samples were quenched with TCA (12.5%) and allowed to precipitate overnight at 4 °C. After centrifugation, the soluble fraction was counted by scintillation. For quantitative kinetic measurements of Arc degradation, Cys^{54} was labeled with Dylight-488 maleimide (Thermo Fisher), and degradation was monitored by de-quenching of fluorescence (excitation 495 nm; emission 515 nm).

Pulse-chase analysis. *E. coli* strains harboring untagged CFA synthase in pTrc99a were grown to early log phase in Luria-Bertani media, washed with M9 salts base, then resuspended in minimal media (without methionine or cysteine) to O.D.= 0.3. The cells were grown for an additional 30 min at 37 °C before they were induced with 50 μM IPTG for 5 min, pulsed with EXPRE^{35}S^{35}S protein labeling mix (20 μCi/mL) for 5 min, then chased with 5 mM phenyl-β-D-galactopyranoside

and 10 mM unlabeled amino acids. Samples were taken at different times and precipitated using TCA. The pellets were washed with acetone, resolubilized in SDS loading buffer, and separated by SDS-PAGE. A sample of purified ^{35}S-labeled CFA synthase was also loaded onto the gel as a molecular-weight standard. The gels were then dried, exposed, and imaged as described above. Uninduced samples were treated in the same way but were incubated without IPTG before pulsing. Half-lives were calculated by densitometry.

Phospholipid analysis. Liquid cultures of *E. coli* strains AR3289 and AR3289 *ΔftsH:kan* were grown overnight, and ~10^{11} cells were harvested and washed with Tris-buffered saline (50 mM Tris-HCl, pH 7.5, 150 mM NaCl) before freezing.

Lipids were extracted as follows: each pellet was thawed and resuspended in residual buffer before transferring to a glass vial and extracting with 3 mL chloroform:methanol (2:1). If necessary, a small amount of water was added to separate emulsions. The organic layer was washed twice with 150 mM NaCl and concentrated *in vacuo* to yield a clear film. Phospholipids were selectively precipitated with acetone for at least 2 h at 4 °C. Precipitates were dissolved in chloroform. Typical yield was 5 mg.

Fatty acid methyl esters (FAMEs) were prepared as described (Ichihara and Fukubayashi, 2010). Briefly, 2.5 mg of dried phospholipid extract was dissolved in toluene (0.1 mL), followed by addition of methanol (0.75 mL) and hydrochloric acid (8% v/v in methanol). The solution was vortexed and incubated at 100 °C for 1 h and then cooled to room temperature. FAMEs were extracted from the solution using hexane (0.5 mL) and water (0.5 mL). GC/MS was performed by the Harvard Small Molecule Mass Spectrometry Facility.

Subunit exchange. An aliquot of purified CFA synthase was desalted into GF buffer (50 mM HEPES, pH 7.5, 100 mM NaCl, 1 mM βME, 10% glycerol) and labeled with six equivalents of Dylight-488 or -650 maleimide (Thermo Fisher) for 30 min at room temperature. The reactions were quenched with 2 mM DTT, and excess dye was removed by desalting. Labeled proteins (2 μM each) were mixed at equal volumes and monitored by fluorescence (excitation 480 nm; emission 675 nm). The curve was fit to a growth equation (Weibull, 1951).

Biolayer interferometry. Assays were performed using an Octet RED96 instrument (ForteBio/Molecular Devices) at 30 °C using GF buffer with 0.05 mg/mL bovine serum albumin. Biosensor tips coated with Anti-Penta-HIS (His1K) antibody were loaded with proteins (400 nM) to a response of ~0.7 nm. The tips were then moved to solutions containing anhydrotrypsin (Molecular Innovations, 150 nM), and responses were monitored at a sampling rate of 5 Hz.

REFERENCES

Abdiche Y, Malashock D, Pinkerton A, Pons J (2008) Determining kinetics and affinities of protein interactions using a parallel real-time label-free biosensor, the Octet. Anal Biochem **377**, 209−217.

Arends J, Thomanek N, Kuhlmann K, Marcus K, Narberhaus F (2016) *In vivo* trapping of FtsH substrates by label-free quantitative proteomics. Proteomics **16**, 3161–3172.

Baytshtok V, Fei X, Grant RA, Baker TA, Sauer RT (2016) A structurally dynamic region of the HslU intermediate domain controls protein degradation and ATP hydrolysis. Structure **24**, 1766–1777.

Bittner LM, Arends J, Narberhaus (2017. When, how and why? Regulated proteolysis by the essential FtsH protease in *Escherichia coli*. Biol Chem 398, 625–635.

Chang YY, Cronan JE, Jr. (1999) Membrane cyclopropane fatty acid content is a major factor in acid resistance of *Escherichia coli*. Mol Microbiol **33**, 249–259.

Chang YY, Eichel J, Cronan JE, Jr. (2000) Metabolic instability of *Escherichia coli* cyclopropane fatty acid synthase is due to RpoH-dependent proteolysis. J Bacteriol **182**, 4288–4294.

Chiba S, Akiyama Y, Ito K (2002) Membrane protein degradation by FtsH can be initiated from either end. J Bacteriol **184**, 4775–4782.

Fei X, Bell TA, Barkow SR, Baker TA, Sauer RT (2020) Structural basis of ClpXP recognition and unfolding of ssrA-tagged substrates. Elife **9**, e61496.

Flynn JM, Neher SB, Kim YI, Sauer RT, Baker TA (2003) Proteomic discovery of cellular substrates of the ClpXP protease reveals five classes of ClpX-recognition signals. Mol Cell **11**, 671-683.

Führer F, Müller A, Baumann H, Langklotz S, Kutscher B, Narberhaus F (2007) Sequence and length recognition of the C-terminal turnover element of LpxC, a soluble substrate of the membrane-bound FtsH protease. J Mol Biol **372**, 485–496.

Gottesman S, Roche E, Zhou Y, Sauer RT (1998) The ClpXP and ClpAP proteases degrade proteins with carboxy-terminal peptide tails added by the SsrA-tagging system. Genes Dev **12**, 1338–1347.

Grogan DW, Cronan JE, Jr. (1986) Characterization of *Escherichia coli* mutants completely defective in synthesis of cyclopropane fatty acids. J Bacteriol **166**, 872–877.

Gur E, Sauer RT (2008) Recognition of misfolded proteins by Lon, a AAA(+) protease. Genes Dev **22**, 2267–2277.

Hari SB, Sauer RT (2016) The AAA+ FtsH protease degrades an ssrA-tagged model protein in the inner membrane of *Escherichia coli*. Biochemistry **55**, 5649–5652.

Hari SB, Grant RA, Sauer RT (2018) Structural and Functional Analysis of *E. coli* Cyclopropane Fatty Acid Synthase. Structure **26**, 1251-1258.

Herman C, Prakash S, Lu CZ, Matouschek A, Gross CA (2003) Lack of a robust unfoldase activity confers a unique level of substrate specificity to the universal AAA protease FtsH. Mol Cell **11**, 659–669.

Herman C, Thevenet D, Bouloc P, Walker GC, D'Ari R (1998) Degradation of carboxy-terminal-tagged cytoplasmic proteins by the *Escherichia coli* protease HflB (FtsH). Genes Dev **12**, 1348–1355.

Herman C, Thevenet D, D'Ari R, Bouloc P (1995) Degradation of sigma 32, the heat shock regulator in *Escherichia coli*, is governed by HflB. Proc Natl Acad Sci USA 92, 3516–3520.

Hoskins JR, Yanagihara K, Mizuuchi K, Wickner S (2002) ClpAP and ClpXP degrade proteins with tags located in the interior of the primary sequence. Proc Natl Acad Sci USA **99**, 11037–11042.

Ichihara K, Fukubayashi Y (2010) Preparation of fatty acid methyl esters for gas-liquid chromatography. J Lipid Res **51**, 635–640.

Jonsson T, Waldburger CD, Sauer RT (1996) Nonlinear free energy relationships in Arc repressor unfolding imply the existence of unstable, native-like folding intermediates. Biochemistry **35**, 4795–4802.

Kenniston JA, Baker TA, Fernandez JM, Sauer RT (2003) Linkage between ATP consumption and mechanical unfolding during the protein processing reactions of an AAA+ degradation machine. Cell **114**, 511–520.

Koodathingal P, Jaffe NE, Kraut DA, Prakash S, Fishbain S, Herman C, Matouschek A (2009) ATP-dependent proteases differ substantially in their ability to unfold globular proteins. J Biol Chem **284**, 18674–18684.

Kraut DA, Matouschek A (2011) Proteasomal degradation from internal sites favors partial proteolysis via remote domain stabilization. ACS Chem Biol **6**, 1087–1095.

Langklotz S, Baumann U, Narberhaus F (2012) Structure and function of the bacterial AAA protease FtsH. Biochim Biophys Acta **1823**, 40-48.

Law JH (1971) Biosynthesis of cyclopropane rings. Acc Chem Res **4**, 199–203.

Lim B, Miyazaki R, Neher S, Siegele DA, Ito K, Walter P, Akiyama Y, Yura T, Gross CA (2013) Heat shock transcription factor sigma32 co-opts the signal recognition particle to regulate protein homeostasis in *E. coli*. PLoS Biol **11**, e1001735.

Meyer AS, Baker TA (2011) Proteolysis in the *Escherichia coli* heat shock response: a player at many levels. Curr Opin Microbiol **14**, 194–199.

Neher SB, Flynn JM, Sauer RT, Baker TA (2003) Latent ClpX-recognition signals ensure LexA destruction after DNA damage. Genes Dev **17**, 1084–1089.

Neher SB, Sauer RT, Baker TA (2003) Distinct peptide signals in the UmuD and UmuD' subunits of UmuD/D' mediate tethering and substrate processing by the ClpXP protease. Proc Natl Acad Sci USA **100**, 13219–13224.

Neher SB, Villén J, Oakes EC, Bakalarski CE, Sauer RT, Gygi SP, Baker TA (2006) Proteomic profiling of ClpXP substrates after DNA damage reveals extensive instability within SOS regulon. Mol Cell **22**, 193–204.

Norby JG (1988) Coupled assay of Na+,K+-ATPase activity. Methods Enzymol **156**, 116–119.

Okuno T, Yamanaka K, Ogura T (2006) An AAA protease FtsH can initiate proteolysis from internal sites of a model substrate, apo-flavodoxin. Genes Cells **11**, 261–268.

Piwko W, Jentsch S (2006) Proteasome-mediated protein processing by bidirectional degradation initiated from an internal site. Nat Struct Mol Biol **13**, 691–697.

Prakash S, Tian L, Ratliff KS, Lehotzky RE, Matouschek A (2004) An unstructured initiation site is required for efficient proteasome-mediated degradation. Nat Struct Mol Biol **11**, 830–837.

Sauer RT, Baker TA (2011) AAA+ proteases: ATP-fueled machines of protein destruction. Annu Rev Biochem **80**, 587–612.

Taylor FR, Cronan JE, Jr. (1979) Cyclopropane fatty acid synthase of *Escherichia coli*. Stabilization, purification, and interaction with phospholipid vesicles. Biochemistry **18**, 3292-3300.

Thomanek N, Arends J, Lindemann C, Barkovits K, Meyer HE, Marcus K, Narberhaus F (2019) Intricate crosstalk between lipopolysaccharide, phospholipid and fatty acid metabolism in *Escherichia coli* modulates proteolysis of LpxC. Front Microbiol **9**, 3285.

Wang AY, Cronan JE, Jr. (1994) The growth phase-dependent synthesis of cyclopropane fatty acids in *Escherichia coli* is the result of an RpoS(KatF)-dependent promoter plus enzyme instability. Mol Microbiol **11**, 1009–1017.

Weibull W (1951) A statistical distribution function of wide applicability. J of Appl Mech 18, 293–297.

Westphal K, Langklotz S, Thomanek N, Narberhaus F (2012) A trapping approach reveals novel substrates and physiological functions of the essential protease FtsH in *Escherichia coli*. J Biol Chem **287**, 42962–42971.

Yang Y, Guo R, Gaffney K, Kim M, Muhammednazaar S, Tian W, Wang B, Liang J, Hong H (2018) Folding-degradation relationship of a membrane protein mediated by the universally conserved ATP-dependent protease FtsH. J Am Chem Soc **140**, 4656–4665.

Yang Y, Gunasekara M, Muhammednazaar S, Li Z, Hong H (2019) Proteolysis mediated by the membrane-integrated ATP-dependent protease FtsH has a unique nonlinear dependence on ATP hydrolysis rates. Protein Sci **28**, 1262–1275.

Yokosawa H, Ishii S (1977) Anhydrotrypsin: new features in ligand interactions revealed by affinity chromatography and thionine replacement. J Biochem **81**, 647–656.

Zhao K, Liu M, Burgess RR (2005) The global transcriptional response of *Escherichia coli* to induced sigma 32 protein involves sigma 32 regulon activation followed by inactivation and degradation of sigma 32 in vivo. J Biol Chem **280**, 17758–17768.

Zhou Y, Gottesman S, Hoskins JR, Maurizi MR, Wickner S (2001) The RssB response regulator directly targets sigma(S) for degradation by ClpXP. Genes Dev **15**, 627–637.

Chapter IV

Future Directions

To understand the degradation mechanism of FtsH more thoroughly, studies that focus on characterizing the determinants of the initial binding step will be important. This chapter includes preliminary results that were gathered in an attempt to assay binding of substrate to FtsH *in vitro* using Biolayer Interferometry (BLI). Ascertaining the conditions that allow formation and detection of a stable recognition complex will be critical in gaining insight about which elements of DHFR are most important for binding. These assays should also be applicable to other FtsH substrates, such as CFAS, for which the recognition mechanism is still uncertain and may also be useful for follow-up studies, which could include probing structural determination of the FtsH-substrate complex.

The initial binding step is critical in establishing the recognition complex and eventually committing the substrate to degradation by a AAA+ protease (Fig. 1.3). Although determining K_M for degradation provides an upper bound on the affinity of substrate for the AAA+ protease, specifically probing the initial binding step will be valuable in understanding the determinants of substrate recognition. One recent approach for studying substrate binding and engagement by ClpXP utilized a fluorescence-quenching assay with a quencher-labelled substrate and a single-chain hexamer of ClpX that was engineered to have a single solvent-exposed cysteine for fluorophore labelling (Saunders et al., 2020). Application of this fluorescence-quenching technique proved to be challenging for FtsH, as I found that the removal of the native cysteines and the introduction of new cysteines for labelling reduced the ATPase activity of FtsH by more than 50%.

Optical biosensors and BLI can be used to determine the kinetics and affinity of molecular interactions (Abdiche et al., 2008). This optical analytical technique detects the change in the number of molecules bound to the fiberoptic sensor tip by analyzing the interference patterns of white light reflecting from the sensor tip (Fig. 4.1A) (Kumaraswamy & Tobias, 2015). BLI can monitor protein-protein interactions in which one of the partner molecules is modified with an epitope tag or a functional group to allow its immobilization on the sensor tip.

In a typical BLI experiment, a biosensor tip is moved between different solutions in a multi-well plate (Fig. 4.1B). First, the tip is moved into a well that contains buffer only to determine the baseline. Then, the tip is moved into a well containing the first macromolecule of interest that becomes immobilized or "loaded" onto the sensor tip via interactions such as biotin-streptavidin. Next, the tip is moved to a well containing the analyte of interest to monitor association. Movement of the tip back into buffer alone allows dissociation of the complex to be analyzed.
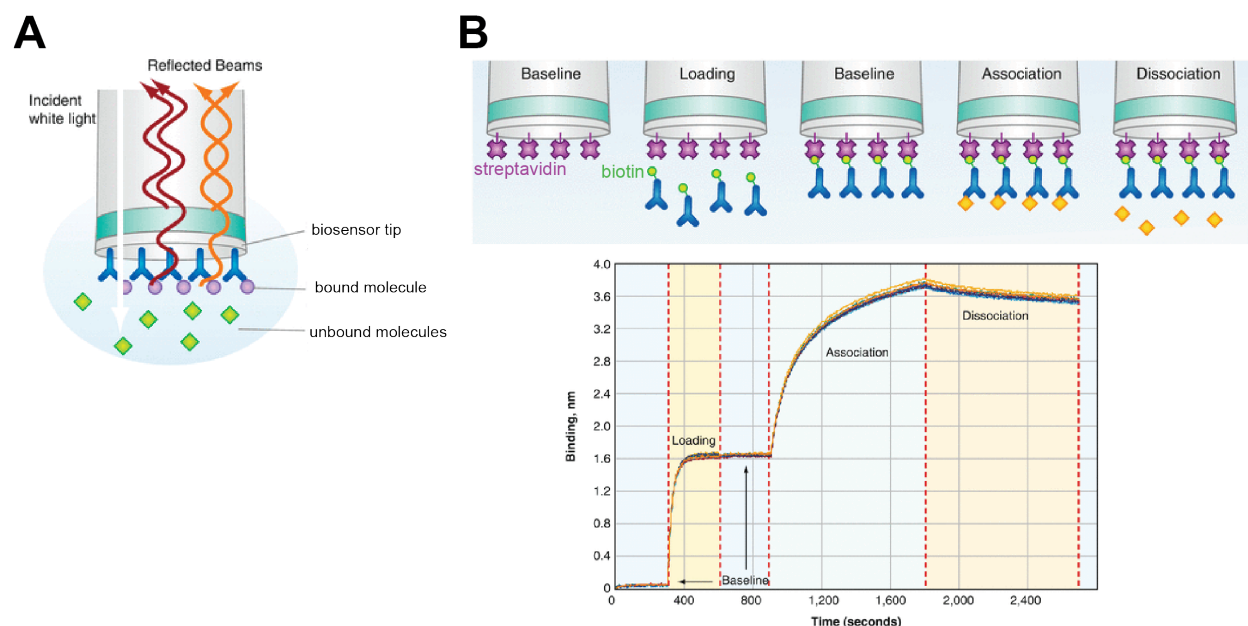

Figure 4.1. BLI as a technique to measure molecular interactions. *A,* A diagram of a biosensor tip. *B,* Kinetics experiment with a biotin (green) - conjugated macromolecule (blue), ligand (orange) and a streptavidin (purple) coated biosensor. All panels adapted from (Kumaraswamy & Tobias, 2015).

The BLI-based binding assay should be able to test the hypothesis that Leu28 and Ala29 in DHFR, which slow FtsH degradation when mutated (Fig. 2.5), also decrease binding for FtsH. The slow rate of FtsH degradation of these DFFR substrates (k_{deg} = 0.2 min^{-1} enz^{-1}) and the use of ATPγS, a slowly-hydrolyzed or non-hydrolysable ATP analog, should reduce the likelihood that DHFR will be consumed during the assay. If degradation proves to be problematic, FtsH variants that are deficient in ATP hydrolysis (Walker-B mutant) or peptide-bond cleavage (Zn^{2+} coordinating mutant) could be used.

BLI, using streptavidin-coated biosensors, has been used to monitor the association and dissociation kinetics of ClpP with biotinylated single-chain ClpX$^{\Delta N}$ pseudo-hexamers (Amor et al., 2016; Amor et al., 2019). In a similar manner, I conjugated a biotin group to the single solvent-exposed cysteine on purified DHFR using maleimide chemistry and showed that different concentrations of DHFR^{biotin} associated with a streptavidin-coated sensor using BLI (Fig. 4.2A). After binding 100 nM DHFR^{biotin} to the streptavidin-coated sensor, it remained stably bound after shifting the sensor into buffer lacking DHFR^{biotin} (Fig. 4.2B).
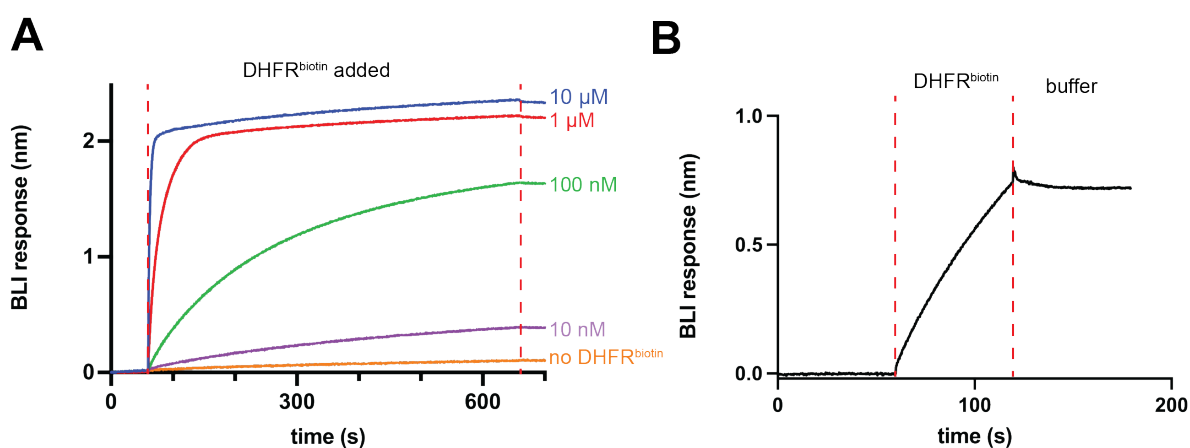

Figure 4.2. Using BLI to develop a DHFR-FtsH binding assay. *A*, Different concentrations of DHFR^{biotin} were loaded onto a streptavidin coated biosensor. *B*, 100 nM biotinylated DHFR was loaded and then the streptavidin-coated sensor tip was moved into FtsH reaction buffer without DHFR^{biotin}.

A pilot experiment showed a small increase in BLI signal (< 0.1 nm) when the sensor tip loaded with DHFR[biotin] was subsequently moved into a well containing FtsH. However, the small signal change observed could have represented non-specific binding to the sensor or signal drift. An important control would be to test FtsH "association" to the sensor tip saturated with DHFR[biotin] versus sensor tip without any DHFR[biotin] loaded to ensure that DHFR-specific binding signal is much greater than any non-specific binding to the sensor tip.

In principle, the FtsH-DHFR BLI binding assay could be optimized to potentially increase the association signal. For example, the temperature and enzyme concentrations could be increased to promote binding. It would also be possible to use a maleimide-biotin with a longer spacer arm length as the proximity of DHFR to the streptavidin-coated sensor tip might inhibit FtsH binding. The high-throughput capabilities of BLI can be harnessed by using multi-well plates, which should accelerate optimization studies.

Establishing conditions for maintaining a stable enzyme-substrate complex could also aid cryo-EM studies of the DHFR-FtsH structure. Detergents, like LMNG, have been shown to be effective in capturing detergent-solubilized membrane protein complexes for cryo-EM studies (Carvalho et al., 2021). Model lipid bilayer systems, including Nanodiscs and bicelles, have also been successfully utilized to study bacterial FtsH (Yang et al., 2018; Prabudiansyah et al., 2021; Liu et al., 2022). These techniques may allow capture of the substrate-bound complex in the lipid bilayer, which would provide valuable insights similar to those obtained from high-resolution EM structures of the eukaryotic orthologs of FtsH and from the structure of *Mycobacterium*

tuberculosis proteasome bound to DHFR with a prokaryotic ubiquitin-like protein (Pup) as the degron (Puchades et al., 2017; Puchades et al., 2019; Kavalchuk et al., 2022).

Many proteins have been proposed to be substrates of FtsH by candidate-based approaches, genetics, and proteomics (Westphal et al., 2012; Arends et al., 2016; Bittner et al., 2017; Lindemann et al., 2018). Binding assays, like the one proposed in this chapter, would provide a technique to analyze these substrates based on affinity, which may reveal novel degrons. The BLI-based assay could also be applied to test hypotheses, such as the proposed length requirement for a cytosolic extension that may be important for targeting certain protein substrates for FtsH degradation (Chiba et al., 2000; Chiba et al., 2002). Developing an assay that specifically monitors the formation of the recognition complex could also be extended to other AAA+ proteases, as the label-free method that does not require modification of the AAA+ protease. Furthermore, this binding technique offers the potential to study the effects on substrate recognition of micromolecular changes at the amino-acid level and the effects of macromolecular changes that occur by association with adaptors or by transitions into higher order quaternary structures.

REFERENCES

Abdiche, Y., Malashock, D., Pinkerton, A., & Pons, J. (2008). Determining kinetics and affinities of protein interactions using a parallel real-time label-free biosensor, the Octet. *Analytical Biochemistry*, *377*(2), 209-217. https://doi.org/https://doi.org/10.1016/j.ab.2008.03.035

Amor, A. J., Schmitz, K. R., Baker, T. A., & Sauer, R. T. (2019). Roles of the ClpX IGF loops in ClpP association, dissociation, and protein degradation. *Protein Sci*, *28*(4), 756-765. https://doi.org/10.1002/pro.3590

Amor, A. J., Schmitz, K. R., Sello, J. K., Baker, T. A., & Sauer, R. T. (2016). Highly Dynamic Interactions Maintain Kinetic Stability of the ClpXP Protease During the ATP-Fueled Mechanical Cycle. *ACS Chemical Biology*, *11*(6), 1552-1560. https://doi.org/10.1021/acschembio.6b00083

Arends, J., Thomanek, N., Kuhlmann, K., Marcus, K., & Narberhaus, F. (2016). In vivo trapping of FtsH substrates by label-free quantitative proteomics. *Proteomics*, *16*(24), 3161-3172. https://doi.org/10.1002/pmic.201600316

Bittner, L. M., Arends, J., & Narberhaus, F. (2017). When, how and why? Regulated proteolysis by the essential FtsH protease in Escherichia coli. *Biol Chem*, *398*(5-6), 625-635. https://doi.org/10.1515/hsz-2016-0302

Carvalho, V., Prabudiansyah, I., Kovacik, L., Chami, M., Kieffer, R., van der Valk, R., de Lange, N., Engel, A., & Aubin-Tam, M. E. (2021). The cytoplasmic domain of the AAA+ protease FtsH is tilted with respect to the membrane to facilitate substrate entry. *J Biol Chem*, *296*, 100029. https://doi.org/10.1074/jbc.RA120.014739

Chiba, S., Akiyama, Y., & Ito, K. (2002). Membrane protein degradation by FtsH can be initiated from either end. *J Bacteriol*, *184*(17), 4775-4782. https://www.ncbi.nlm.nih.gov/pmc/articles/PMC135282/pdf/0311.pdf

Chiba, S., Akiyama, Y., Mori, H., Matsuo, E., & Ito, K. (2000). Length recognition at the N-terminal tail for the initiation of FtsH-mediated proteolysis. *EMBO Rep*, *1*(1), 47-52. https://doi.org/10.1093/embo-reports/kvd005

Kavalchuk, M., Jomaa, A., Müller, A. U., & Weber-Ban, E. (2022). Structural basis of prokaryotic ubiquitin-like protein engagement and translocation by the mycobacterial Mpa-proteasome complex. *Nature Communications*, *13*(1), 276. https://doi.org/10.1038/s41467-021-27787-3

Kumaraswamy, S., & Tobias, R. (2015). Label-free kinetic analysis of an antibody-antigen interaction using biolayer interferometry. *Methods Mol Biol*, *1278*, 165-182. https://doi.org/10.1007/978-1-4939-2425-7_10

Lindemann, C., Thomanek, N., Kuhlmann, K., Meyer, H. E., Marcus, K., & Narberhaus, F. (2018). Next-Generation Trapping of Protease Substrates by Label-Free Proteomics. *Methods Mol Biol*, *1841*, 189-206. https://doi.org/10.1007/978-1-4939-8695-8_14

Liu, W., Schoonen, M., Wang, T., McSweeney, S., & Liu, Q. (2022). Cryo-EM structure of transmembrane AAA+ protease FtsH in the ADP state. *Commun Biol*, *5*(1), 257. https://doi.org/10.1038/s42003-022-03213-2

Prabudiansyah, I., van der Valk, R., & Aubin-Tam, M. E. (2021). Reconstitution and functional characterization of the FtsH protease in lipid nanodiscs. *Biochim Biophys Acta Biomembr*, *1863*(2), 183526. https://doi.org/10.1016/j.bbamem.2020.183526

Puchades, C., Ding, B., Song, A., Wiseman, R. L., Lander, G. C., & Glynn, S. E. (2019). Unique Structural Features of the Mitochondrial AAA+ Protease AFG3L2 Reveal the Molecular Basis for Activity in Health and Disease. *Mol Cell*, *75*(5), 1073-1085.e1076. https://doi.org/10.1016/j.molcel.2019.06.016

Puchades, C., Rampello, A. J., Shin, M., Giuliano, C. J., Wiseman, R. L., Glynn, S. E., & Lander, G. C. (2017). Structure of the mitochondrial inner membrane AAA+ protease YME1 gives insight into substrate processing. *Science*, *358*(6363). https://doi.org/10.1126/science.aao0464

Saunders, R. A., Stinson, B. M., Baker, T. A., & Sauer, R. T. (2020). Multistep substrate binding and engagement by the AAA+ ClpXP protease. *Proc Natl Acad Sci U S A*, *117*(45), 28005-28013. https://doi.org/10.1073/pnas.2010804117

Westphal, K., Langklotz, S., Thomanek, N., & Narberhaus, F. (2012). A trapping approach reveals novel substrates and physiological functions of the essential protease FtsH in Escherichia coli. *J Biol Chem*, *287*(51), 42962-42971. https://doi.org/10.1074/jbc.M112.388470

Yang, Y., Guo, R., Gaffney, K., Kim, M., Muhammednazaar, S., Tian, W., Wang, B., Liang, J., & Hong, H. (2018). Folding-Degradation Relationship of a Membrane Protein Mediated by the Universally Conserved ATP-Dependent Protease FtsH. *J Am Chem Soc*, *140*(13), 4656-4665. https://doi.org/10.1021/jacs.8b00832